How to Improve both Fatigue Strength and Anti-Loosening Performance of Pitch Difference Nut

(ピッチ差付きボルト・ナット締結体における疲労寿命向上と緩み防止性能向上の両立)

By

WANG Biao

Department of Mechanical Engineering

Kyushu Institute of Technology

Acknowledgements

First of all, I would like to express my deepest thanks to my professor Nao-Aki Noda in Kyushu Institute of Technology for giving me the opportunity study in Japan. I am grateful for the 4 years guidance and help of Prof. Noda.

I appreciate the financial support of The Ministry of Education, Culture, Sports, Science and Technology of Japan.

I appreciate those useful suggestions from professor Weiming Feng, my senior Fei Ren and Professor Xin Lan for my 4 years studies in Japan.

I would like to express my sincere thanks to Dr. Yoshikazu Sano and Dr. Yasushi Takase, who helped me a lot.

I would like to thank the members of the Bolt team: Dr Xi Liu, Mr. Shutaro Kubo, Mr. Kousuke Tateishi, Mr. Yuto Inui, Mr. Ryo Kawano; the member of Joints team: Dr. Dong Chen, Mr. Rei Takaki, Mr. Sirui Wang; Prof. Kazuhiro Oda from Oita University and professor Tatsujiro Miyazaki from University of the Ryukyus, who helped me a lot in my researches.

I am thankful to Guowei Zhang, who helped so much at my first year in Japan. Besides, I am thankful to my seniors and friends, Guowei Zhang, Yunting Huang, Yunong Shen, Jian Song, Hongfang Zhai, Xuchen Zheng, Geng Gao, Zifeng Sun, Xianghua Meng, Lu Chen, Beifen Siew, Mohd Radzi Bin Aridi and Rahimah Abdul Rafar who left me good memories in KIT.

Contents

Abstract

Bolt nut connections are widely used to connect mechanical elements in the industry because they are easy to install, remove and maintain. When subjected to complex working environments, failure of bolt nut connections may happen and even cause accidents. For example, the transverse load may cause self-loosening of the bolt nut connections, and cyclic axial load may cause fatigue failure of the bolt nut connections. Therefore, bolt nut connections with high fatigue strength, anti-loosening performance, and low cost are always needed.

In our teams' previous researches, it has been found that both fatigue life and anti-loosening performance of the bolt nut connections can be improved by introducing a pitch difference between the nut and the bolt. For pitch difference bolt nut connections, the load distribution gradually decreases from the free side to the clamped side of the nut rather than decreases from the clamped side to the free side of the nut as common bolt nut connections, and this is the reason why the fatigue life of pitch difference nut can be improved. Besides, when the pitch difference is large enough, a prevailing torque, which is commonly used for anti-loosening, will occur and prevent the nut from self-loosening effectively. However, when the pitch difference is small, the fatigue life can be improved significantly, and the improvement of anti-loosening performance is limited. On the other hand, when the pitch difference is relatively large, the bolt nut connections show excellent anti-loosening performance and the improvement of fatigue life is much smaller than that when the pitch difference is small. In one word, significant improvement of the fatigue life and anti-loosening performance cannot be achieved at the same time only by introducing a pitch difference to a common bolt nut connection.

In this study, the mechanism of anti-loosening performance of pitch difference bolt nut connections is investigated. Besides, the effect of some geometric aspects of pitch difference bolt nut connections, such as thread root radius and nut height, are investigated to obtain high fatigue life and excellent anti-loosening performance at the same time. This thesis is composed of a total of 5 chapters and organized as follows.

In Chapter 1, the history of bolt nut connections and some typical failures of bolt nut connections are introduced. Besides, previous researchers' efforts on improving fatigue life and anti-loosening performance of bolt nut connections are summarized. In addition, previous researches on pitch difference nut of our team are introduced.

In Chapter 2, the mechanism of anti-loosening performance of the pitch difference nut is studied by Junker experiments and finite element simulation. Loosening experiments of M12 bolt nut connection with a pitch difference of α=0, 30, 40, 50μm are done by Junker's type loosening test. According to DIN 25201, when the baseline fastener loosens after 300 ± 100 cycles vibration, and the residual axial force of the test specimen is no less than 80% with 2000 vibration cycles, the anti-loosening performance of the test specimen can be regarded as excellent. It is found that α =40, 50μm meet the standard. Although $\alpha = 35\mu m$ does not meet the criteria, the clamping force $F = 4.0$kN (27%) is maintained at vibration number n =1500, and the loosening resistance is substantially maintained. The relationship between clamping

force and tightening torque ($F-T$ relation) and the loosening process of pitch difference nuts are analyzed FEM. It is found that at the early stage of vibration, the elastic energy releases and the clamping force decreases fast. With the loosening of the nut, two sides of the nut contact the bolt thread. Owing to the elastic energy stored between two ends of the nut, a tightening process occurs and the tightening angle in every cycle increases with the decrease of clamping force. Thus, the decrease rate of the clamping force becomes slower with the increasing the vibration number, when the clamping force decreases to a certain value, the tightening angle almost equals to the loosening angle in one vibration cycle, i.e., a residual clamping force and a residual prevailing torque remains steady and loosening of the bolt nut connection will not continue.

In Chapter 3, the effects of thread root radius on fatigue and anti-loosening performance of pitch difference nut are studied experimentally and analytically for M16 bolt nut connections. It is found that by enlarging the root radius from ρ_0 to $2\rho_0$, the fatigue life of bolt nut connections can be improved by more than 30% because both stress amplitude and mean stress at the thread roots can be reduced. In addition, by introducing a suitable pitch difference between the root radii enlarged bolt-nut connections, the fatigue limit can be further improved by 25%. This is because when no pitch difference, the crack initiation always occurs at $No.1$ or $No.2$ threads close to the bolt head, causing the final failure; however, under a suitable pitch difference, the crack initiation occurs at $No.6$ or $No.7$ threads far away from the bolt head. Good anti-loosening performance can be expected for the bolt-nut connections having enlarged root radius because the prevailing torque T_P = 19Nm and the residual prevailing torque T_P^u = 10Nm are not smaller compared to other special bolt-nut connections. Since those values are not smaller compared to other special nuts such as U-Nut and Super Slit Nut, good anti-loosening performance can be expected for the enlarged root radius of bolt-nut connections under the suitable pitch difference.

In Chapter 4, the effect of nut height on anti-loosening performance and fatigue life of M12 bolt nut connections having a pitch difference between the nut and the bolt is investigated in this study. The relations between tightening torque and clamping force under different nut heights and pitch differences are obtained by experiments and finite element analysis. It has been found the anti-loosening property for pitch difference bolt nut connections depends on the produce of pitch difference and thread number n. Besides, the stresses at the thread roots of the bolt are analyzed using the axisymmetric model. When the pitch difference is less than 25μm, the fatigue life increment remains steady if increasing the nut height from 10.5mm to 14.0mm. It can be concluded that by increasing the nut height and decreasing the pitch difference at the same time, a better combination of anti-loosening performance and fatigue properties can be obtained.

Chapter 5 provides the major conclusions, the most significant outcomes and contributions, and suggestions for future works.

List of Figures

List of Tables

Nomenclatures

AS	Australian Standard
BSF	British standard fine thread
BSW	British standard whitworth thread
CD bolt	Critical design for fracture
DIN	Deutsches Institut für Normung
DTB	Double thread bolt, Dual thread bolt
FEM	Finite element method
HLN	Hyper lock nut
ISO	International organization for standardization
JIS	Japanese Industrial Standards
NAS	National aerospace standard
SLB	Step lock bolt
SSN	Super slit nut
USS	United states standard
3D	Three dimensional

C_x	Thread clearance in the transverse direction
C_z	Thread clearance in the axial direction
D	Nominal diameter of the bolt
d_2	Pitch diameter of the bolt
d_w	Effective diameter of the bearing surface
E	Young's modulus
F	Clamping force of the bolt nut connection
F_a	Amplitude of the axial cyclic loading
F_c	Cyclic axial force
F_{m}	Mean axial force
F_u	Residual clamping force
H	Nut height
H_c	Height of the clamped body
K	Nut factor
K_t	Stress concentration factor
m	Complete thread number
n	Transverse vibration cycle number of the clamped body
p	Thread pitch
R	Stress ratio
T	Tightening torque of the nut
T_P	Prevailing torque
T_P^u	Residual prevailing torque
T_{slip}	Slip torque
T_R^u	loosening resistance torque

$\tilde{T}_R^u$	median loosening resistance torque
u_x	Transverse displacement of the clamped body
α	Pitch difference between the nut and the bolt
β	Half angle of the thread
θ	Nut rotation angle
θ_B	Twist angle of the Bolt
θ_L	Loosening angle of the nut
θ_N	Twist angle of the nut
μ_s	Thread coefficient factor
μ_w	Bearing surface, under-heading coefficient factor
ν	Poisson's ratio
ρ	Thread root radius
σ_a	Stress amplitude
σ_B	Tensile stress
$\sigma_{\max}$	Maximum stress at the thread root
$\sigma_{\min}$	Minimum stress at the thread root
σ_{w}	Fatigue strength
σ_y	Yield stress
$\mathrm{II_B}$	Nut tightening process
$\mathrm{II_F}$	Nut loosening process

Chapter 1. Introduction

1.1 Background

Bolt nut connection is one of the most essential and widely used elements in industries such as large aircraft, large power generation equipment, automobiles, high-speed trains, large ships. Therefore, in many cases, the working environment of bolt nut connections is complex. To ensure the safety of the structures connected by bolt nut connections, cheap bolt nut connections with excellent anti-loosening performance and high fatigue strength are always needed.

Structures with a screw shape have been used for over 2000 years. The record of usage of bolted joints can date back to 15th century [1]. At the early time, screws are made by hand. In 1760, Job and William Waytt patented a design that can be used to produce screws automatically, and opend a factory to produce screws 16 years later. In 1797, Henry Maudsley invented a large screw cutting lathe that can be used to produce accurately sized screws massively. However, the biggest problem then was there was no uniform standard for screws.

In 1941, Joseph Whitworth British published a paper in the Institution of Civil Engineers, designed a thread form and was accepted by Engineering Standards Association. This kind thread shape is so called British Standard Fine (BSF) thread form, as shown in Fig. 1.1, and have been using until now [2]. The thread angle of BSF is 55 degree. In 1964, William Sellers developed the published a thread form [3], and it was accepted as United States Standard (USS) thread in 1898 and no longer supported now. The thread angle of this type of thread is 60 degrees. In 1947, the International Organization for Standardization (ISO) thread was accepted, see Fig. 1.2, and it is the most commonly used thread worldwide. The thread angle of ISO thread is also 60 degrees.

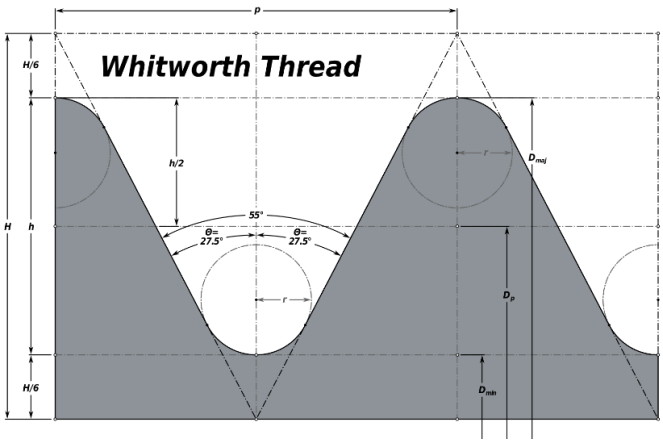

Fig. 1.1 British Standard Whitworth (BSW) thread dimensions

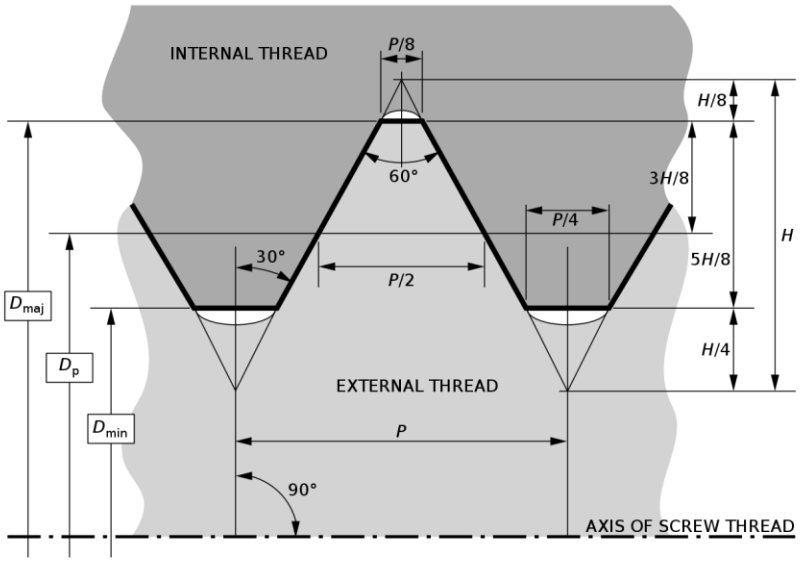

Fig. 1.2 ISO, DIN, AS, JIS thread dimensions

However, these standard threads can not meet the requirement for some special use of bolt nut connections. Researches on threads have always been a topic for engineers. When subjecting cyclic axial force, fatigue failure may happen. When subjecting transverse load, self-loosening may happen. Besides, special cases like impact, drastic temperature changes can also cause the failure of bolted joints.

Accidents caused by failure of bolted joints are sometimes happening. According to the report by Petroleum Safety Authority in 2019, about 3% of incidents in their database are related to bolts [4]. In 1979, the roof of the stadium under construction in Kansas City, US collapsed, and killed 5 workmen. Failure of the high-strength bolt nut connections under wind load is the reason of this accident. In 2015, a wind turbine in Lemnhult, Sweden collapsed because of fatigue failure of bolt nut connections, see Fig. 1.3.

According to a survey by Campbell et al., about 25% of wing accidents of aircraft are related to screws [5]. In 2013, an aircraft in Oita, Japan caught fire in the right engine, the report by Japan Transport Safety Board says the reason maybe the loosening of the B nut connection the right engine manifold and the injector $No.14$, see Fig. 1.4 [6]. In 2014, an accident during helicopter maintenance check flight happened because loosening of B-Nut. In April 2015, an airplane in Offutt Air Force base, Nebraska, US caught fire caused a loss of 64.2 million US dollars, and the reason for this accident is loosening of a nut connecting oxygen tubing [7].

Fig. 1.3 Accident of wind turbine in Lemnhult, Sweden caused by fatigue failure of bolt nut connections.

Fig. 1.4 Exterior view of the right engine in the accident of JA206J airplane

1.2 Previous researches on fatigue of bolt nut connections

Since fatigue failure of bolted joints causes failure of structures and even major accident industry, many efforts have been made to improve fatigue life of bolted joints.

These studies on fatigue properties of bolted joints can be roughly divided into four types, using washers, size or thread shape changing of bolts, improving manufacturing method, and special post treatment process.

1.2.1 Effect of washers on fatigue

Majzoobi et al. did a series of experiments about washer effects on fatigue life of bolt nut connections [8]. According to the experimental results, the fatigue life of bolt nut connections with washers is almost 2 times longer than that of bolt nut connections without washers. Silva et al. investigated the effect of the material of plain washer on the fatigue life of bolted joints and found that the fatigue life of bolt nut connections with 304 stainless steel washers is longer than that of connections with carbon steel washers [9]. Ji found that the fatigue life of bolt nut connections can be significantly improved by putting a ceramic gasket under the nut [10].

1.2.2 Effect of bolt or thread shape on fatigue

Griza et al. investigated bolt length effect on M24 studs, and found that increasing the bolt length can increase the fatigue strength of the joint [11]. It is considered that the bolt stiffness is reduced by increasing the length of the bolt. Heywood investigated the relationship between fatigue and stress concentration and found that the fatigue strength is related to the absolute size of the notch, material, and the stress concentration factor [12]. Gregor et al. investigated the effect of cyclic loading on the mechanical behavior of three kinds of materials; from these experiments, it can be found that by enlarging the root radius, both fatigue limits and fatigue strength of the materials can be improved [13,14]. Walker et al. studied the thread parameters' effects on the fatigue life, and they found that the reduced stress concentration may improve the fatigue strength [15]. Dragoni investigated the effect of pitch difference on the fatigue life of steel bolted connections and found that for small bolts of low-grade steel the fatigue life slightly increases with decreasing the pitch and remarkably increasing the endurance load of large bolts made by high-grade steel with increasing the pitch [16]. Majzoobi et al. also investigated the effect of pitch on the fatigue life of bolted joints, and found that ISO standard coarse threaded bolts have a higher fatigue life than the fine threaded bolt [17]. Yoshimoto et al. found increasing the flank angle by 5 degrees in the pressure flank and reducing the pitch by 0.15% for M24 may improve the fatigue strength of bolt nut connections [18]. Honarmandi et al. investigated the thread root shape effect on fatigue life of bolt nut connections by using four different thread root shapes; triangular thread, trapezoidal thread, negative buttress thread, and positive buttress thread, shown in Fig. 1.5 [19]. The FE analysis shows that the stress concentration factor K_t at the thread for positive buttress thread, triangular thread, negative buttress thread, and Trapezoidal thread is 3.75, 3.34, 3.16 and 2.59, respectively. The experimental results show that for the four types of thread root shapes, the larger the K_t is, the shorter the fatigue life of the bolt nut connection is. It is well known that for common bolt nut connections, the stress distributions at the bolt thread

root gradully decreases from the bearing surface side to the free end side. Thus, the maximum stress always occurs at the first engaged thread. Therefore, if the K_t at the first thread can be reduced, the fatigue life is supposed to be extended. Nishida et al. investigated the effect of thread shape, root radius and material on fatigue life, and proposed a kind of bolt, named CD bolt (Critical Design for Fracture), shown in Fig. 1.6. It is found that the fatigue life for CD bolt is about twice that of common bolts [20,21]. In Honarmandi's study [19], this method is called Fatigue Bolt Improvement method, but in fact, it is almost the same as CD bolt, the only difference between them is the gradient of the CD shaping. For a common bolt nut connection, fracture sometimes happens at the runout of the bolt, so the thread runout should be gradual to decrease the stress concentration, as shown in Fig. 1.7(a) [22]. Besides, when tapering the nut at the bearing side at a 15-degree angle, the fatigue life can be improved by 20%.

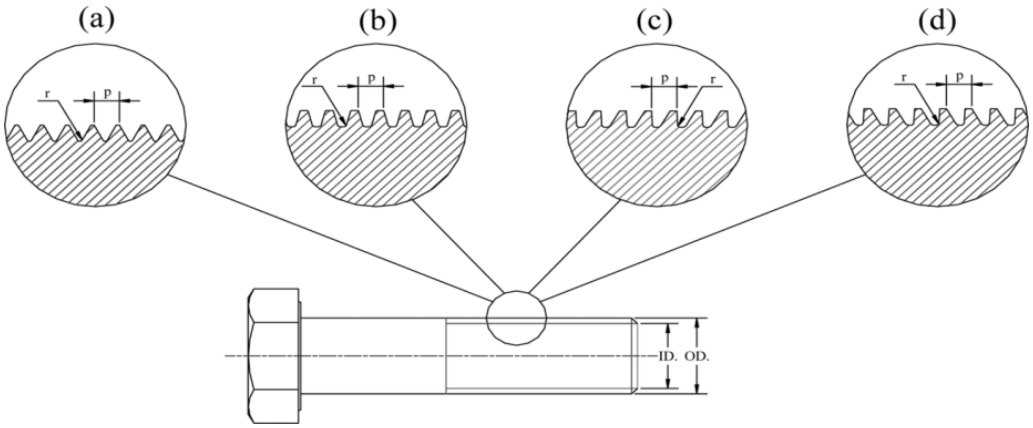

Fig. 1.5 thread root shapes (a) triangular (b) trapezoidal (c) negative buttress (d) positive buttress

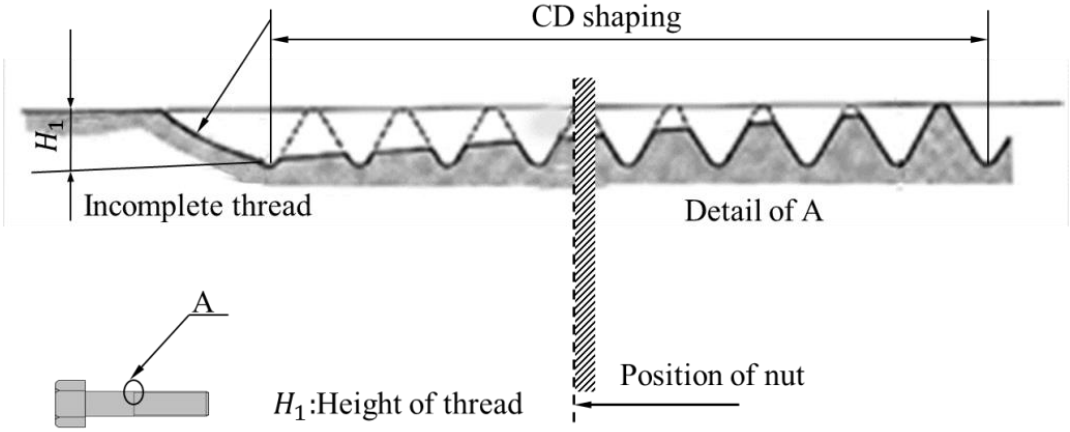

Fig. 1.6 Typical shape of CD bolt

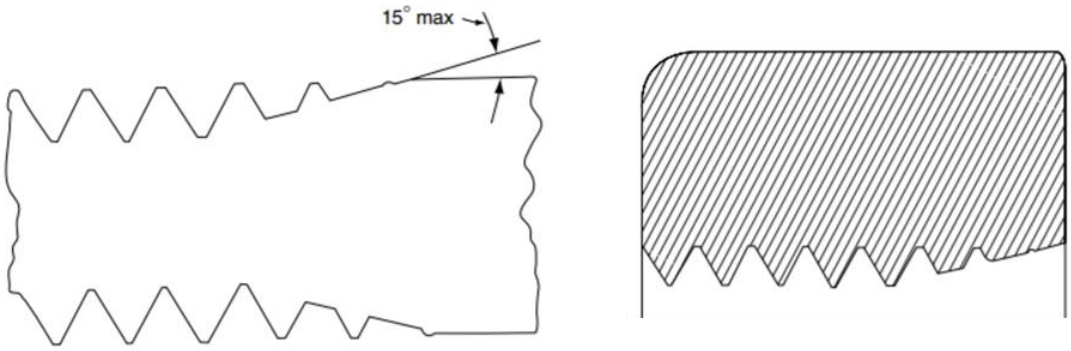

(a) Thread runout tapering (b) Tapering at the bearing side of the nut

Fig. 1.7 Tapering at the runout and the bearing side of the nut

1.2.3 Effect of the manufacturing process on fatigue

There are many methods to manufacture threads. It is widely accepted that the fatigue life of rolled bolt nut connections is longer than that of bolt nut connections made by cutting. In the rolling process, a compressive residual stress occurs in the thread, thus, the hardness of the thread increases gradually from the bolt axial to the thread root, as shown in Fig. 1.8 and Fig. 1.9 [23]. Knight et al. found that modifying the thread root by cold deformation process may reduce the stress concentration factor and surface residual compressive stresses improving the fatigue life [24]. There are some micro-cracks occur in the thread manufacturing process. Liu et al. found that reducing these micro-cracks can effectively improve the fatigue performance of the bolted joints [25,26]. There are several different processes when manufacturing thread, and heat treatment is a common way to improve fatigue properties. Ifergane et al investigated the effect of rolling and heat treatment effect on fatigue properties by experiments. Four types of threads are used, cold rolling before heat treatment, cold rolling after heat treatment, machining before heat treatment, machining after treatment. Among the four methods, cold rolling after heat treatment can get the maximum fatigue lifetime [27,28]. There are some other researchers studied the order effect of the manufacturing process on fatigue, the conclusions are the same as above, the fatigue life of the threads rolled after heat treatment is longer than the threads rolled before heat treatment. In addition, the fatigue strength of the threads rolled after heat treatment is also much larger than the that of the threads rolled before heat treatment [29,30]. Recent years, ultrasonic thread root rolling technology has widely used in industry. Cheng et al. found that fatigue life of the bolt made by ultrasonic rolling technology can be 5 times as long as the bolt without using this technology [31,32].

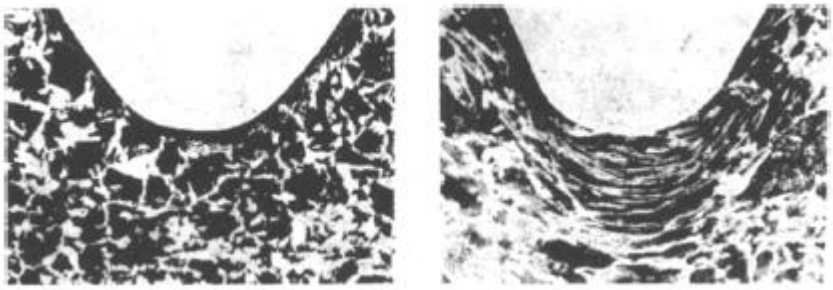

(a) (b)

Fig. 1.8 Microstructure of specimens with thread (a) by cutting (b)by rolling

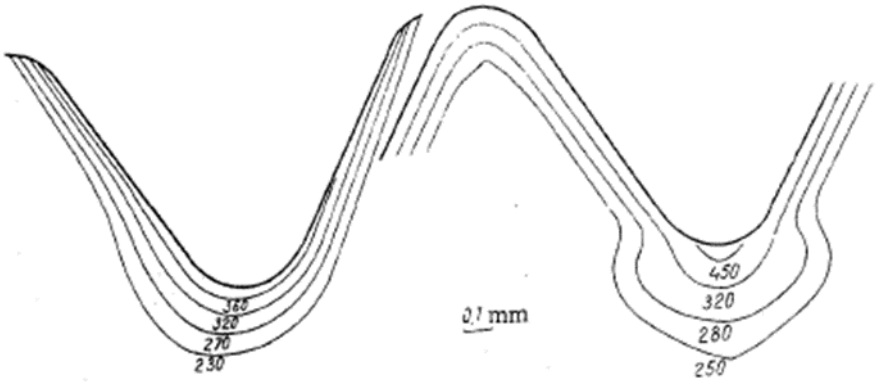

(a) (b)

Fig. 1.9 Microhardness of specimens with thread (a) by cutting (b)by rolling

1.2.4 Effect of post treatment process on fatigue

Surface peening treatment is a popular research field in recent years and can be used to improve fatigue life of materials [33–36]. Therefore, some researcher tried this technology on bolt treatment. Shen et al. found that fine particle peening may improve the fatigue life because of eliminating the influential tool marks on the bolt head fillet, decreasing the surface roughness and improving the hardness [37]. Zhan et al. found that the fatigue life can be improved by 87.8% by using shot peening treatment of a nut [38]. Besides, Sun et al. found that the fatigue life of threads can be improved by using plasma nitriding treatment [39].

1.3 Previous researches on anti-loosening of bolt nut connections

Junker found that for bolt nut connections, dynamic loads in the transverse direction are more likely to cause loosening failure than forces in the axial direction [40]. Junker test has been adopted into international fastener standards and is widely used worldwide [41–43]. Indeed, other factors such as dynamic axial force [44], thermal stress [45,46], dynamic bending moment [47], and impact loads [48,49] can also cause loosening of bolt nut connections, these special factors are not taken into consideration.

There are many researches available focusing on improving anti-loosening

performance of bolt nut connections. These methods can be simply divided into three kinds, i.e., using special washers, changing nut, changing bolt geometry.

1.3.1 Washer effects on anti-loosening

There are many kinds of washers available in the market. Some typical types of washers are shown in Fig. 1.10 Nord lock washer, which uses a pair of washers with cams and radial serrations on their two sides, can utilize tension instead of friction to prevent loosening of bolt nut connections because the cam inclination is greater than the thread of the bolt [50,51]. Sawa et al. [51,52] did a series of loosening experiments about different types of M12 nuts and washers by using Junker's type loosening machine, and it is found that the anti-loosening performances of a bolt nut connections without a plate washer, spring washer, toothed washer or Nord lock washer is worse than that of bolt nut connections with a washer. Besides, the anti-loosening performance of different types of washers depends on the bolt preload. Among all the four types of washers, the anti-loosening performance of spring washers is the worst, but still much better than that of bolt nut connections without a washer. Moreover, when the preload is relatively small, plate washer shows better anti-loosening performance than toothed washer and Nordlock washer; when the preload is large, the anti-loosening performance is better than that of the toothed washer and plate washer. Dravid et al. [53] also found that the plain washer has a better anti-loosening performance than a spring washer. NBK group [54] invented a type of eccentric lock washer, it shows better anti-loosening performance compared to plate washer and spring washer. Panja [55] found that outside serrated toothed washer has better loosening resistance ability compared to the inside serrated toothed washer.

Fig. 1.10 Different types of washers

1.3.2 Nut geometry effect on anti-loosening

The second method is changing the nut geometry. Fig. 1.11 shows some typical types of geometry changed anti-loosening nut. As shown in Fig. 1.11(a), a flange nut is a nut with a wide flange at the bearing side of the nut, and this flange acts as a washer. Besides, the bearing surface side of the flange is usually a serrated shape. Thus, the serrated shape flange can resist the loosening of the nut. It is reported that 110 percent of the tightening torque is needed to loosen them [56]. Flange nuts are mostly used for wood and plastic. Slotted nut, also known as castelled nut, has some slots on the free end side of the nut, and is usually used together with a pin. This type of nuts is extremely well for low-torque applications [56]. Saper lock nut is a kind of wire inserted nut and is widely used in industries such as transportation, bridges [57]. Different from the common nut, this type of nuts can be reused several times. Since there is a spring inserted in the thread, when vibrating the bolted joints, the loosening energy can be absorbed and transfer to a locking torque. Except for the anti-loosening nut above, prevailing torque is also widely used for anti-loosening [58]. Nylon insert nut, super slit nut, U nut, Outer cap nut, and super lock nut shown in Fig. 11 are all prevailing torque nuts. For prevailing torque type nuts, the prevailing torque after several times of usage is usually smaller than the prevailing torque for the first usage. For example, detailed values of the prevailing torque of U nut after usage can be found from the official website of Fuji Seimitsu. The experimental results of anti-loosening performance are different, even for the same kind of nuts. For example, the percentage of residual clamping force for Nylon insert nut is different from the papers cited[51,52,55,59]. This may because the materials and experimental conditions are different. Therefore, the anti-loosening nuts should follow the manual of the products. Daiki industry and Tokyo university developed a kind of nut name Super Slit Nut (SSN), part of the nut is cut, and the thinner part of the nut is pressed to deformation. For M12 SSN, the experimental results and FEM results of prevailing torque are between 15Nm and 19Nm, and the anti-loosening performance of SSN is much better than that of common nut [60]. Nishiyama et al. designed a kind of nut, named Hyper Lock Nut (HLN) [61]. The shape of HLN is similar to SSB, both of the two types of nut has a cut part as shown in Fig. 1.11(e), and the different part is, for HLN, instead of pressing the thinner part of nut to plastic deformation, very small part of the bearing surface side of the nut is cut, the included angle of the cutting surface and the bearing surface is 1 degree. HLN can provide good anti-loosening performance without a complicated tightening process. U nut is a type of prevailing torque type nut which is widely used in the whole world [62]. As shown in Fig. 1.11(f), U nut is made of two parts, a nut and a friction ring (special spring). The friction ring is fixed to the upper surface of the nut by caulking and integrated. When the friction ring comes into contact with the thread of the bolt and the state shown on the left is reached, stress P is generated due to the spring action. Along with the reaction force P' again, the thread of the bolt is strongly pressed to generate friction torque (preveling torque) that prevents free rotation. Aparting from this, there are many kinds of anti-loosening nut similar to U nut, for

instants, V nut (COMWELL Fujisawa Co., Ltd.), E lock nut (Osaka Forming Co., Ltd), Cosumolock nut (KOSUMOROKKU), Precision Lock Nut (Nikki Trading Corp.) available in the market. Fig. 1.11(g) shows the outer cap nut. Initially, this outer cap nut can be rotated smoothly by hand until the nut touches the fixing plate. However, loosening prevention performance can be achieved by deforming the outer cap after tightening the outer cap nut and generating the contact force of the screw in the outer cap area [63]. Fig. 2(h) shows the super lock nut. There is a thin tube between the upper and lower parts, which can be deformed along the axial direction, so that phase-difference of lowers and needle threads are generated. Due to this phase difference, opposite forces are applied to the surfaces of the upper and lower parts, and loosening prevention performance is exhibited [64]. Wakabayashi designed a nut pair that consists of an upper nut and a lower nut that eccentrically engage with each other to avoid loosening, named Hard Lock. This kind of bolt nut connection has witnessed the success of Japan Shinkansen for several decades [65].

(a) Flange nut (b) Slotted nut (c) Saper lock nut

(d) Nylon insert nut (e) Super slit nut (f) U nut

(g) Outer cap nut (h) Super lock nut (i) hard lock nut

Fig. 1.11 Some typical types of anti-loosening nut

1.3.3 Bolt geometry effect on anti-loosening

The third method for anti-loosening is changing the bolt thread geometry. Sase et al. developed and optimized a bolt named step lock bolt (SLB) which aims at preventing bolt torsion [66,67]. The thread is alternately composed of the stepped part and inclined part, as shown in Fig. 1.12(a). Excellent anti-loosening performance of SLB has been confirmed by a displacement based loosening test. Another effective way of anti-loosening is using a double thread, named as Double Thread Bolt (DTB), also known as Dual Threaded Bolt. Takemasu developed a kind of DTB, for which the pitch ratio of the coarse thread and the fine thread is 2:1. The anti-loosening performance was confirmed by using a vibration test based on NAS3354, after over 10 million cycles of vibration, neither a crack or any damage was observed, this proved the excellent anti-loosening of the rolled DTB [68]. Shinbutsu et al. designed a new type of DTB, called DTB-II thread, which composed of a coarse single thread and coarse multiple threads, and it is found that the anti-loosening performance of this kind of threads is much better than conventional DTB-I thread [68–70]. The DTB is now available in the market, and its product name is Perfect Lock Bolt.

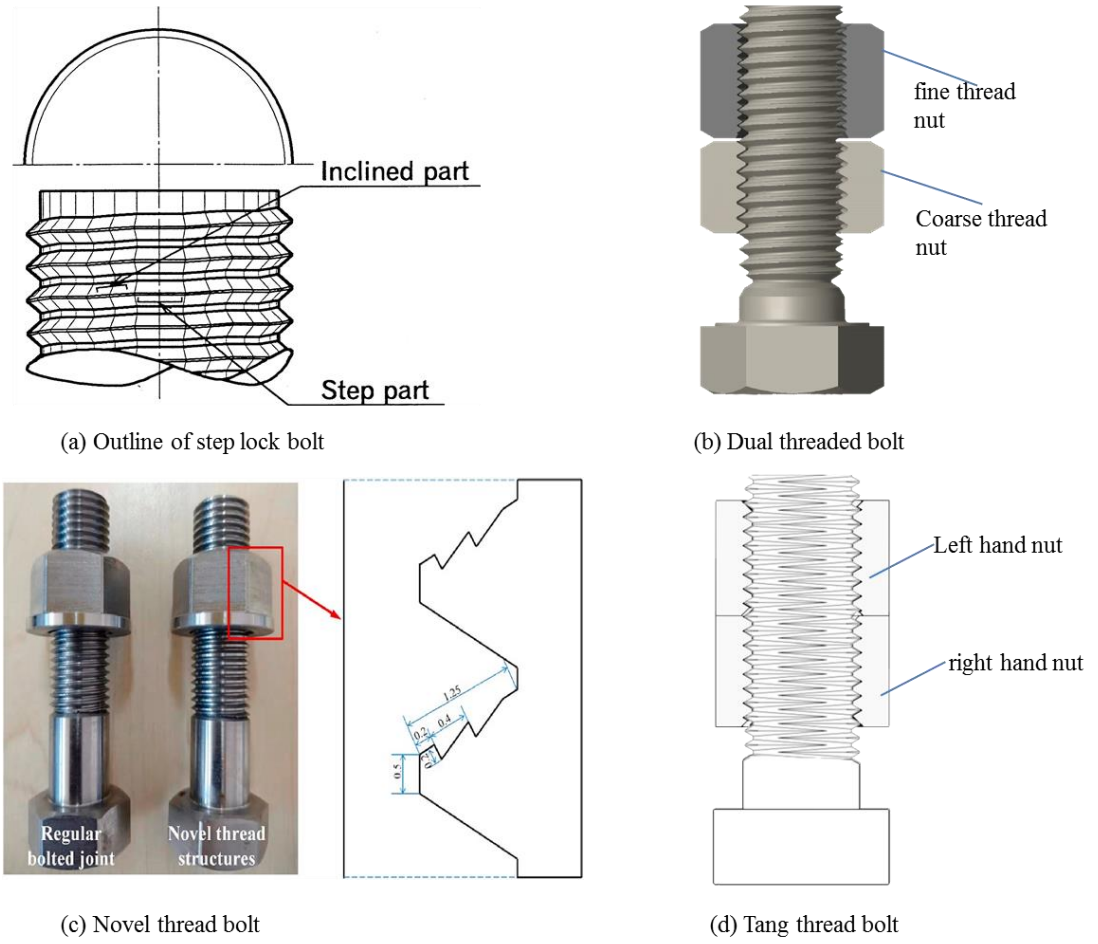

(a) Outline of step lock bolt

(b) Dual threaded bolt

(c) Novel thread bolt

(d) Tang thread bolt

Fig. 1.12 Examples of bolt thread changed structures

Gong et al. designed a novel anti-loosening structure, shown in Fig. 1.12(c). For the newly proposed thread structure, both internal and external threads are changed, it is considered that the modified thread shape can effectively inhibit relative sliding along the radial direction. The Junker test results showed that the axial clamping force is even smaller larger after the vibration test [71]. Fig. 1.12(d) shows the basic structure of a famous anti-loosening bolt in China, named Tang thread bolt [72,73]. For a tang thread bolt, the upper side is a left hand nut, and the lower side is a right hand side. The upper nut can stop the loosening of the lower side nut under vibration.

1.4 Previous researches on pitch difference nut of our team

Xiao et al. studied pitch difference effect on fatigue strength and anti-loosening performance of Tapering Thread Bolt (CD bolt) for M12 bolt nut connections [74]. However, different from common bolt nut connections, the clearances of the specimens used are set as 0. By using axis-symmetric finite element analysis, it is found that when there is a suitable pitch difference between the nut and the bolt, the maximum stress at the thread root can be reduced by 28.6% compared to that of common M12 bolt nut connections. Besides, for CD bolt and nut, the maximum stress at thread root can be further reduced by 4.5%. Moreover, it is found that the prevailing torque increases with the increase of pitch difference, which means the anti-loosening performance can be better. For the M12 bolt nut connections used in this study, when the pitch difference increases from 1μm to 5μm, the prevailing torque increases from 4.93Nm to 24.67Nm, accordingly. According to Izumi et al.'s research on Super Lock Nut [60], when the prevailing torque reaches to 13.5Nm, the anti-loosening performance is good enough.

Akaishi et al. studied the effect of slight pitch difference on fatigue strength of M16 bolt nut connections [75]. The pitch differences used are 0μm, 5μm and 15μm. The clearances for the specimens in the axial direction are 125μm. From the experimental fatigue results, it can be found that the fracture positions for the pitch difference bolt nut connections are the runout surface, No.-3 thread, as shown in Fig. 1.13. Even though, the fatigue lives of the pitch difference nuts ($\alpha = 5\mu m$ and $\alpha = 15\mu m$) are much longer than that compared to common M16 bolt nut connections.

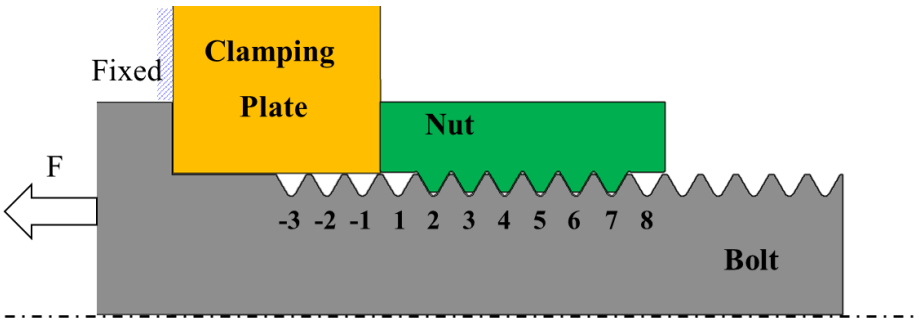

Fig. 1.13 Sketch for M16 bolt nut connections

Chen et al. studied pitch difference effect on the fatigue life of M16 bolt nut

connections with pitch differences [76–80]. The fatigue life for $\alpha = 15\mu m$ can be extended to about 1.5 times compared to the common bolt nut connections. Even the fatigue life of $\alpha = 33\mu m$ is shorter compared to that of $\alpha = 15\mu m$, it is still much longer than that of common bolt nut connections. That is to say, with the increasing of pitch difference, the fatigue life of the bolt nut connections increases at first and then decreases. Besides, the mechanism of fatigue life improvement of pitch difference nut has been found. For common bolt nut connections, the maximum stress of the bolt thread locates on the contact part of the thread near the bearing surface, $No.2$ thread as shown in Fig. 1.13. Thus, an initial crack occurs here and final fracture happens the same position later. However, for pitch difference bolt nut connections, the maximum stress of the bolt thread occurs at the right side, $No.7$ thread. Then, the cracks extent to the left side, $No.2$ thread, and final fracture occurs at the left side. This also can be observed from the cross section of the bolt thread. Besides, the anti-loosening performance of different pitch difference nuts has been confirmed by the Loosening experiment device based on NAS3350, and the anti-loosening performance of pitch difference nuts is also confirmed by the plastic deformation obtained by the axisymmetric FE model. The most important conclusions can be summarized as shown in Fig. 1.14. When the pitch difference is small, the fatigue life improvement is quite good, but the improvement of anti-loosening performance is relatively low. On the other side, when the pitch difference is large, anti-loosening performance is excellent, but the fatigue life improvement is smaller than that when pitch difference is relatively small.

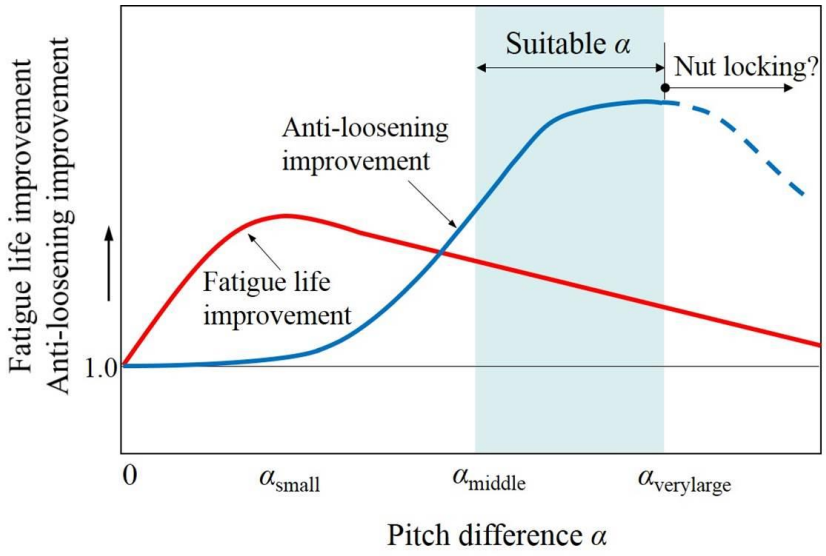

Fig. 1.14 Schematic illustration of the fatigue life improvement and anti-loosening improvement

Liu proposed an effective way to detect and correct manufacturing errors [81]. Besides, Liu et al. studied the relation between the clamping force F and tightening torque T (F-T relation) and the relation between prevailing torque and pitch difference using the 3D finite element model [81–85].

Chapter 2. Mechanism of anti-loosening performance of pitch difference bolt nut connections under transverse vibration

2.1 Introduction

Loosening test is quite a good way to measure the anti-loosening performance of bolt nut connections. Junker found that for bolt nut connections, dynamic loads in the transverse direction are more likely to cause loosening failure than forces in the axial direction [40]. Junker test has been adopted into international fastener standards such as DIN 65151 and used worldwide. There are mainly two kinds of loosening test machines. One kind is transverse impact vibration testing machines based on NAS 3350 (National Aerospace Standard), as shown in Fig. 2.1. However, for this kind of machine, the amplitude of vibration is time-varying, and the criteria is the nut does not drop after 30000 cycles of vibration. Thus, it is hard to simulate the loosening process. The other kind is Junker's type transverse cyclic vibration testing machines. Fig. 2.2 shows a sketch of a Junker test machine based on DIN 65151, a sensor connected with the fixed part can be used to record the change of clamping force, and the moveable plate is on rollers and can move frictionless in the transverse direction. Since the amplitude of transverse vibration of the moveable plate is constant; it is easy to simulate the loosening process by using Junker's type loosening test.

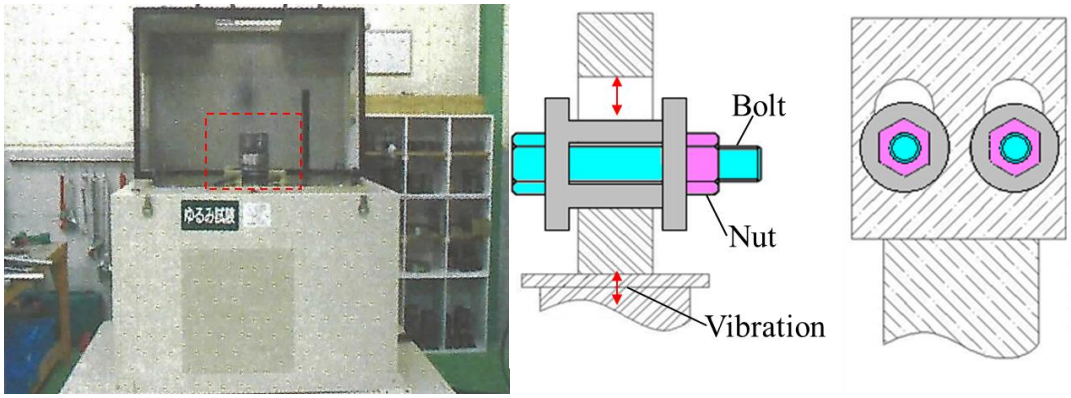

(a) Test machine (b) Sketch of the test machine

Fig. 2.1 Loosening test machine based on NAS 3350 (National Aerospace Standard)

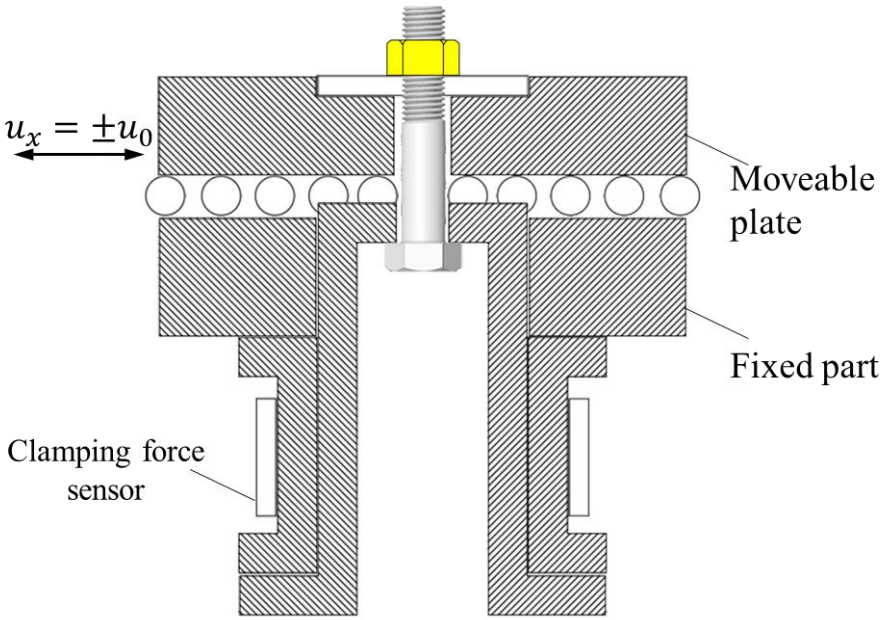

Fig. 2.2 Sketch of Junker's type loosening test machine based on DIN 65151

In our team's previous studies, the relations between tightening torque and clamping force have been studied. Fig. 2.3 shows the screwing process, tightening process, untightening process, and unscrewing process of the nut [84]. Screwing process, before the nut contacts the clamped body, a prevailing torque between the nut and the bolt will occur and then remains steady after the whole nut is screwed into the bolt, shown as Fig. 2.3(a). Tightening process, after the nut contacts the clamped body, a tightening force F between the bolt and the nut will occur and increase, shown as Fig. 2.3(b). Untightening process, the tightening force F decreases until to zero with the loosening of the nut, shown as Fig. 2.3(c). Unscrewing process, there will be a residual prevailing torque smaller than the prevailing torque that occurred in the screwing process, shown as Fig. 2.3(d). But in the untightening process, the nut is untightening by hand, which is far from the loosening process in reality. In this study, the untightening process is replaced by the Junker loosening test, and the FEM model is shown in Fig. 2.4.

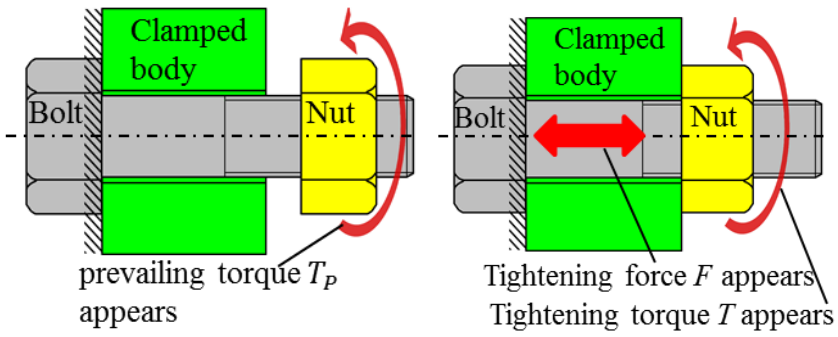

(a) Screwing process (b) Tightening process

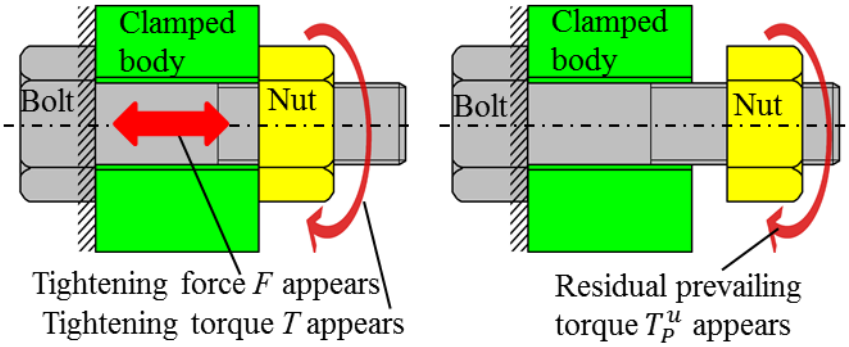

(c) Untightening process (d) Unscrewing process

Fig. 2.3 Schematic illustration for (a) screwing process (b) tightening process (c) untightening process and (d) unscrewing process

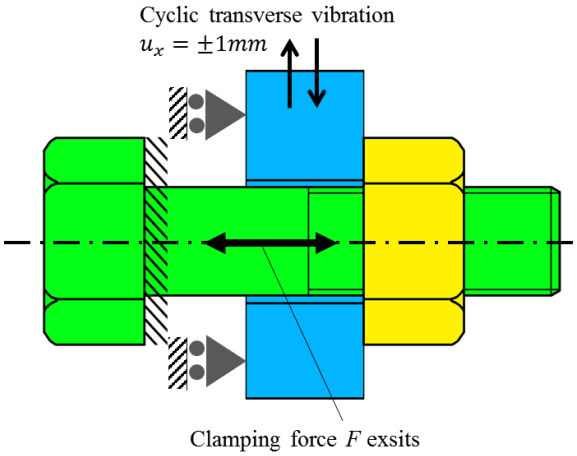

Fig. 2.4 FEM model of Junker's type loosening test

2.2 Specimens used for Junker test

In this study, Japanese Industrial Standard (JIS) M12 bolt nut connections are used. The size of the bolt and the nut are shown in Fig. 2.5. For common M12 coarse thread bolt nut connections, both the pitch of the bolt and the nut are $p = 1750\mu m$. For pitch difference bolt nut connections, the pitch of the bolt is the same as a common bolt, and the pitch of the nut is α µm larger than that of the bolt. Three different pitches $\alpha = 35, 40, 50$ µm are used in this study. Besides, a common nut $\alpha = 0$ is also used as a reference. For the common bolt nut connection, the clearance between the bolt and nut in the axial and transverse directions are $C_z = 59\mu m$ and $C_x = 102\mu m$, respectively, as shown in Fig. 2.6. The bolts are made by Chromium-molybdenum steel SCM 435, and its strength is 8.8. The nuts are made by medium carbon steel S45C, and their strength is 8. The material properties of the bolt and the nut are shown in Table 2.1. Both the bolt and the nut are made by cutting with the manufacturing error within 3µm. All bolts used in this chapter are full threaded bolts.

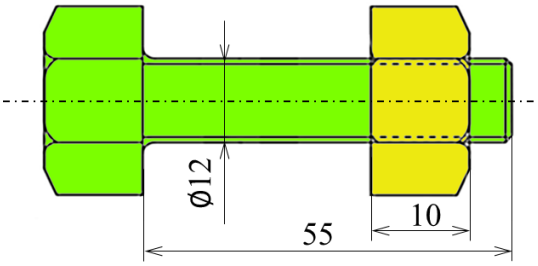

Fig. 2.5 Size of the bolt nut connection used for Junker loosening test (unit: mm).

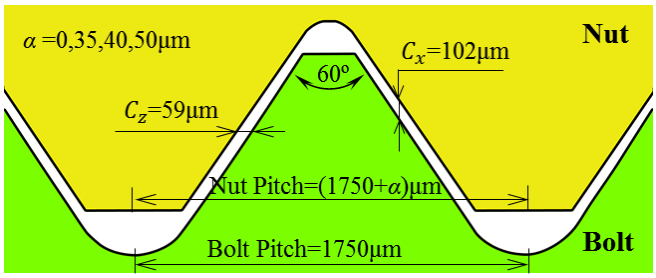

Fig. 2.6 Pitch difference and clearance between threads of the bolt and nut.

Table 2.1 Material properties of the bolt and the nut.

	Young's modulus E (GPa)	Poisson's ratio ν	Yield strength σ_y (MPa)	Tensile strength σ_B (MPa)
SCM435 (Bolt)	206	0.3	800	1200
S45C (Nut)	206	0.3	530	980

For pitch difference nut, when the pitch difference is big enough, two ends of the nut will contact the bolt before it contacts the clamped body. Thus, a prevailing torque will occur and increase until the whole nut is screwed onto the bolt and then remains steady. The contact status when the prevailing torque appears is shown in Fig. 2.7. The relation between the screwing in cycles and the tightening torque is shown in Fig. 2.8.

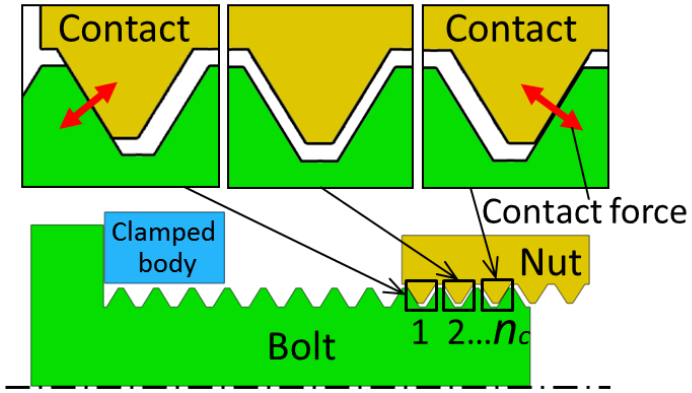

Fig. 2.7 Contact status when the prevailing torque appears between bolt and nut.

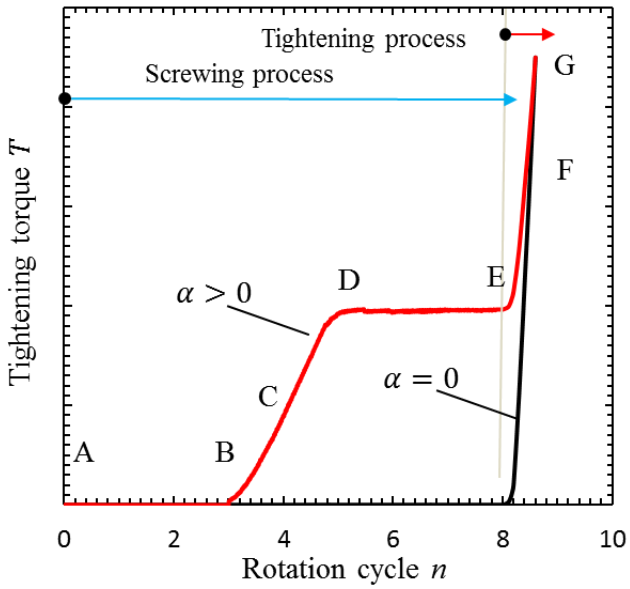

Fig. 2.8 Sketch of relation between rotation cycle and prevailing torque for common bolt nut connections and pitch difference bolt nut connections

2.3 Experimental conditions and results

2.3.1 Experimental conditions

Fig. 2.9(a) shows the Junker vibration test machine based on DIN 65151 used for the loosening tests, and Fig. 2.9(b) is a schematic diagram of the main part. The movable plate is fastened to the fixed plate with bolts and nuts via rollers, and the initial tightening force before loosening is $F_{22.3\%} = 15\text{kN}$. Since the movable plate is supported by rollers, the friction with the fixed plate can be ignored. Thus, the simplified FEM model is shown in Fig. 2.4.

For pitch difference nut, as shown in Fig. 2.7, a prevailing torque generates in the screwing process when two ends of the nut start to contact with the bolt, and the prevailing torque will increase until the whole nut is screwed onto the bolt. During the loosening process, the eccentric shaft shown in Fig. 2.9(a) rotates at a frequency of 8 Hz. Thus, the moveable plate (clamped body in Fig. 2.3)) vibrates in the transverse direction at the same frequency of the shaft. The vibration displacement applied to the moveable plate is determined based on DIN 65151. That is, the clamping force decreases to $F = 0$ after $n = 300 \pm 100$ cycles vibration. According to this, the amplitude of the moveable plate is ± 1 mm. Table 2.2 shows all the test conditions, including the amplitude. When the vibration number n reaches 1500, the experiment ends. In the revised DIN25201 as an evaluation of loosening resistance performance, the criterion of good anti-loosening performance is that the residual axial force is 80% of the initial clamping force after 2000 times of vibration. In this study, the criteria are

that the residual clamping force is 80% of the initial clamping force after 1500 times of vibration [86].

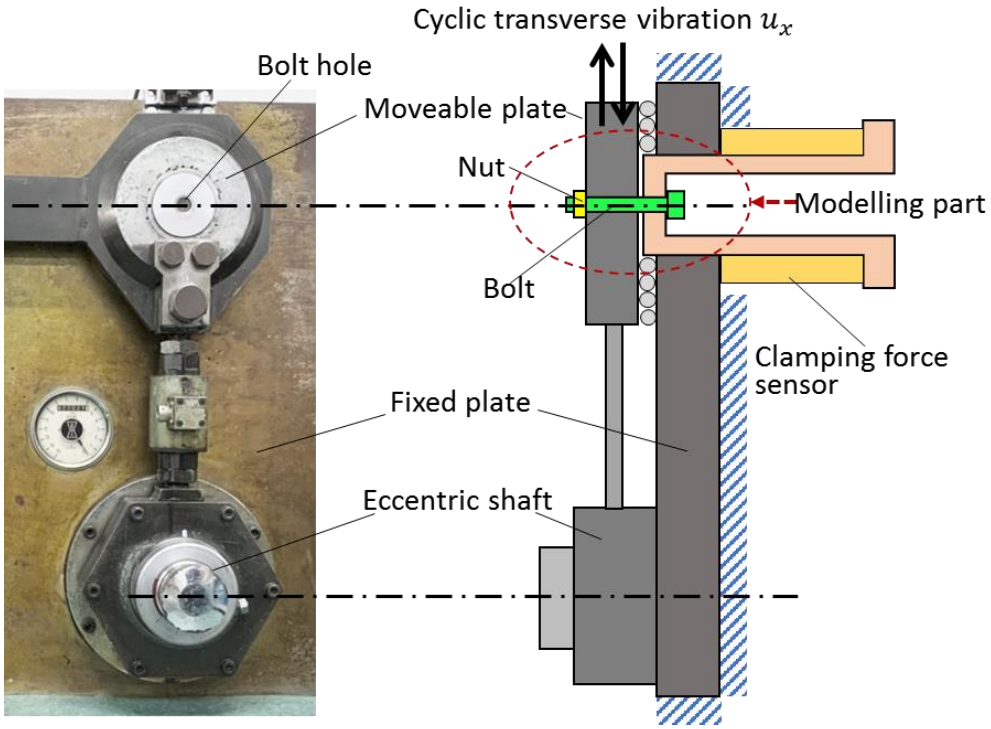

(a) Photo of Junker's device. (b) Schematic illustration.

Fig. 2.9 Junker type nut loosening experimental device based on DIN series (DIN 65151).

Table 2.2 Testing conditions

Displacement amplitude (mm)	Frequency (Hz)	Initial clamping force (kN)	Number of cycle (n)
±1	8	15	1500

2.3.2 experimental results

Fig. 2.10 shows the relationship between the transverse vibration cycles n and the clamping force F obtained by Junker's type loosening test when the initial clamping force is 15kN, and the sample points are obtained 3 times in one loading cycle. Since the data at the beginning of the experiment was irregular regardless of the magnitude of the pitch difference, the experimental results are considered without considering the data of the vibration cycle $n < 10$ in which this irregular tendency is remarkable.

From Fig. 2.10(a), it was clarified that the descent rate of clamping force F decreases with the pitch difference α increases. The criteria for this loosening resistance meet the DIN standard when the pitch difference α = 40 and 50μm. When the pitch difference $\alpha = 35\mu m$, the residual clamping force did not meet the standard. However, the residual clamping force $F = 4.0\text{kN}$ (27%) is maintained when the vibration number

reaches to $n = 1500$, and the loosening resistance remains steady as shown in Fig. 2.10(a). The mechanism of this anti-loosening effect will be explained in section 2.5.

As shown in Fig. 2.10(b), when the pitch difference is small, i.e., $\alpha = 0$ and $\alpha = 35\mu m$, the clamping force F shows an even decreasing waveform with the vibration cycle increases at the initial vibration stage $n = 0\sim50$. On the other hand, when the pitch difference is large, i.e., $\alpha = 40\mu m$ and $\alpha = 50\mu m$, the waveform is not regular. Therefore, in order to show the behavior of the waveform in detail, the relation between the clamping force F and the vibration cycles n ($F - n$ relations) when $n = 10\sim15$ and $n = 45\sim50$ are shown in Fig. 2.10(c1) and Fig. 2.10(c2), respectively. Since the waveforms in Fig. 2.10(c1) and (c2) are close to each other, it can be regarded that the loosening progresses steadily when the vibration number n is over 10. From Fig. 2.10(c2), it can be seen that, during 5 cycles of vibration, $F - n$ relation fluctuates within 2 times when $\alpha = 40\mu m$ and $\alpha = 50\mu m$, and fluctuates 4 times when $\alpha = 0$ and $\alpha = 35\mu m$. Therefore, it was confirmed that the clamping force decreases almost every cycle at the initial vibration stage when $\alpha = 0$ and $\alpha = 35\mu m$.

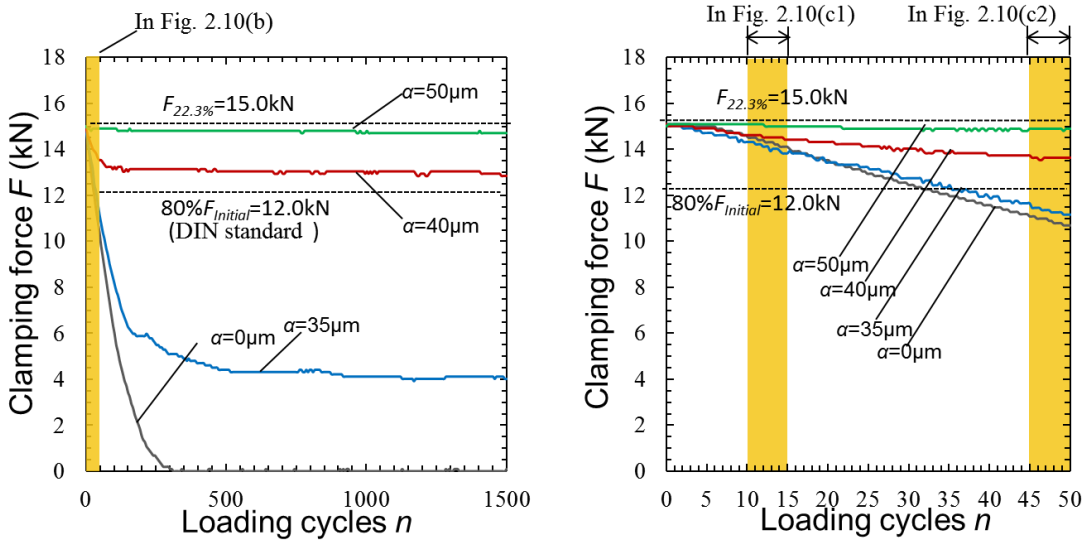

(a) 0~1500cycles (b) 0~50cycles

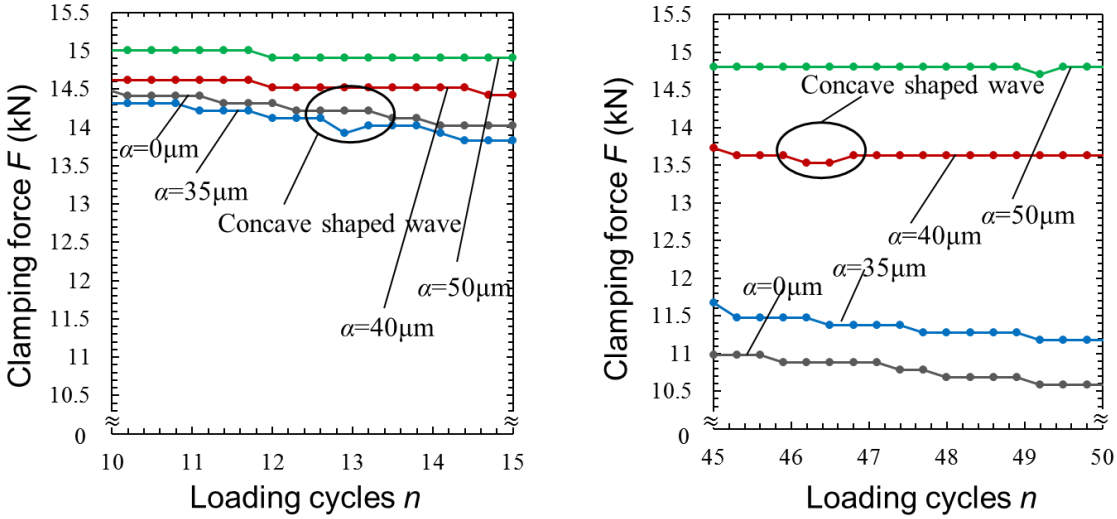

(c1) 10~15cycles (c2) 45~50cycles

Fig. 2.10 Clamping force F vs loading cycles n.

2.4 Analysis of loosening process due to transverse loading

2.4.1 Analytical method

The effect of the pitch difference on loosening is also simulated by finite element analysis. The fastening part of the bolt nut connection, shown in Fig. 2.9(b), is simplified as the three-dimensional model shown in Fig. 2.11. As shown in Fig. 2.11(a), in order to simplify the physical shape, the hexagonal part of the bolt head and nut was replaced with a cylindrical shape. The length, width, and thickness of the movable plate used in the FE model is 40mm, 40mm, and 15mm, respectively. 8 node elements are used for meshing, and the minimum mesh size of the threaded part is 0.048mm. The total number of elements is about 8.0E+4, and the number of nodes is about 1.51E+5. The penalty method was used for the contact analysis, and the non-linearity of the material was taken into consideration. To save the simulation time, the stress-strain relations of the materials are simplified in bilinear. The thread coefficient factor $\mu_s = 0.12$ and the under-head coefficient factor $\mu_w = 0.17$ are used in the simulation [81]. The finite element method analysis software ANSYS Workbench 16.2 is used for the analysis. The analysis can be divided into two parts, the tightening process shown in Fig. 2.11(b) and the loosening process shown in Fig. 2.11(c).

In the tightening process, the nut is tightened until the clamping force reaches 15kN, which corresponds to 22.3% of the bolt strength. During the tightening process, the under-head side of the bolt head and the surface opposite to the bearing surface of the clamped body are fixed. Here, for bolt nut connections with a pitch difference, in order to save the simulation time, the distance between the clamped body and the nut is set as 0.05mm at the very beginning of the analysis. For normal bolt nut connections

without a pitch difference, the analysis starts from the state the nut contacts the moveable plate.

In the loosening process, after the clamping force reaches to 15kN (Fig. 2.11(b)), Changing the boundary as shown in Fig. 2.11(c). The surface opposite to the bearing surface of the clamped body (moveable plate) is set as frictional in the transverse direction of the bolt, and the moveable plate vibrates in the transverse direction cyclically. This amplitude is given as a periodic displacement in the x direction in Fig. 2.11(c) by the movable plate. The same as the experimental condition, the amplitude is set as ± 1 mm. The analysis is performed until the vibration cycle n reaches to 50.

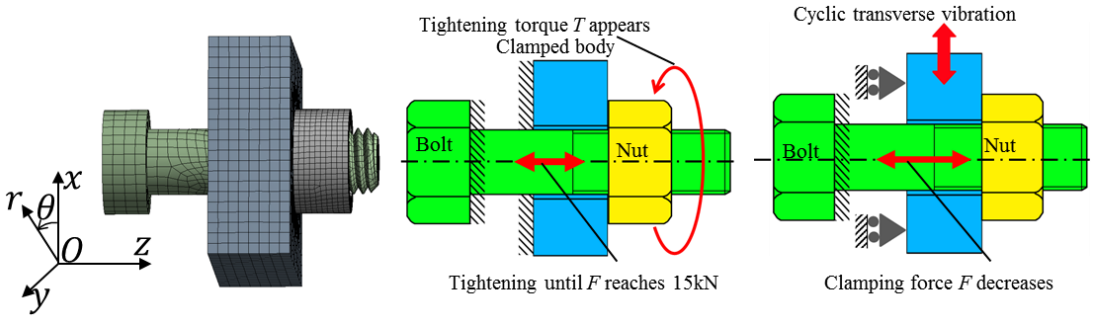

(a) FEM model

(b) Boundary conditions of tightening process.

(c) Boundary conditions of loosening process due to transverse loading.

Fig. 2.11 FEM model and boundary conditions for tightening process and loosening process.

2.4.2 Comparison of FEA results and experimental results of loosening process

Fig. 2.12 shows the analytical results of the relationship between the tightening torque T and the clamping force during the tightening process. From Fig. 2.12, it can be seen that the prevailing torque increases with the increasing of pitch difference. Besides, for pitch difference $\alpha = 35\mu m$, the relation between tightening torque and clamping force is close to a bilinear line, and the slope ratio before the clamping force reaches 8kN is much larger than that of the clamping force is larger than 8kN. For pitch difference $\alpha = 40\mu m$ and $\alpha = 50\mu m$, the relations are linear.

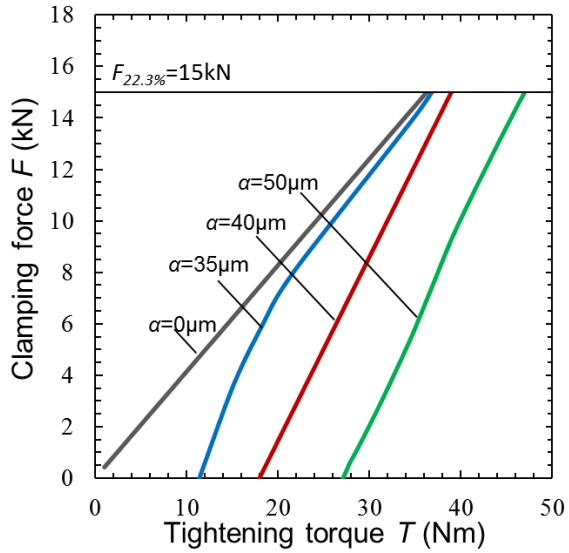

Fig. 2.12 Relation between clamping force F and tightening torque T.

Fig. 2.13 shows the analytical results of the relationship between the clamping force F and the vibration cycle n in the loosening process until the vibration cycle number reaches to 50. Comparing the analysis results (Fig. 2.13) and the experimental results (Fig. 2.10), the tendency of loosening speed, that is, the magnitude relationship of d_F/d_n is consistent, i.e., $\alpha = 0 < \alpha = 35\mu m < \alpha = 40\mu m < \alpha = 50\mu m$. In the analytical results shown in Fig. 2.13(c), the clamping force F fluctuates immediately after the movable plate reaches maximum displacement. The clamping force decreases slightly after the vibration when the pitch difference is over $40\mu m$, and remains steady when the pitch difference is no larger than $35\mu m$. In the experimental results shown in Fig. 2.10(c2), there are flat parts and stepped parts, and the clamping force decreases at the stepped part. Regarding the difference between the waveforms of the analytical and experimental results, such as the transmission loss of vibration by the experimental equipment, the difference in the number of data samplings can be considered. In the experiment, data were acquired 3 times per cycle, whereas, in the analysis, data were acquired 20 times per cycle.

Focusing on the waveforms in Fig. 2.13(c) and (d), $\alpha = 35\mu m$ and $\alpha = 40\mu m$ have the same shape, and when $\alpha = 0$, the fastening force $F \approx 0$, so the waveforms are different. In Fig. 2.13(c) and 10 (d), the fastening force F increases (or decreases) immediately after the moveable plate reaches the maximum value. Using the Gaussian symbol $[n]$ (the integer part of the vibration cycle n that is a real number), the position of the maximum displacement and the position where the fastening force F increases (or decreases) are expressed as follows, and it is independent of vibration number n. Position where maximum displacement is $n - [n]$ = 0.25,0.75. Position where the fastening force F increases (or decreases): $n - [n]$ = 0.25 to 0.35, 0.75 to 0.85.

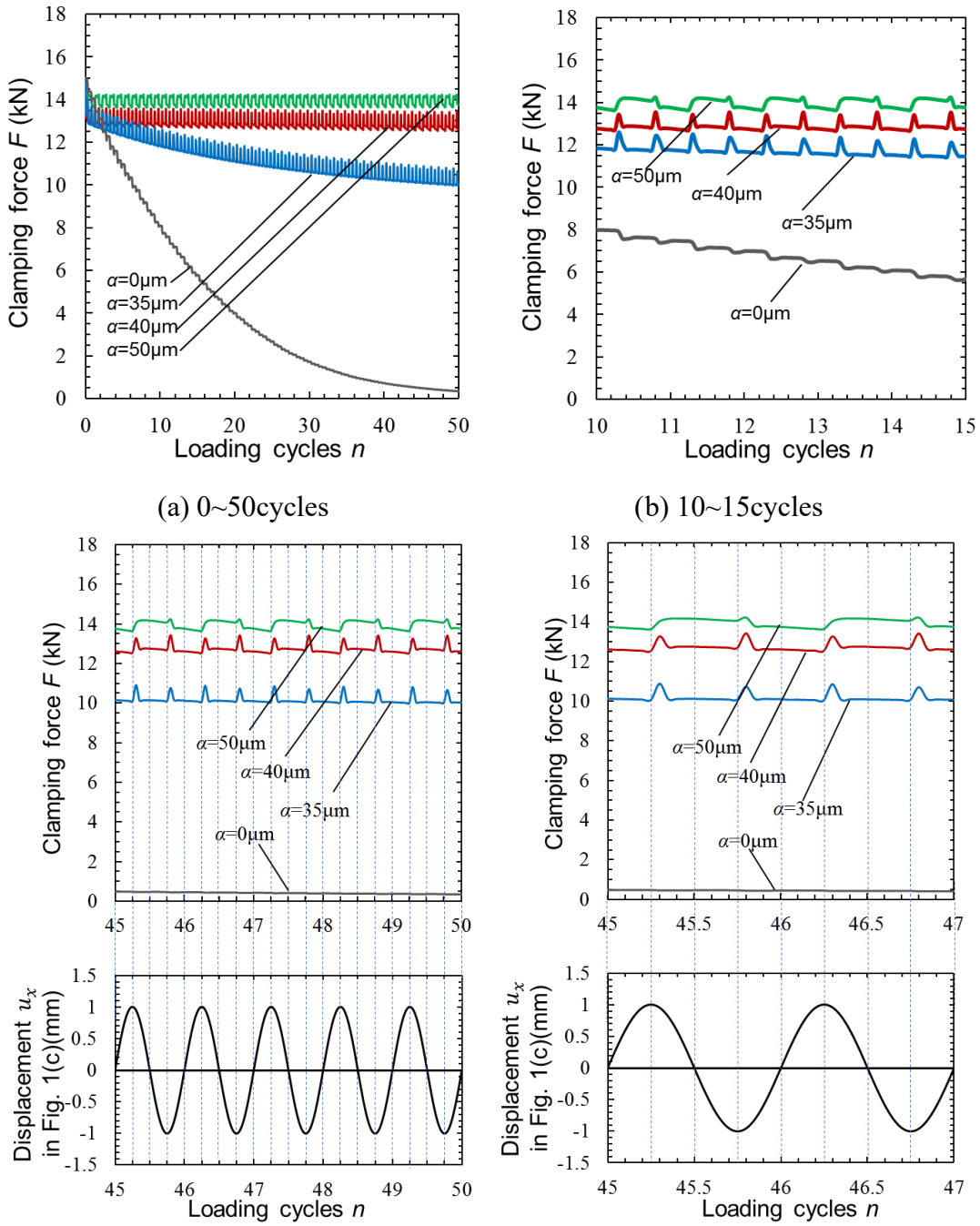

(a) 0~50cycles (b) 10~15cycles

(c) 45~50 cycles (d) 45~47 cycles

Fig. 2.13 Relation between clamping force F and transverse vibration cycles n.

Fig. 2.14 shows the contact state between the bolt and nut thread surfaces during the tightening process. The reason the clamping force fluctuates when the displacement of the moveable plate reaches maximum value is the difference in the direction of the frictional force caused by the pitch difference α. As shown in Fig. 2.14, when the movable plate vibrates, the nut also vibrates in the same direction due to the friction between the movable plate and the nut bearing surface. The transverse displacement of the moveable plate and the nut are shown in Fig. 2.15. From the figure, it can be seen

that from the position the displacement reaches to the maximum value to a point before the nut returns to the central axis of the bolt, the nut moves in the transverse direction with the moveable plate. Comparing Fig. 2.13 and Fig. 2.15, it can be found that the clamping force fluctuates when the nut moves together with the moveable plate.

As shown in Fig. 2.14(b), when the pitch difference $\alpha \geq 35\mu m$, both outer sides of the nut thread surface contact with the bolt thread, and an axial force $F_\alpha > 0$ exists in the bolt sandwiched by the nut thread (see Fig. 2.16, [79]). It should be noticed that the F_α is referred as the bolt axial force due to the nut both ends contact. Due to this axial force F_α, frictional force is generated at both ends of the nut, and the direction of the frictional force in the circumferential direction of both ends is different. When the movable plate is vibrated in the x-direction, the bolt and nut are twisted and released due to the difference in the direction of the frictional force acting on both ends of the nut. The axial force acting on the nut changes. The reason why the fastening force F decreases or increases immediately after the moveable plate reaches maximum displacement is due to this change in the axial force. On the other hand, from Fig. 2.14(a), when $\alpha = 0$, only the screw surface on the opposite side of the nut bearing surface is always in contact with the screw surface of the bolt. Therefore, when the movable plate vibrates, the nut also vibrates in the same direction, so the axial force between the screw surfaces becomes small and the nut loosens.

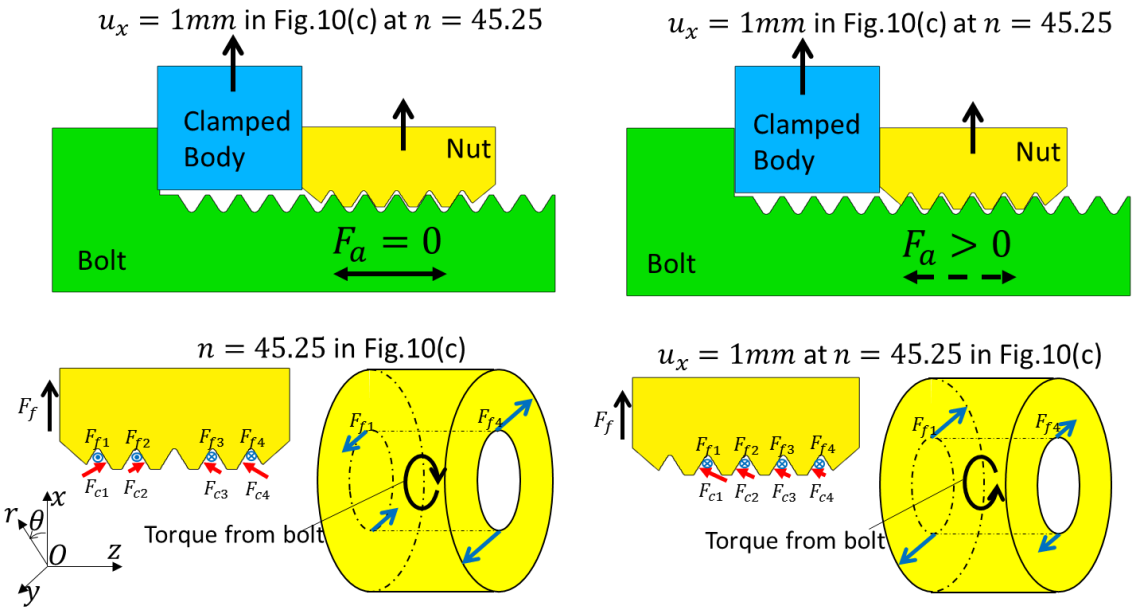

(a) $a \geq 40\mu m$ (b) $a = 0$

Fig. 2.14 Contact status in Fig. 2.4.

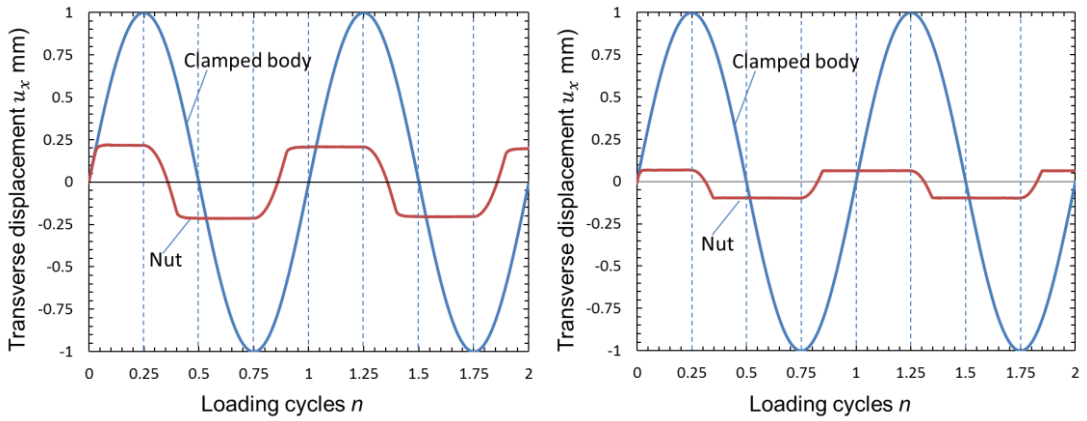

(a) $\alpha = 0$ (b) $\alpha = 40\mu m$

Fig. 2.15 Displacement of nut due to the vibration of moveable plate

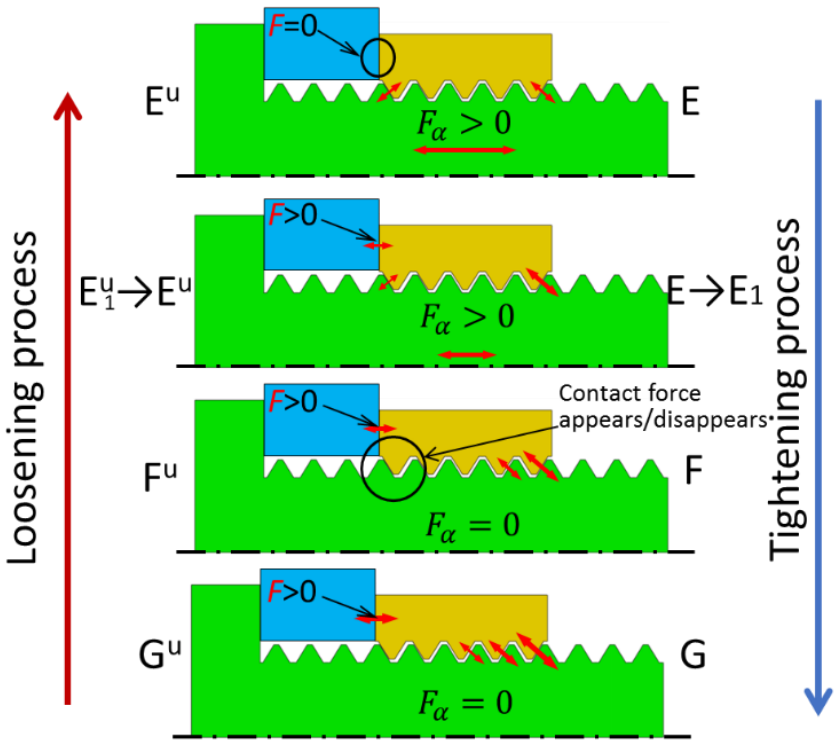

Fig. 2.16 Contact status in tightening and untightening process of nut.

2.5 Consideration of loosening process of nut with pitch difference

2.5.1 F-T relation during the loosening process of nuts with a pitch difference(Stage Ⅰ ~StageⅢ)

Fig. 2.17(a) and Fig. 2.18(a) show the relation between clamping force and vibration cycles for a nut with a pitch difference $\alpha = 35\mu m$ and $\alpha = 40\mu m$, respectively. In Fig. 2.17(a) and Fig. 2.18(a), there are a stage A in which the clamping force F decreases monotonically, and a stage B in which the decrease in the clamping force F becomes small and F becomes almost constant. To explain this, the relationship between the clamping force F and the tightening torque T ($F-T$ relationship, see Fig. 2.17(b) and Fig. 2.18(b)) in the loosening process of the previous study (Noda et al., 2020) is used. In the $F-T$ relationship shown in Fig. 2.17(b) and Fig. 2.18(b), the process of nut loosening can be classified into stage I, stage II, and stage III shown below. The phenomenon different from that of common bolts is typical when the pitch difference is $\alpha = 35\mu m$. Stage II does not appear when the pitch difference α is over $40\mu m$.

Stage I: The process in which the nut is almost integrally with the bolt and the initial twist energy of the bolt is released (between point G and point Gu in Fig. 2.17(b)). The contact point of the screw surface and the $F-T$ relationship are the same as $\alpha = 0$. In addition, there is almost no decrease in the clamping force F. (In the Junker loosening test described later, the initial twist of the bolt is not released, and there is a stage where the nut and bolt are almost integrated with each other, so this is referred to as I^{*}).

Stage II: The process from when the nut starts to slide with respect to the bolt thread surface to the state when both ends of the nut begin to contact with the bolt thread (between point Gu and point Fu in Fig. 2.16). Stage II exists when the pitch difference $\alpha = 35\mu m$, shown in Fig. 2.17(b), but does not exist at $\alpha = 40\mu m$, shown in Fig. 2.18(b). In stage II ($\alpha = 35\mu m$), the contact state of the nut thread surface with the bolt is between points Gu and Fu. Only one side of the nut contact with the bolt thread, as shown in Fig. 2.16, and the contact status is close to that of a normal nut $\alpha = 0$. Therefore, in stage II, the $F-T$ relationship is the same as that of common nut, as shown in Fig. 2.17(b). Stage II does not exist when pitch difference is $\alpha = 40\mu m$, as shown in Fig. 18(b). The reason is that since the pitch difference α is large, when the clamping force reaches to 15kN, the two ends of the nut still contact with the bolt thread. This can also be explained by the $F-T$ relation in Fig. 2.12. When the $F-T$ relation in Fig. 2.12 becomes bilinear, it means that the clamping is big enough to make the bearing surface side of the nut thread separates from the bolt thread. Thus, there is no stage Gu and Fu in Fig. 2.16. Therefore, the $F-T$ relationship of $\alpha = 40\mu m$ at the beginning of loosening is different from that of $\alpha = 35\mu m$ as shown in Fig. 2.18(b). (In the Junker loosening test described later, there are $\mathrm{II_F}$ when the nut loosens and $\mathrm{II_B}$ when the nut tightens).

Stage III: The process in which the bearing surface end of the nut thread starts to contact the bolt thread, and the contact force on this side nut increases. The axial force between threads $F_a > 0$ in Fig. 2.16 also increases (point Fu in Fig. 2.16). The $F-T$ relationship between Eu) is different from $\alpha = 0$. Stage III is between the points Fu and Eu in Fig. 14, and since the contact state of the screw surface is different from the normal nut α = 0, the $F-T$ relationship is also different as shown in Fig. 2.17(b), and the fastening force F is unlikely to decrease. From this, it can be expected that the nut with pitch difference has loosening resistance even if the axial force after 1500 times is less than 80% at $\alpha = 35\mu m$. On the other hand, when $\alpha = 40\mu m$, loosening resistance can be expected from the initial stage of loosening.

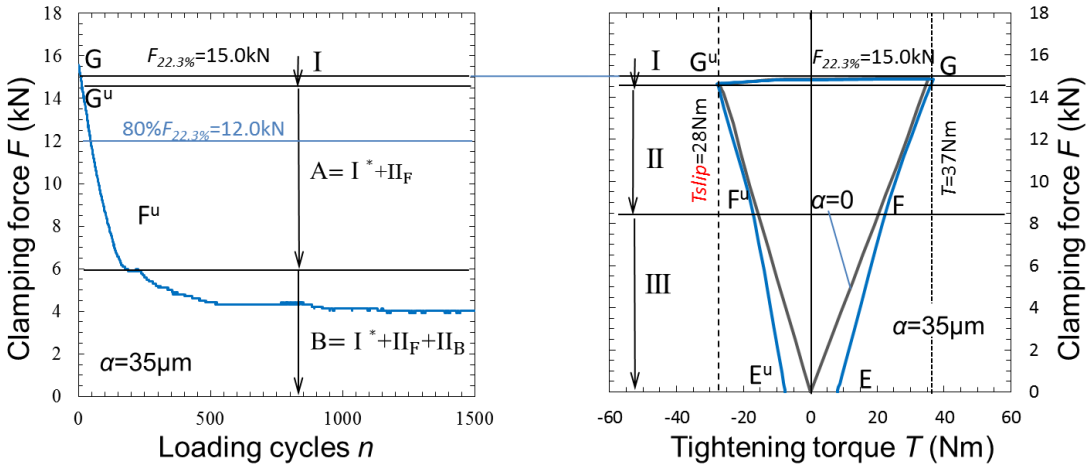

(a) Clamping force F vs loading cycles n of $\alpha = 35\mu m$. (b) Clamping force F vs tightening torque T of $\alpha = 35\mu m$.

Fig. 2.17 Clamping force F vs loading cycles n relation explained by $F-T$ relation of $\alpha = 35\mu m$.

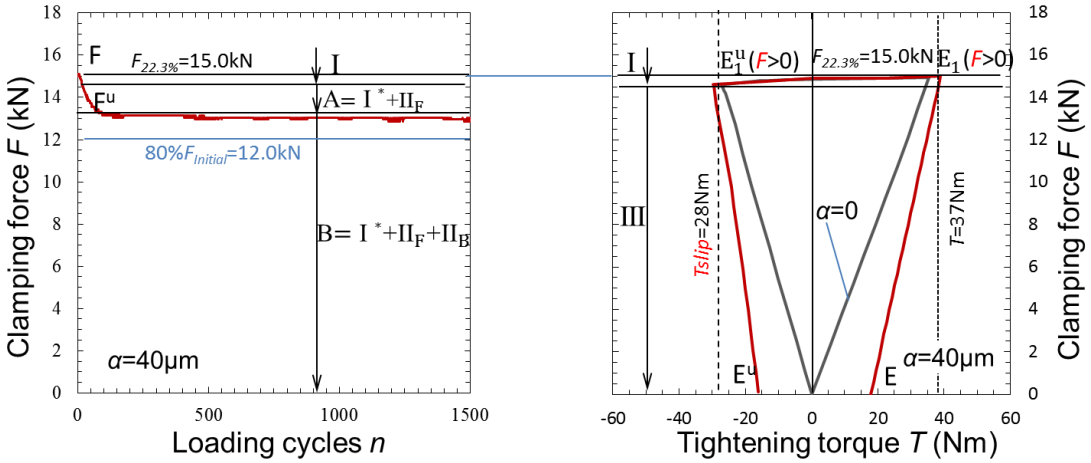

(a) Clamping force F vs loading cycles n of $\alpha = 40\mu m$. (b) Clamping force F vs tightening torque T of $\alpha = 40\mu m$.

Fig. 2.18 Clamping force F vs loading cycles n relation explained by $F-T$ relation of $\alpha = 40\mu m$.

2.5.2 Loosening process in the Junker's type loosening test (Stage A~ Stage B)

Fig. 2.19 shows the relationship between the nut loosening angle θ_L and the number of repetitions in the loosening test, and it can be used to explain stage I and stage A and stage B in Fig. 2.17(a) and Fig. 2.18(a). In these figures, the slack angle θ_L on the vertical axis is the relative twist angle θ_L of the nut defined by the difference $\theta_L = \theta_N - \theta_B$ between the twist angle θ_N of the nut and the twist angle θ_B of the bolt. Figure 15 (a) shows the results of α = 0, 35, and 40 μm at the initial clamping force $F = 15$kN. Fig. 2.19(b) shows the result of analysis with the initial clamping force set to $F = 6$kN in order to reproduce the number of repetitions n = 0 to 2 (see Fig. 2.17(a)) at which stage II starts in the experiment at α = 35μm. In Fig. 2.19(a), the loosening angle θ_L increases sharply when the transverse vibration number n = 0 to 0.07. This is the same as stage I described in previous section, the twist elastic energy of the bolt stored in the tightening process is released in this stage. Next, when the vibration number n = 0.05 ~ 2, α = 0μm and α = 35μm can be regarded as stage A because the loosening angle θ_L increases steps by steps. That is, the section that increases on the stairs is the $F - T$ related stage II, and the other sections with a constant clamping force F are the $F - T$ related stage I. On the other hand, $\alpha = 40$μm in Fig. 2.19(a) has stage A with the vibration number n = 0 to 0.05, but it is mainly stage B in other sections. In this stage B, the loosening angle θ_L is almost constant. Although the loosening angle is increasing and decreasing alternately, the loosening angle fluctuates in a very small range compared to that of $\alpha = 0$μm and $\alpha = 35$μm. This stage B is clearly shown in Fig. 2.17(b) which shows the relation between vibration cycles and loosening angles of α = 35μm when the tightening force is $F = 6$kN.

In Fig. 2.19(b), the specimen of α = 35μm is in stage B, and it can be seen that stage II and stage I are repeated alternately. In particular, unlike stage A, stage II in stage B includes stage II_F in which θ_L increases and loosening progresses, and stage II_B in which θL decreases and tightening occur. Therefore, since α = 0μm and α = 35μm in Fig. 2.19(a) are stage A, the nut is loose because it is stage B, but $\alpha = 40$μm in Fig. 2.19(a) and α = 35μm in Fig. 2.19(b). In stage B, loosening does not happen. On the other hand, in Fig. 2.19(b), when the initial clamping force is 6 kN for α = 35μm, the loosening rate is less than 1/30 compared to the first several vibration cycles, so it can be regarded that a quite good loosening resistance of the nut is remaining.

From this, the loosening process in the loosening test can be expressed by the following stages A and B.

Stage A: This is a section where stage I and stage II occur alternately, and in stage II, loosening always progresses.

Stage B: This is a section where stage I and stage II occur alternately. In stage II, loosening and tightening occur alternately.

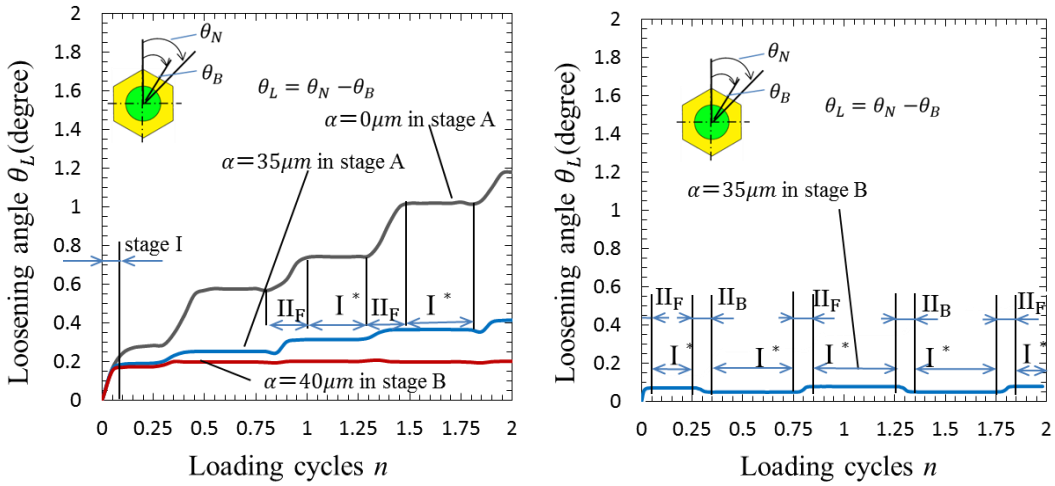

(a)when $F = 15$kN (b) when $F = 6$kN

Fig. 2.19 Loosening angles θ vs loading cycles.

Typically, the change from stage A to stage B can be explained from the simulation of the loosening process of $\alpha = 35\mu m$. Fig. 2.20 shows the relation between the vibration cycles and the clamping force obtained by FEM and experiments of Junker's type loosening test when the pitch difference is $\alpha = 35\mu m$. The trend of the change of clamping force with the change of loading cycles coincides with each other. The FEM result shows a significant tendency of the change of clamping force with loading cycles. That is, with the increasing of loading cycle, the decreasing rate of clamping force becomes smaller and smaller.

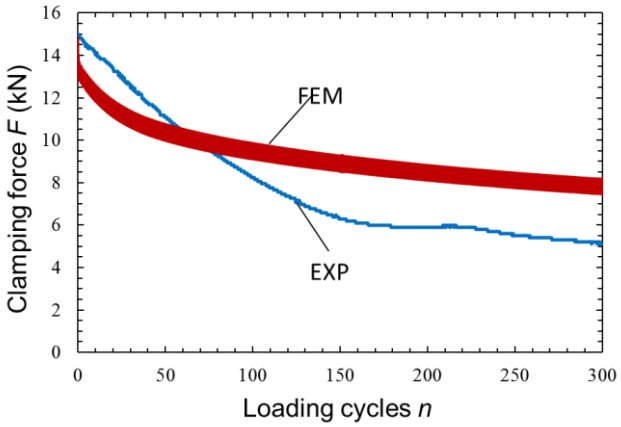

Fig. 2.20 Relation between the vibration cycles and the clamping force obtained by FEM and experiments when the pitch difference α is 35μm.

Fig. 2.21 relation between the vibration cycles and the loosening angle, the rotation angle of the bolt, and the rotation angle of the bolt obtained by FEM when the pitch difference α is 35μm. Fig. 2.22 and Fig. 2.23 show some detail of Fig. 2.21. From Fig. 2.21 and Fig. 2.23, it can be seen that the rotation angle of the bolt remains steady after a relatively large rotation at the very beginning of the vibration. Therefore, Except for the initial stage of vibration of the moveable plate, the rotation angle of the nut can

be used to represent the loosening of the nut.

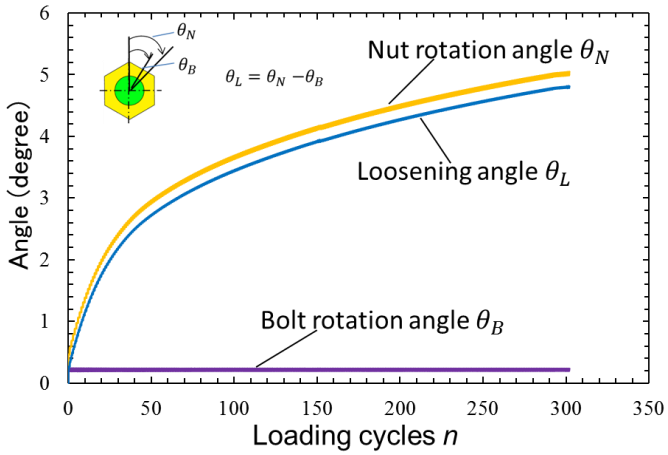

Fig. 2.21 Relation between the vibration cycles and the loosening angle, the rotation angle of the bolt and the rotation angle of the bolt obtained by FEM when the pitch difference α is 35μm.

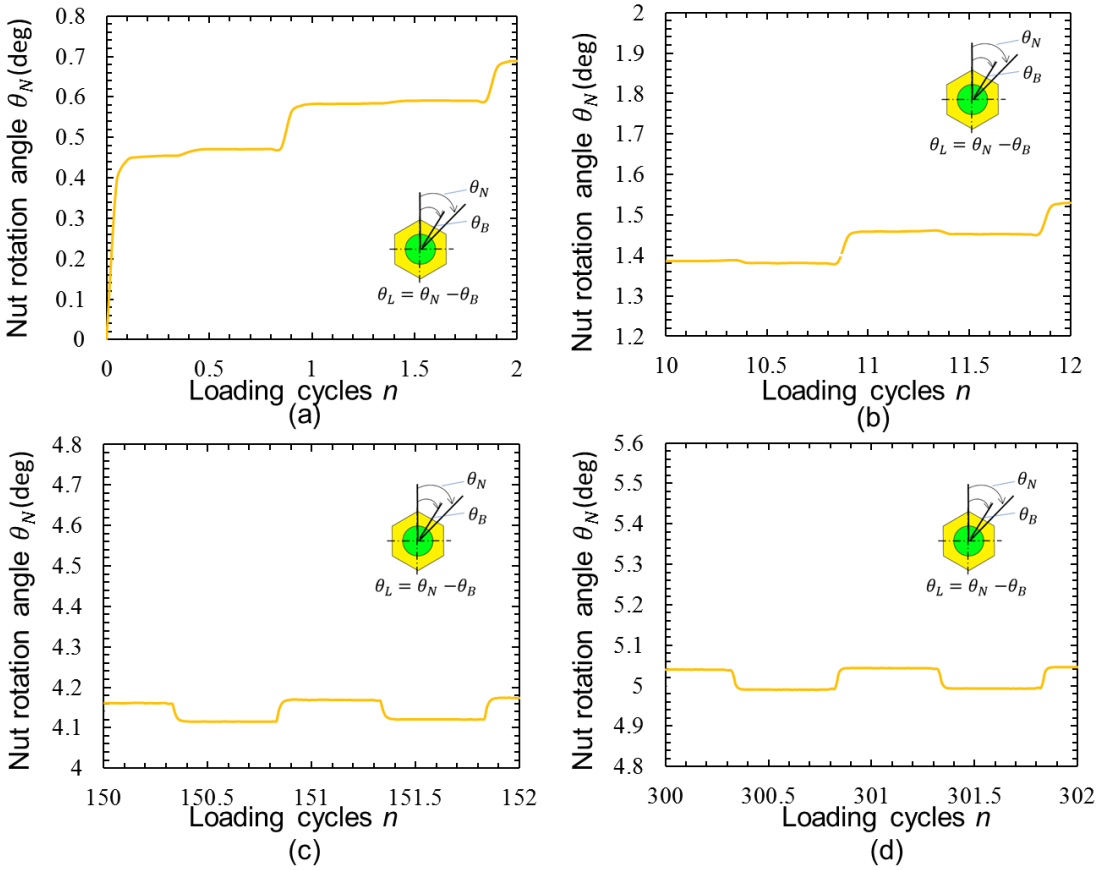

Fig. 2.22 Some details of nut rotation angle shown in Fig. 2.21

From Fig. 2.22, it can be seen that, in the first several cycles, the loosening process and unloosening process occur alternately. Then, a tightening process occurs in every cycle, and the tightening angle is much smaller compared with the loosening angle in

one loading cycle. Thus, loosening progresses in every cycle. When the loading cycle reaches 150, the loosening angle and tightening angle in one cycle almost equals to each other. By comparing Fig. 2.20 and Fig. 2.22, it can be seen the smaller the absolute loosening angle in one cycle is, the slower the decreasing rate of the clamping force is.

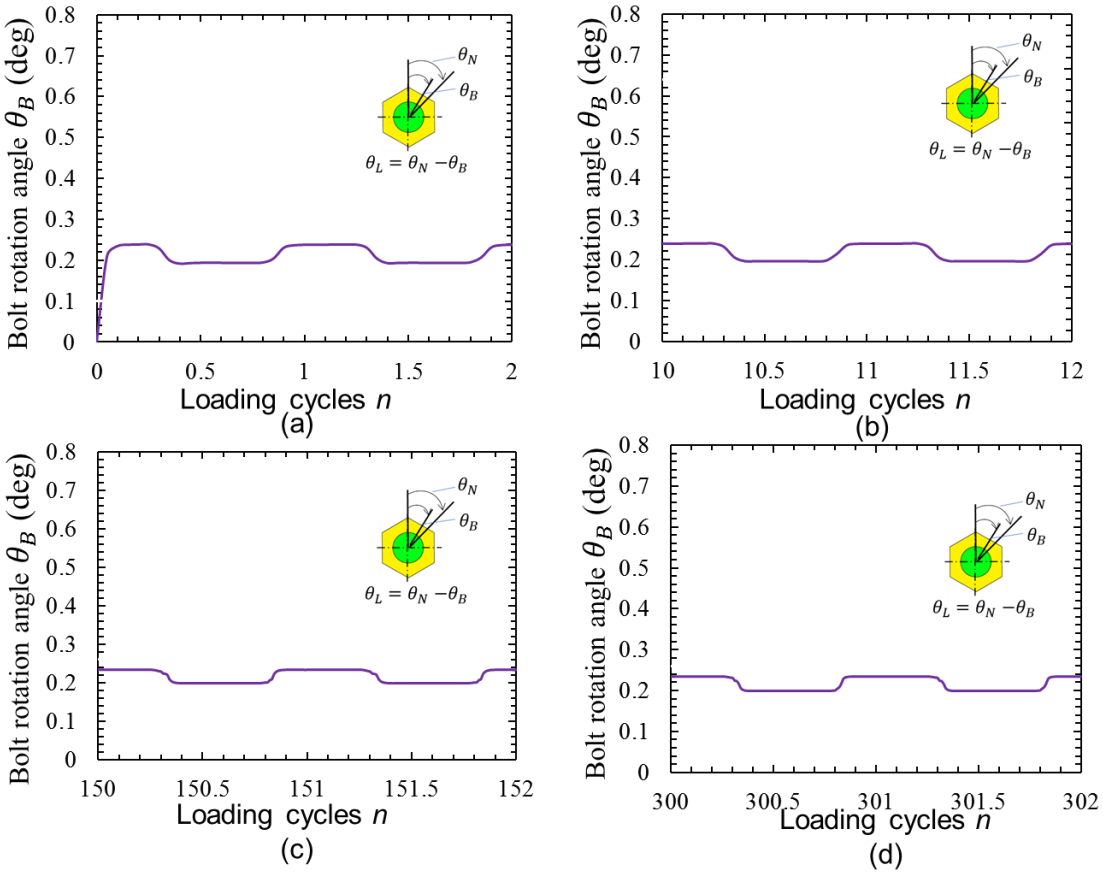

Fig. 2.23 Some details of bolt rotation angle shown in Fig. 2.21

2.6 Conclusions

In this chapter, we considered the loosening process of pitch difference nuts. The Junker vibration test was used for the loosening test, and a simplified 3-dimensional model was built for the loosening simulation analysis. The loosening resistance performance and loosening resistance mechanism were considered with reference to the relationship between the clamping force F and the torque T, which has been studied in our team's previous research [81,84]. The conclusions obtained are summarized below.

(1) According to the looseness resistance judgment standard based on DIN25201, for which the residual axial force should at least be 80% of the initial axial force after 1500 cycles of vibration, the nut with a pitch difference of $\alpha = 40, 50\mu m$ has a good anti-loosening performance. Although the pitch difference of $\alpha = 35\mu m$ does not meet the criteria, the residual clamping force F_u=4kN, which is about 27% of initial axial force,

is maintained when the vibration cycles reach to 1500, and the loosening resistance is substantially maintained.

(2) Regarding the relationship between axial force F and torque T, which is one of the basic characteristics of bolt nut connections, when the nut with pitch difference $\alpha = 35\mu m$, the loosening process can be divided into the following three different stages. Stage I: the stage where the nut and bolt are integrated. Stage II: From the state the nut starts to slide against the bolt thread surface to the state both ends of the nut start to contact the bolt thread. Stage III: from the stage where two ends of the nut contact the bolt thread and the contact force at bearing surface side of the thread increases to the state the nut is separate from the clamped body.

(3) According to the relationship between the relative twist angle θ_L of the nut and the number of vibration cycles n. The loosening process by the Junker test can be classified into stage A and stage B. In these processes A and B, stages I and II related to $F-T$ exist alternately. In stage A, only the stage II nut loosening process $\mathrm{II_F}$ exists, but in stage B, the stage II tightening process $\mathrm{II_B}$ exists, which is different from stage A.

(4) In stage B, the loosening angle of the nut in one loading cycle remains steady, while the tightening angle in one loading cycle becomes increases with the increasing of the loading cycle. Thus, the loosening rate of the nut becomes smaller and smaller until the loosening angle equals to the tightening angle in one loading cycle, the clamping force remains steady.

Chapter 3. Root radius effect on fatigue strength and anti-loosening performance of pitch difference bolt nut connections

3.1 Introduction

Bolt nut connections are one of the essential mechanical elements used in various industrial fields; for instance, about 2000 bolt nut connections are needed in one vehicle [87]. When subject to dynamic and impact loading with vibrations, self-loosening and fatigue failure of bolt nut connections may happen and even causes serious accidents. Several kinds of bolt failure under complex working environments are discussed in recent studies [88–92]. Therefore, low-cost bolt nut connections with excellent anti-loosening performance and high fatigue strength, long fatigue life are always needed in the industry.

The bolt fatigue failure sometimes happened without the nut loosening. This is because the large stress concentration always appears at the bolt thread root. Since it is difficult to reduce the stress concentration, few pieces of research are available for improving the fatigue strength compared to anti-loosening. Table 3.1 shows a comparison of some special bolt nut connections. Most special bolt-nuts have either more components or very special geometry, leading to a complex manufacturing process and a high cost, which is usually more than 3 times of the common bolt nut connections.

Usually, the anti-loosening ability affects the fatigue strength and the cost significantly. Most previous studies concern either anti-loosening or high fatigue life and few studies aimed at improving both anti-loosening and fatigue strength. In our team's previous research, it has been found that the fatigue life and the anti-loosening performance of bolt nut connections can be improved by introducing a suitable pitch difference between the bolt and the nut [76,80]. The sketch of pitch difference effect on fatigue life and anti-loosening performance is shown in Fig. 1.14 Gregor et al. investigated the effect of cyclic loading on the mechanical behavior of three kinds of materials, from these experiments, it can be found that by enlarging the root radius, both of fatigue limits and fatigue strength of the materials can be improved [13,14]. Thus, better combination of fatigue life improvement and anti-loosening performance may be obtained by increasing the root radius of pitch difference bolt nut connections.

This chapter will focus on the coupled effect of the root radius ρ and the pitch difference α on the fatigue strength in bolt nut connections. Based on the authors' previous researches, three kinds of root radii α for M16 bolt nut connections are chosen. Furthermore, at the same time, enlarging the thread root radius ρ to reduce the

concentration aiming at improving the fatigue life and fatigue limit. The fatigue strength improvement will be discussed from the S-N curve and fatigue limit diagram based on the experiments and FEM analysis. The anti-loosening effect will be confirmed since the coupled effect of the thread root radius ρ and the pitch difference α may affect the anti-loosening as well as the fatigue strength.

Table 3.1 Comparison of some special bolt–nut connections.

Method	Anti-loosening performance improvement	Fatigue limit improvement	Fatigue life improvement	Machinability	Low cost
This study	◎	◎	○	◎	◎
Pitch difference Nut (Chen et al., 2015; Noda et al., 2016)	◎	△	○	◎	◎
SPR (Noda et al., 2008)	○	△	△	×	×
Hard Lock Nut (Wakabayashi, 2002)	◎	△	△	×	×
CD Bolt (Nishida et al., 1997)	△	○	○	△	△
Low strength nut (SNCM630→S20C) (Nishida,2004)	○	○	○	◎	◎
Double Structure Bolt (DTB-II) (Shinbutsu et al., 2017)	◎	△	△	×	×
Standard bolt-nut	△	○	○	◎	◎

×:bad, △:fair, ○:pretty, ◎:remarkable.

3.2 Fatigue strength improvement

3.2.1 Fatigue test specimen

This study focuses on high strength Japanese Industrial Standards (JIS) M16 bolt nut connections. Three kinds of new bolt shapes whose root radii are larger than that of JIS M16 bolt are prepared, aiming at improving both the fatigue life and fatigue limit. Japanese Industrial Standards (JIS) specifies the standards used for industrial activities in Japan and ISO, JIS and DIN standards are based upon the metric system and are closely related. The screw thread specifications based on JIS also apply to ISO and DIN

threads. Although the nut height dimension H=16mm in Fig. 3.1 varies depending on the standard, when there is no pitch difference between the bolt and the nut, the effect of nut height on fatigue strength is negligible. Table 2 shows nut height and nut width according to different standards. This study focuses on the pitch difference nut when H=16mm is based on JIS M16. The effect of the nut height on the fatigue life and anti-loosening performance for the nut height under a small pitch difference will be discussed in the next chapter.

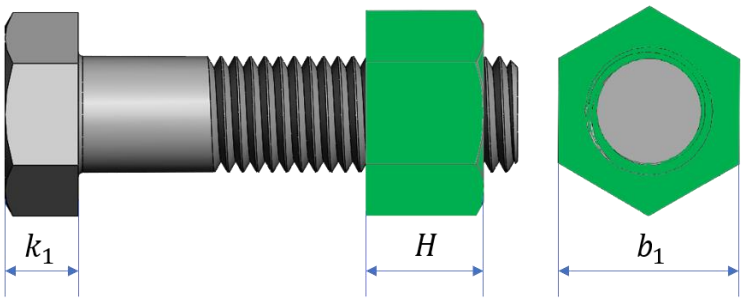

Fig. 3.1 Sketch of a bolt nut connection

Table 3.2 Nut height and nut width according to different standards

Nut		M12 (mm)	M16 (mm)
Width b1(mm)	DIN/JIS B1181	19	24
	JIS B1220	-	23.2-24
	ISO4032/AS1112-200 JIS B1199-2	17.73-18	23.67-24
	JIS B1186	-	26.2-27
Nut Height H(mm)	ISO4032/AS1112-200	10.37-10.8	14.1-14.8
	DIN555	9.25-10.8	12.1-13.9
	ISO4034 ISO type1	10.4-12.2	14.1-15.9
	DIN934	9.64-10.0	12.3-13.0
	ISO4032,ISO8673	10.37-10.8	14.1-14.8
	ISO4033 ISO type2	11.75-12.0	15.7-16.4
	JIS B1220	-	12.1-13.9
	JIS B1199-2	11.57-12.0	15.7-16.4
	JIS B1181 type2	10	13
	JIS B1181 1xd	12	16
	JIS B1186	-	15.65-16.35

The suggested nut in this study can be manufactured as the same way as the normal nut, and the cost is predicted to be about 1.5 times of the normal nut considering the modification of thread tap as well as the checking procedure on the pitch difference. Fig. 3.2(a) illustrates a bolted joint whose thread is numbered as -3, -2, ... 7, 8 from the

bolt head side to the other side. As shown in Fig. 3.2(b), since nut chamfers are commonly used, the threads are neglected at two ends, as shown in Fig. 3.2(a) in the simulation. Instead of the standard JIS M16 pitch p=2000μm, the nut pitch is α μm larger than that of the bolt pitch p=2000μm in this study. The length of the threaded part of the bolt is 44mm, and the length of the shank part of the bolt is 96mm. When $\alpha = 0$, the thread contact is shown in Fig. 3.2(c) where the largest stress appears at the root of $No.2$ thread. Instead, when $\alpha > 0$, the thread contact is shown in Fig. 3.2(d) where the largest stress appears at the root of $No.7$ thread [76]. In previous studies, Patters showed that the longer nut has the longer the fatigue [93]. Griza described that bolts with longer length tend to have high fatigue strength for bolt joints under the same tightening torque [11]. According to JIS B 1181 - 1993 Type 2, Grade A, Hexagon Nuts, the nut height is between 15.7mm and 16.4mm. To eliminate the effect of nut length, all the height of the nuts used in this study are 16mm. Fig. 3.3 illustrates the shape and dimension of the thread designed in the study. Instead of the standard root radius JIS M16 $\rho = \rho_0 = 0.29\,\mathrm{mm}$, the newly designed bolt specimens have a root radius $\rho = 2\rho_0$ and $\rho = 3\rho_0$. To evaluate the stress reduction conveniently, we consider the stress concentration factor K_t of a round bar having a circumferential 60° notch shown in Fig. 3.3(d) whose K_t formula is available [94,95]. The stress concentration factor K_t decreases from 4.53 to 2.90 by increasing the thread root radius from $\rho = \rho_0$ to $\rho = 2\rho_0$, and the stress concentration factor K_t is reduced to 2.4 when the bolt root radius becomes $\rho = 3\rho_0$.

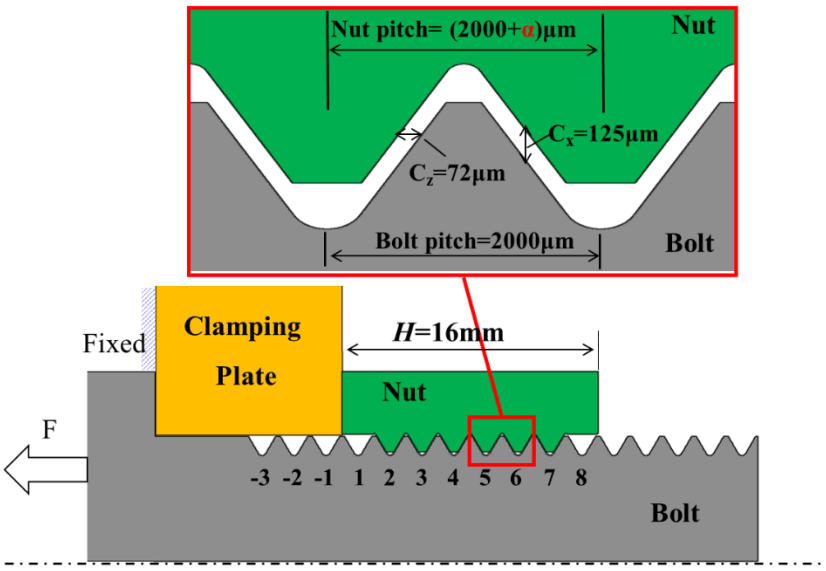

(a)

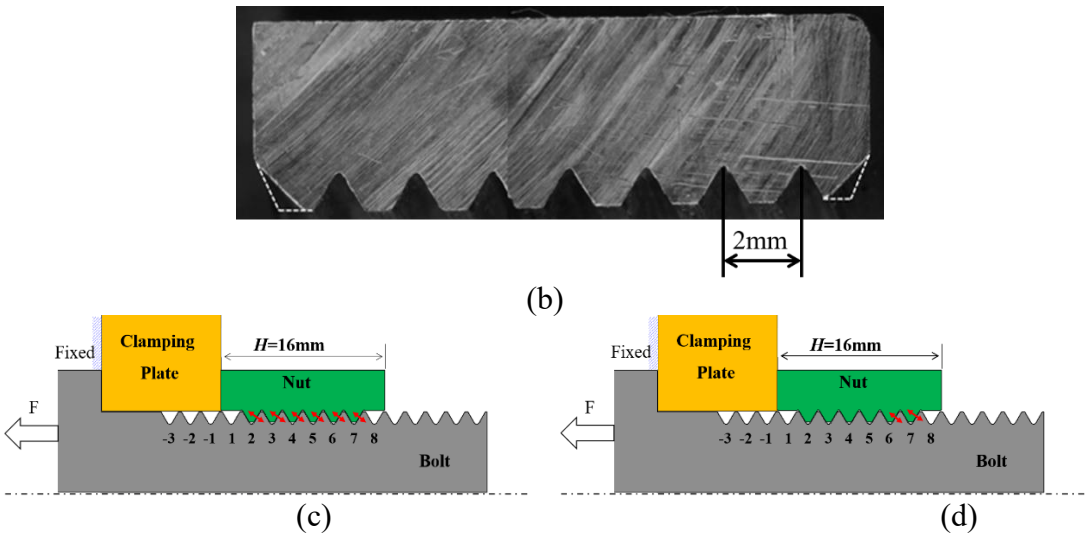

Fig. 3.2 Schematic illustration of (a) bolted joint, (b) nut chamfer at nut ends, (c) threads contact when $\alpha = 0$ and (d) thread contact when $\alpha > 0$.

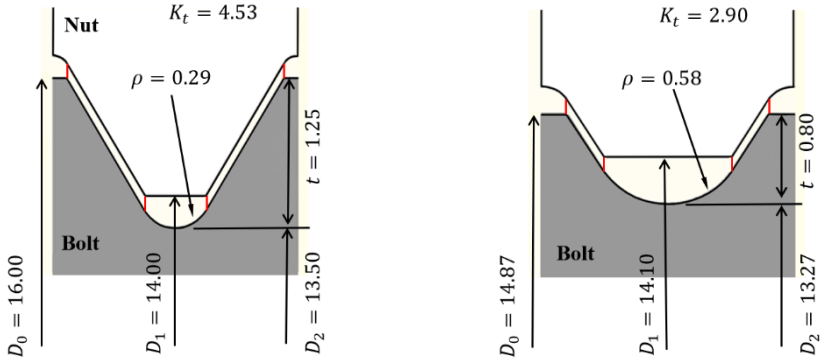

(a) ρ=ρ0 (K_t=4.53 in Fig. 3.3(d)) (b) ρ=2ρ0 (K_t=2.90 in Fig. 3.3(d))

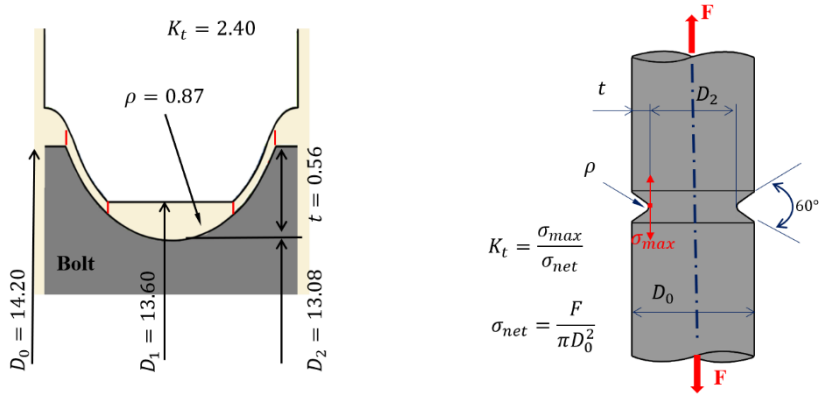

(c) ρ=3ρ0 (K_t=2.40 in Fig. 3.3(d)) (d) Notched bar

Fig. 3.3 Three types of bolt specimens with different thread shapes

3.2.2 experimental conditions

Fig. 3.4 illustrates the assembled state of a bolt nut connection in the fatigue experiment. As shown in Fig. 3.4, the bolt head side and the nut side are in the two

different frames on the device. The lower side frame is fixed on the machine, and the upper side subjects to a cyclic loading F_c. Table 2.1 shows the bolt-nut materials JIS SCM435 steel and JIS S45C steel. Similar to the previous papers [76,77,80], a 392kN (400 ton) servo fatigue tester is used, the frequency is set to 5 or 10 Hz, and the mean load F_{m} is 30kN. Esmaeili et al. found that the tightening torque T can affect the fatigue strength of bolt joints [96]. To eliminate the effect of tightening torque T, in the fatigue experiments in this study, the tightening torques T =0. Table 3.3 shows the loading conditions set in the experiments. The S-N curve was obtained from the experimental results under five levels of stress amplitude with a fatigue limit of 2×10^6 cycles.

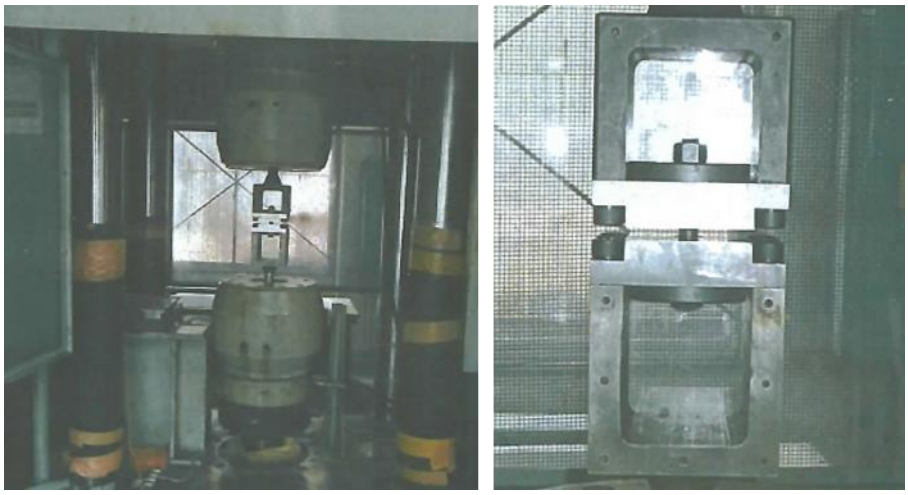

(a) fatigue experiment device

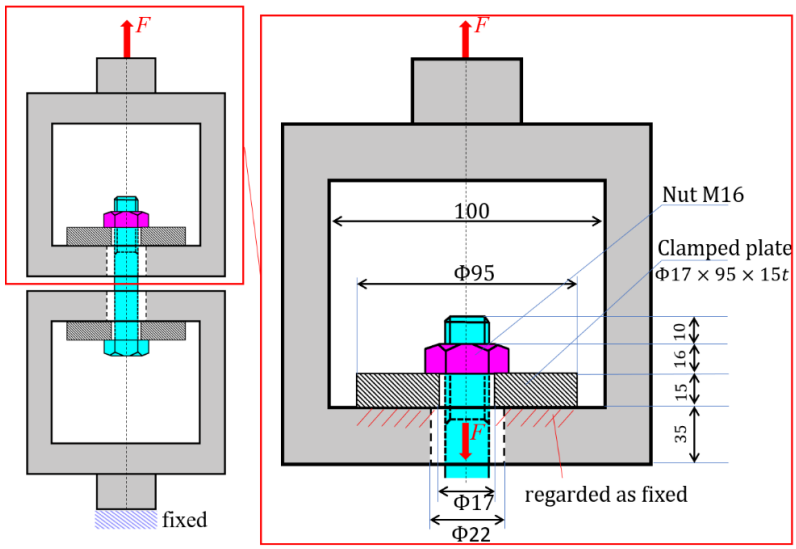

(b) Schematic illustration of fatigue test.

Fig. 3.4 fatigue experiment device and sketch of the specimen part

Table 3.3 Experimental conditions.

Load (kN)		Stress (MPa)		$R = \frac{\sigma_m - \sigma_a}{\sigma_m + \sigma_a}$
Mean load	Load amplitude	Mean stress σ_m	Stress amplitude σ_a	
30	22.6	213	160	0.14
30	18.3	213	130	0.24
30	14.1	213	100	0.36
30	11.3	213	80	0.45
30	8.5	213	60	0.56

3.2.3 Fatigue strength improvement due to enlarged root radius

Previously, Walker et al. [15], Yoshimoto [18] and Nishida [20] studied the root radius effect on the fatigue strength without providing pitch difference. Those results did not show significant fatigue strength improvement although the stress concentration can be reduced. To clarify the root radius effect and to verify the fatigue limit improvement, a series of fatigue tests are conducted on the specimen in Fig. 3.3. Fig. 3.5 shows the S-N curve obtained by varying the thread root radius as $\rho = \rho_0$, $\rho = 2\rho_0$ and $\rho = 3\rho_0$ under the pitch difference (a) $\alpha = 0\mu m$ and (b) $\alpha = 15\mu m$.

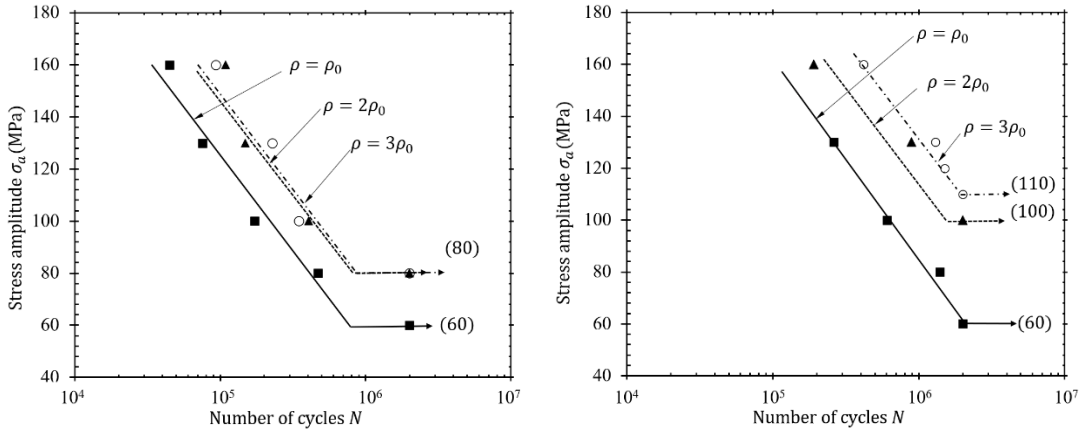

(a) α=0μm (b) α=15 μm

Fig. 3.5 S-N curves for bolt nut connections by varying the thread root radius

From Fig. 3.5(a), when α=0μm, it can be seen that by enlarging the root radius from standard $\rho = 1\rho_0$ to $\rho = 2\rho_0$ and $\rho = 3\rho_0$, the fatigue limit of the bolt nut connections increases from 60MPa to 80MPa. Besides, the fatigue life of $\rho = 3\rho_0$ is 3.00 times larger than that of $\rho = \rho_0$. From Fig. 3.5(b), when α=15 μm, it can be seen that the fatigue life of $\rho = 2\rho_0$ was improved more than two times than that of $\rho = \rho_0$ when the stress amplitude is 130MPa. When increasing the root radius from $\rho = \rho_0$ to $\rho = 2\rho_0$, the fatigue limit was improved from 60MPa to 100MPa. The fatigue limit increases to 110MPa when the root radius increases to $\rho = 3\rho_0$. That is to say by

enlarging the root radius to $\rho = 2\rho_0$ and $\rho = 3\rho_0$ the fatigue limit of the bolt nut connections can be improved by 67% and 83%, respectively. It may be concluded that enlarging bolt root radius and choosing suitable pitch differences may improve the fatigue life and fatigue limit of the bolt nut connections efficiently.

3.2.4 Fatigue strength improvement due to pitch difference

In the authors' previous papers, the pitch difference effect on the fatigue strength was discussed experimentally and theoretically [76,80]. In this paper, the pitch difference effect is discussed coupled with the root radius effect to improve both the fatigue life and the fatigue limit. Fig. 3.6 shows the S-N curves of bolt nut connections when α=0 and α=15μm coupled with $\rho = 1\rho_0$ and $\rho = 2\rho_0$. In Fig. 3.6, when $\rho = \rho_0$ with increasing the pitch difference from α=0 to α=15μm, the fatigue life can be significantly improved although the fatigue limit remains the same. For example, the fatigue life for a bolt with a root radius of $\rho = 2\rho_0$ is twice that of the bolt with a root radius of $\rho = \rho_0$ when α=0, and besides, the fatigue limit is improved from 60MPa to 80MPa by 33%. Moreover, by introducing a pitch difference of α=15μm coupled with enlarging the root radius to $\rho = 2\rho_0$, the fatigue limit is improved by 67%, and besides, the fatigue life is improved by 162% when the stress amplitude is 160MPa. In a word, both the fatigue life and fatigue limit of bolt nut connections can be significantly enhanced by enlarging the root radius and introducing an appropriate pitch difference between the bolt and the nut at the same time.

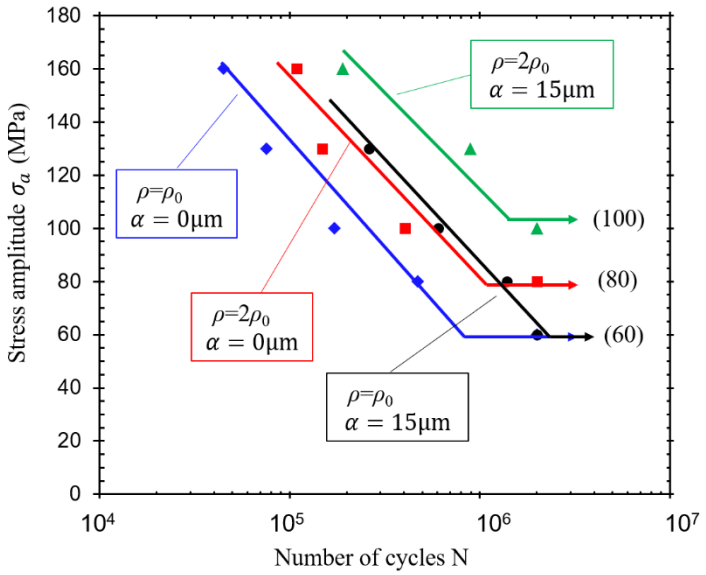

Fig. 3.6 S-N curves for bolt nut connections when α=0 and α=15 μm.

3.3 Stress and crack appearing at bolt threads

3.3.1 Crack observation

Fig. 3.7 illustrates the crack configuration observed from the bolt outer surface after the fatigue experiments. When α=0, as shown in Fig. 3.7(a) and (b), a crack is observed only at $No.1 \sim No.3$ threads. This is because $No.1 \sim No.3$ threads carry most of the load as shown in Fig. 3.2(c). Then, the crack initiated at $No.1$ or $No.2$ thread propagates and causes the final bolt fracture at the same thread without extending to other threads.

On the other hand, when α=15μm, as shown in Fig. 3.7(c) and Fig. 7(d), cracks can be observed between $No.2$ and $No.7$. When α=15μm, cracks initiate at $No.6$ and $No.7$ threads because those threads carry most of the load as shown in Fig. 3.2(d). After the cracks propagate at $No.6$ and $No.7$ threads, another crack initiates and propagates at $No.5$, $No.4$… toward $No.1$ thread consecutively until causing the final bolt failure. The consecutive crack extension is caused by the crack initiation and propagation at each thread, which changes the thread contact state between the bolt and nut due to the pitch difference [76].

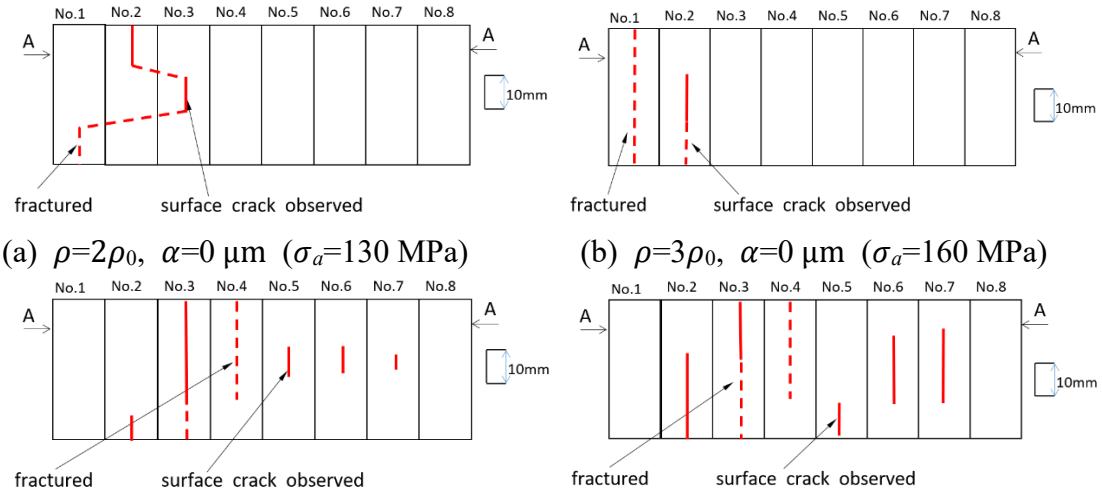

(a) ρ=2ρ_0, α=0 μm (σ_a=130 MPa) (b) ρ=3ρ_0, α=0 μm (σ_a=160 MPa)

(c) ρ=2ρ_0, α=15 μm (σ_a=130 MPa) (d) ρ=3ρ_0, α=15 μm (σ_a=160 MPa).

Fig. 3.7 Sketch of the cracks observed from the bolt outer surface after the fatigue experiments.

Fig. 3.8 Crack configuration observed from the fractured specimen surface, and it can be seen that no thread stripping occurred in the threads of both the nut and the bolt. Fig. 3.8(c) and Fig. 3.8(d) shows an example of the bolt thread surface with the nut cross section after the fatigue tests when $\sigma_m = 213\text{MPa}$ and $\sigma_a = 130\text{MPa}$. As shown in Figure 2, increasing the root radius of the bolt thread necessitates truncating the internal thread, which may reduce the shear strength of the bolt thread. However, the thread surface status of $\alpha = 15\mu\text{m}$ is nearly the same in Fig. 3.8(c) when $\rho = 1\rho_0$ and in Fig. 3.8(d) when $\rho = 2\rho_0$. No thread stripping can be seen within this fatigue strength study by enlarging thread root radius. Although slight wear can be seen at the nut thread in Fig. 3.8(d), the wear site is far away from the crack initiation site in Fig.

3.7(c) at *No.5* thread root. It should be noted that in this study, high strength nut with a height of 16mm is used. For common M16, of which the nut height is 13mm and the yield strength is lower than that used in this study, more works are needed to check if thread stripping occurs or not.

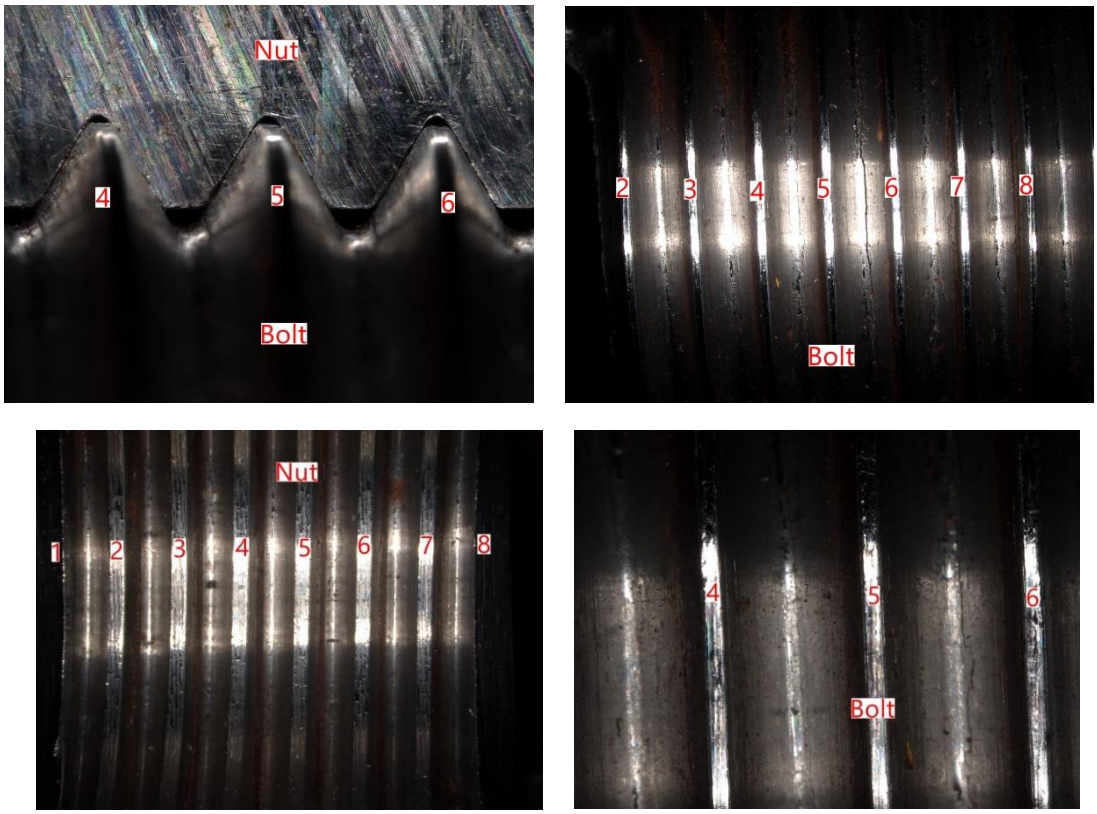

(a) $\rho=\rho_0$, α=15 μm (σ_a=130 MPa)

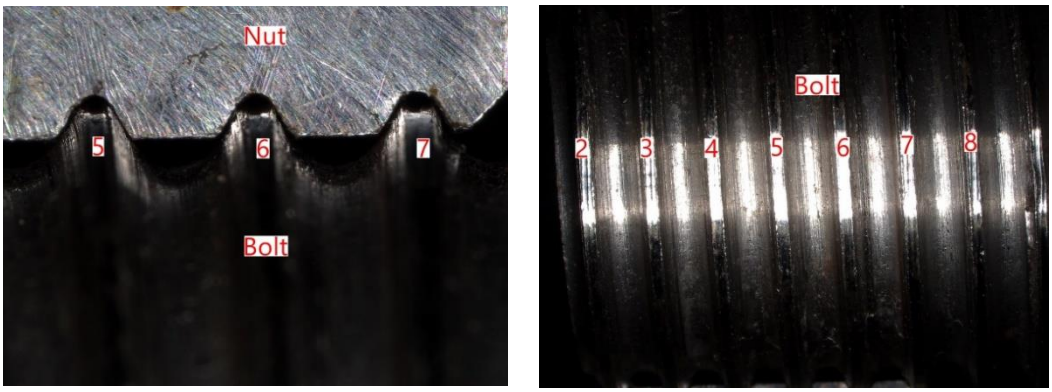

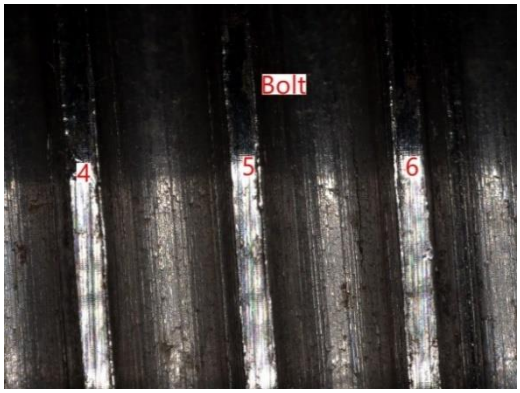

(b) ρ=2ρ_0, α=15 μm (σ_a=130 MPa)

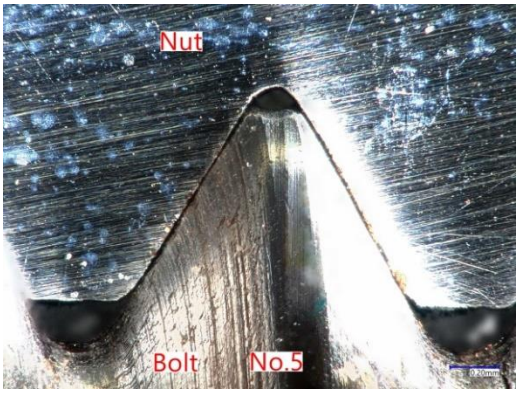

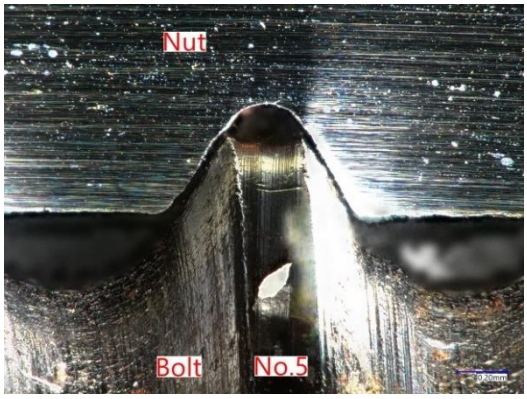

(c) ρ=ρ_0, α=15 μm (σ_a=130 MPa) (d) ρ=2ρ_0, α=15 μm (σ_a=130 MPa)

Fig. 3.8 Crack configuration observed from the fractured specimen surface.

3.3.2 FEM modeling and boundary conditions

The stress at the thread root is calculated by applying the FEM software MSC.Marc/Mentat, 2012. Fig. 3.9 shows an example of FEM mesh used in the axisymmetric analysis where 4-node QUAD elements are used, and the minimum element size near the bolt root is about 0.01 mm x 0.01 mm. The material properties are shown in Table 2.1. The elasto-plastic analysis of the FEM model is performed under the same loading conditions as the experiments. The multi-linear stress-strain curves used in the simulation is shown in Fig. 3.10. The bolt head side of the clamped body is fixed, and axial force F_c = 30 ± 14.1 kN is applied to the bolt head. Thus, the corresponding stress amplitude and the nominal stress amplitude at the bolt roots are σ_a=213 MPa and σ_m=100 MPa, respectively.

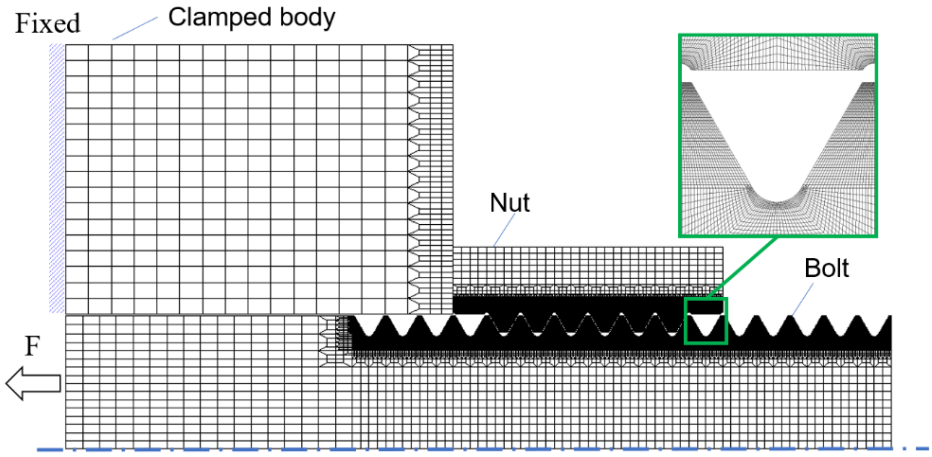

Fig. 3.9 Axisymmetric FEM model when $\rho = 1\rho_0, \alpha = 0$.

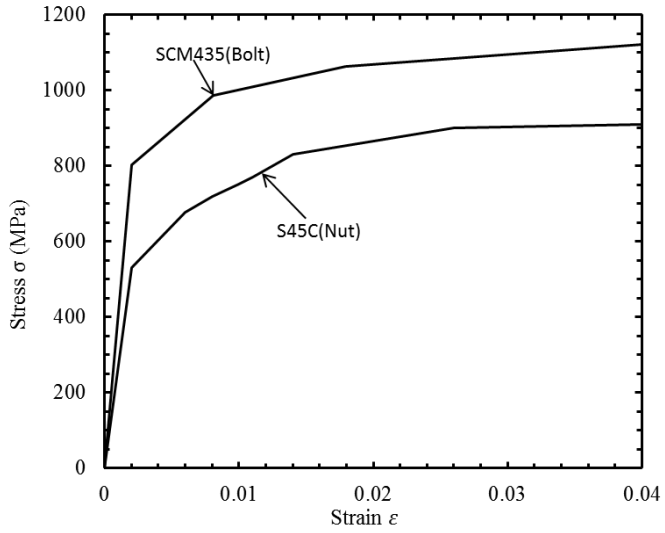

Fig. 3.10 Stress strain curves used in the axi-symmetric analysis

3.3.3 Stress amplitude versus mean stress under no pitch difference

Fig. 3.11 shows the endurance limit diagrams with the Soderberg line of the plane specimen. Here, σ_w represents the fatigue strength under reversal stress σ_m =0 and σ_y is the yield strength. The maximum tangential stress at each thread obtained by the FEM is plotted in terms of the stress amplitude $\sigma_a = (\sigma_{max} - \sigma_{min}) / 2$ and the mean stress $\sigma_m = (\sigma_{max} + \sigma_{min}) / 2$. Due to no stress gradient in plain specimens, the fracture stress in notched specimens is always larger than that in the plain specimens. Therefore, it should be noted that the stress data plotted beyond the line ($(\sigma_m/\sigma_y)+(\sigma_a/\sigma_w) > 1$) does not represent the real fracture at the bolt thread. Several previous studies investigated the endurance limit after a certain amount of mean stress level [97–100]. In this paper, the Soderberg line of the plain specimen is used to discuss the relative hazard at the bolt roots.

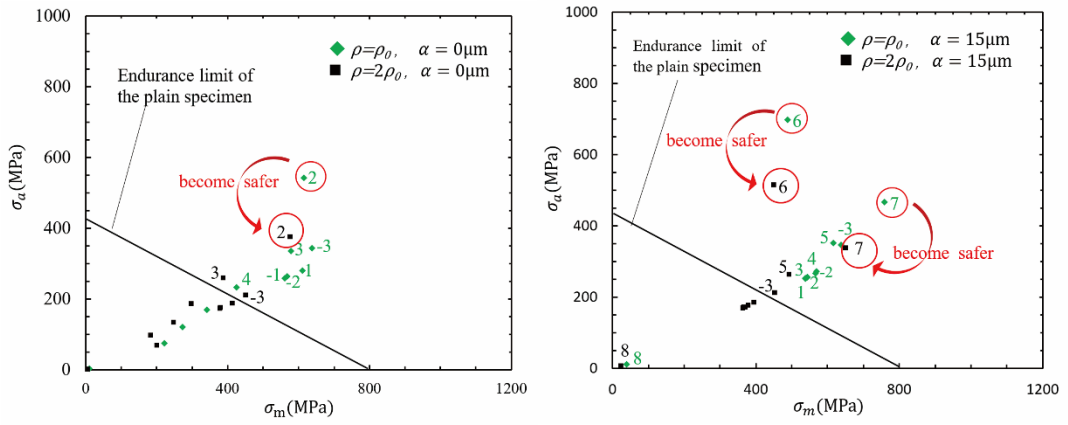

(a) ρ=ρ_0, 2ρ_0 when α=0μm (b) ρ=ρ_0, 2ρ_0 when α=15μm

Fig. 3.11 Endurance limit diagram when $F_a = 14.1$kN

When α=0, from Fig. 3.11(a), the most dangerous part locates at *No*.2 thread. By enlarging the root radius from $\rho = \rho_0$ to $\rho = 2\rho_0$, at *No*.2 thread, the mean stress decreases by about 6% and the stress amplitude decreases by about 38%. When $\alpha = 15\mu m$, from Fig. 3.11(b), the most dangerous part locates around *No*.6 and *No*.7 threads of the bolt. By enlarging the root radius from $\rho = \rho_0$ to $\rho = 2\rho_0$, at *No*.6 thread, the mean stress decreases by about 8% and the stress amplitude decreases by about 26%. The same trend can be found when the pitch difference α=33μm. Those analytical results in Fig. 3.11 are in good agreement with the fracture surface observation in Fig. 3.7. For bolt nut connections without pitch difference α=0, both initial cracks and final breaks of the bolt occur at *No*.2 thread close to the bolt head side. For bolt nut connections with pitch differences $\alpha \neq 0$, the initial crack occurs *No*.6 and *No*.7 threads far from the bolt head and then extend to *No*.2 thread near the bolt head side, where the final break occurs.

3.3.4 Stress amplitude versus mean stress under pitch differences

Fig. 3.12 is an endurance limit diagram obtained using the analytical results. Here, the mean stresses and stress amplitude under two different kinds of pitch difference when root radius $\rho = \rho_0$ and $\rho = 2\rho_0$ are compared. From Figure 9, it can be seen that when increasing the pitch difference from $\alpha = 15\mu m$ to $\alpha = 33\mu m$, the stress distributions for the bolt with a root radius of $\rho = \rho_0$ and $\rho = 2\rho_0$ are the same. The maximum stress amplitude and the mean stress occurred at the side far from the bolt head are consistent with the experimental results.

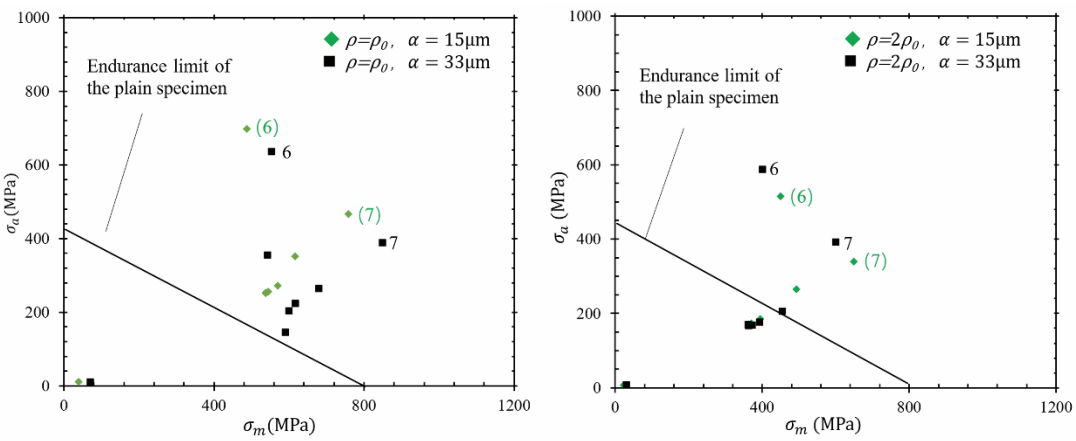

(a) $\rho = \rho_0$ when α=15μm and 33μm (b) $\rho = 2\rho_0$ when α=15μm and 33μm

Fig. 3.12 Endurance limit diagram when Fa=14.1kN

3.4 Anti-loosening performance under enlarged root radius

As described in the above sections, the fatigue limit improvement was experimentally verified, and the stress reduction was analytically clarified by enlarging the thread root radius ρ and providing suitable pitch difference α. However, those results can be expected only when the nut loosening does not happen. In this section, therefore, anti-loosening is confirmed by applying three-dimensional FEM simulation to the nut screwing and tightening processes.

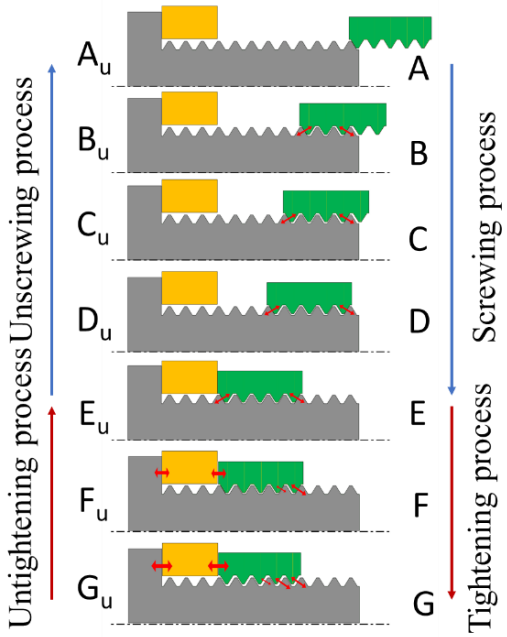

Fig. 3.13 Illustration of the thread contact status during the screwing, tightening, untightening, and unscrewing of pitch difference nut.

3.4.1 Analysis method

Fig. 3.13 illustrates the nut screwing process from A to D, and the nut tightening process from E to G. Fig. 3.13 also illustrates the nut untightening process from Gu to Eu and the nut unscrewing process from Du to Au. When the pitch difference α=0, the prevailing torque T_P required in the nut screwing is zero as T_P=0, but when $\alpha \neq 0$, the prevailing torque T_P is no longer 0 as $T_P \neq 0$. This prevailing torque T_P is commonly used to characterize the anti-loosening performance of bolt nut connections. As an example, Eccles et al. explained that all prevailing torque type nuts detach from the bolt when the external load is larger than the bolt tightening force [58]. Under a larger tightening force, therefore, the prevailing torque type nuts can be used safer.

This paper discusses the effect of the root radius on the anti-loosening performance focusing on the prevailing torque obtained from the three-dimensional FEM simulation. To clarify the impact of root radius on loosening performance, the dimensions of M16 bolt-nut are chosen to be the same. The length of the bolts used for anti-loosening experiments is 76mm, and the thread length and the grip length are 42mm and 18mm, respectively. The recent study showed the 3D FEM results are in good agreement with the experimental results for JIS M12 bolt-nuts [84].

Three-dimensional FEM models were simulated by ANSYS WORKBENCH 16.2. As shown in Fig. 3.14, the bolt head and the nut shapes are simplified by cylinders to save the calculation time. Fig. 3.14(a) shows the FEM mesh for M16 bolt-nut when the pitch difference α=0 and the root radius ρ=ρ_0 with the total element number 175907 and the total node number 346712. The results are confirmed to be accurate enough since the maximum relative error is less than a few percent by applying the refined smaller mesh to the contact surface with a much larger calculation time. Fig. 3.14(b) shows the boundary condition assuming the initial nut location at 0.1mm away from the clamped body. The bolt head and the left side of the clamped body are fixed, and the nut is screwed onto the bolt in the clockwise tightening direction. The prevailing torque T_P can be obtained before the nut contacts to the clamped body. Since the pitch of a standard JIS M16 bolt is 2mm, when rotating the nut by the angle θ=18 degree, the nut moves to the left by 0.1 mm and touches the clamped body. The material property in Table 2 is used in FEM analysis, assuming the clamped body is also SCM435. Bilinear elasto-plastic stress-strain relations are applied instead of multi-linear relations to save the calculation time. Then, the Newton-Raphson approach is used to solve nonlinear problems. The upper thread of the bolt is supposed to contact to the lower thread of the nut, and the lower thread of the bolt is supposed to contact to the upper thread of the nut. The friction coefficient between the threads is denoted as μ_s, and the friction coefficient between the nut and the clamped body is denoted as μ_w. Previous studies have proven that the thread friction coefficient μ_s is in the range 0.11 to 0.15, and the underhead friction coefficient μ_w is in the range 0.16 to 0.18 [101]. In this study, $\mu_s = 0.12$ and $\mu_w = 0.17$ are used in the FEM analysis by considering the previous study where the molybdenum disulfide paste spray was used in the nut screwing process [81]. Elliott et al. studied the behaviour and strength of bolted

connections failing in shear, and found that the shear resistance of a bolted connection is not significantly affected by the hole clearances [92]. In this section of this study, all the diameters of bolt holes are 16.8mm.

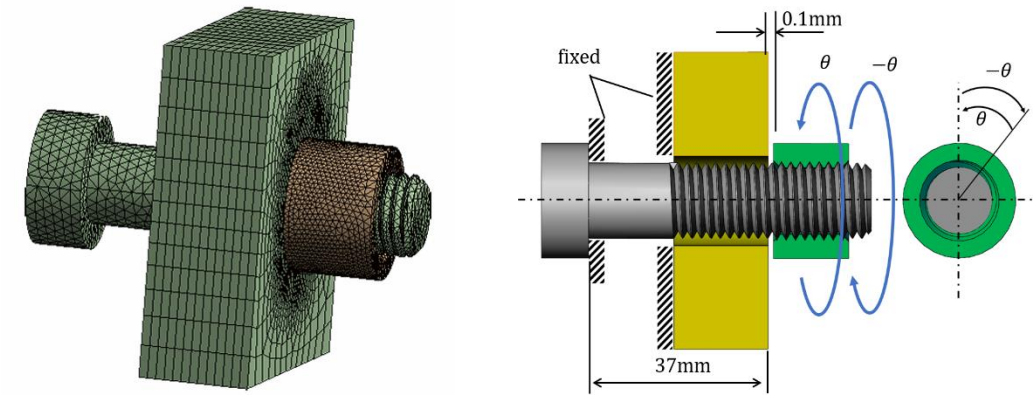

(a) FEM mesh model (b)Boundary conditions.

Fig. 3.14 FEM model and boundary conditions for tightening and untightening process.

After the nut contacts the clamped body, the tightening force F v.s. tightening torque T relation, that is the $F-T$ relation can be obtained from point E to point G in Fig. 3.13. After the tightening process is finished, the loosening process can be analyzed subsequently from point G to point E as shown in Fig. 3.13. The nut rotation angle θ to produce specified clamping force $F_{25\%}$, which is 25 percent bolt axial yielding force, cannot be known beforehand. Therefore, the analysis is performed as shown in the following step (i) and step (ii).

(i) Applying a sufficiently large rotation angle θ to the nut. When the rotation angle θ is sufficiently large, the tensile stress of the bolt may exceed the yield stress. Thus, a rotation angle $\theta_{25\%}$ corresponding to the fastening force $F_{25\%}$can be obtained.

(ii) Tightening the nut by using the rotation angle $\theta_{25\%}$ obtained in the process (i). After the tightening force reaches $F_{25\%}$, untighten the nut by an anti-tightening angle $-\theta_{25\%}$.

3.4.2 Results and discussion for $T-\theta$ relation

Fig. 3.15 shows the $T-\theta$ relation, that is, the tightening torque T versus the nut rotation angle θ relation during the screwing and tightening processes when the bolt root radius $\rho = 1\rho_0$. During the nut screwing, $T_P = 0$ when $\alpha = 0$; however, $T_P \neq 0$ when $\alpha \neq 0$. During the nut tightening, it should be noted that the gradient $dT/d\theta$ varies depending on the pitch difference α. The gradient $dT/d\theta$ when $\alpha = 0$ is larger than the gradient $dT/d\theta$ when α =33μm. During the entire nut tightening process, $dT/d\theta = const$ when $\alpha = 0$; however, when $\alpha \neq 0$, the gradient $dT/d\theta = const$ but the constant value is slightly changed at point F2 as in Fig. 3.15. In

Fig. 3.15, the slope ratio of the lines E_1G_1, E_2F_2, and F_2G_2 are denoted by $tan\theta_1$, $tan\theta_2$ and $tan\theta_3$, respectively. It is found that the angles have the relation $\theta_1 > \theta_3 > \theta_2$. This can be explained in the following way.

Fig. 3.16 illustrates why the $T-\theta$ relation can be depicted as shown in Fig. 3.15 by illustrating the thread contact status. From Fig. 3.16, it is seen that when $\alpha = 0$, the slope ratio is closely related to the clamped body deformation whose height is H_c. This is because $No.1$ or $No.2$ nut thread near the bolt head may carry most of the load. When $\alpha \neq 0$, however, the slope ratio is closely related to the deformation due to the clamped body and the nut whose height is $H_c + H$. This is because $No.6$ or $No.7$ nut thread near the nut end may carry most of the load. At the nut position from E_2 to the nut position F2 in Fig. 3.16 (b), the thread contact status changes at $No.1$ or $No.2$ nut thread. This is the reason why the slope slightly changes at Point F_2 in Fig. 3.15. In the case of Fig. 3.15, the angle $\theta_1 = 165$ degree $> \theta_3 = 157$ degree $> \theta_2 = 156$ degree.

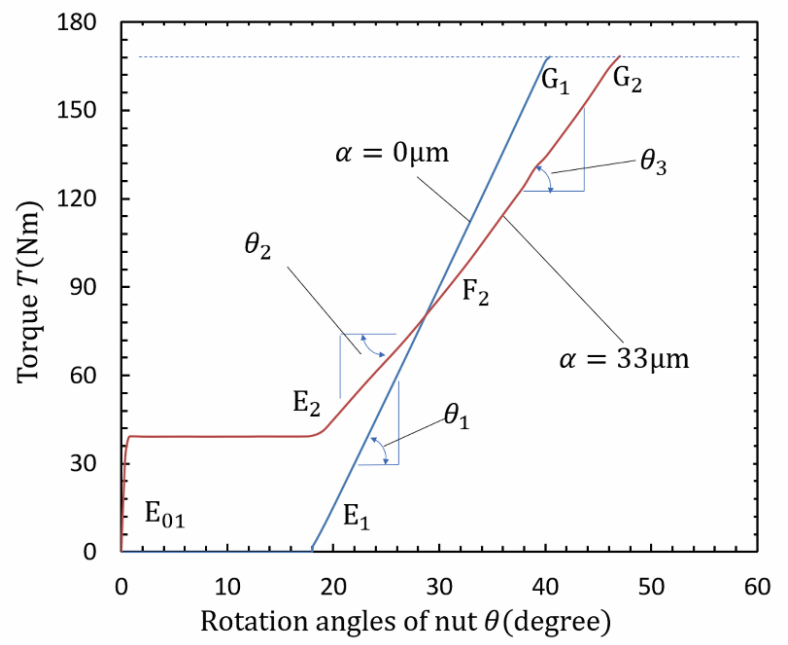

Fig. 3.15 Relationship between the and tightening torque T and the nut rotation angle θ during the screwing and tightening process when ρ=1ρ_0

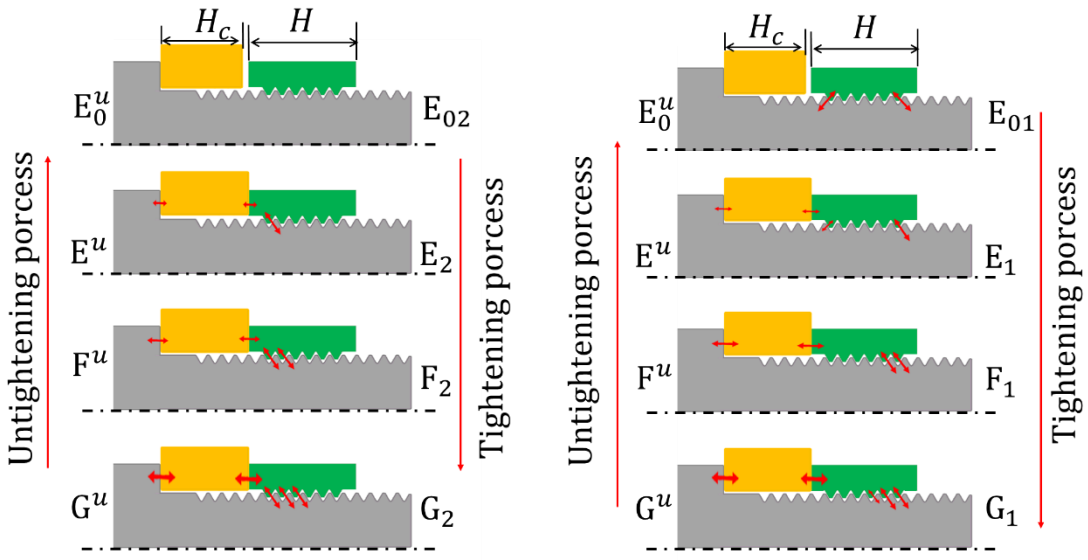

(A) α=0μm (B) α > 0μm

Fig. 3.16 Illustration why the $T-\theta$ relation can be depicted as shown in Fig. 3.15 during the tightening and untightening processes

3.4.3 Results and discussion for $F-T$ relation

Fig. 3.17 shows the tightening force T vs. the torque T relation when $\rho = 1\rho_0$ and $\rho = 2\rho_0$ with $\alpha = 0$ and $\alpha = 33\mu m$. In the previous study, the authors conducted impact-vibration test prescribed in NAS3350 (National Aerospace Standard) for M16 pitch difference nut. Then, anti-loosening is confirmed for $\alpha \geq 33\mu m$ showing the prevailing torque $T_P = 3039$Nm for JIS M16 [80]. Such good anti-loosening was also reported for "U-nut" widely used in the world although U-nut has relatively smaller prevailing torque T_P=1.5Nm for JIS M12 [62]. Another special nut named "Super Slit Nut" is also accessible in the market showing T_P= 15Nm ~19Nm for JIS M16 with good anti-loosening [60]. As shown in Fig. 3.17, the FEM analysis shows that the pitch difference nut has T_P= 19Nm even when $\rho = 2\rho_0, \alpha = 33\mu m$. Considering other special nuts such as U-nut and Super Slit Nut, good anti-loosening performance can be expected for the enlarged root radius of pitch difference nut considered in this paper.

As shown in Fig. 3.17, when $\alpha = 0$, the clamping force F appears once T applies. However, when $\alpha = 33\mu m$, the clamping force F appears only after the torque exceeds the prevailing torque as $T \geq T_p$. After the tightening force reaches F=$F_{25\%}$ producing 25% of the bolt yield stress σ_y=800MPa (see Table 2.1), untightening process starts by reversing torque T. During this process, tightening force F decreases with decreasing the magnitude of T. When $\alpha = 33\mu m$ the magnitude of T is always larger than that of $\alpha = 0$. And even when $F = 0$ the reverse torque is not zero as T=T_p^u> 0, which is named as residual prevailing torque and discussed in the recent paper [84]. In Fig. 3.17, the light green zone illustrates the difference between $\alpha = 0$ and $\alpha = 33\mu m$ defined in equation (2-1). Such torque difference in equation (2-1) can be regarded as the loosening resistance torque T_p^u contributing to anti-loosening (see Appendix A).

$$T_P^u = |T_P|_{\alpha>0} - |T_P|_{\alpha=0} \quad (2\text{-}1)$$

As shown in Fig. 3.17(b), when $\rho = 2\rho_0$ and $\alpha = 33\mu m$, the light green zone region T_p^u in equation (1) is comparatively smaller. However both T_p and T_p^u appear in a similar way of $\rho = 1\rho_0$ and $\alpha = 33\mu m$ in Fig. 3.17(a) and those values T_p and T_p^u are not smaller compared to U-nut and Super Slit Nut as described above. The recent study showed that the loosening resistance torque T_p^u increases with increasing the pitch difference α as well as the prevailing torque T_p [84]. Therefore, Fig. 3.17(b) suggests that even when the bolt root radius is enlarged, the anti-loosening performance can be expected under the suitable pitch difference.

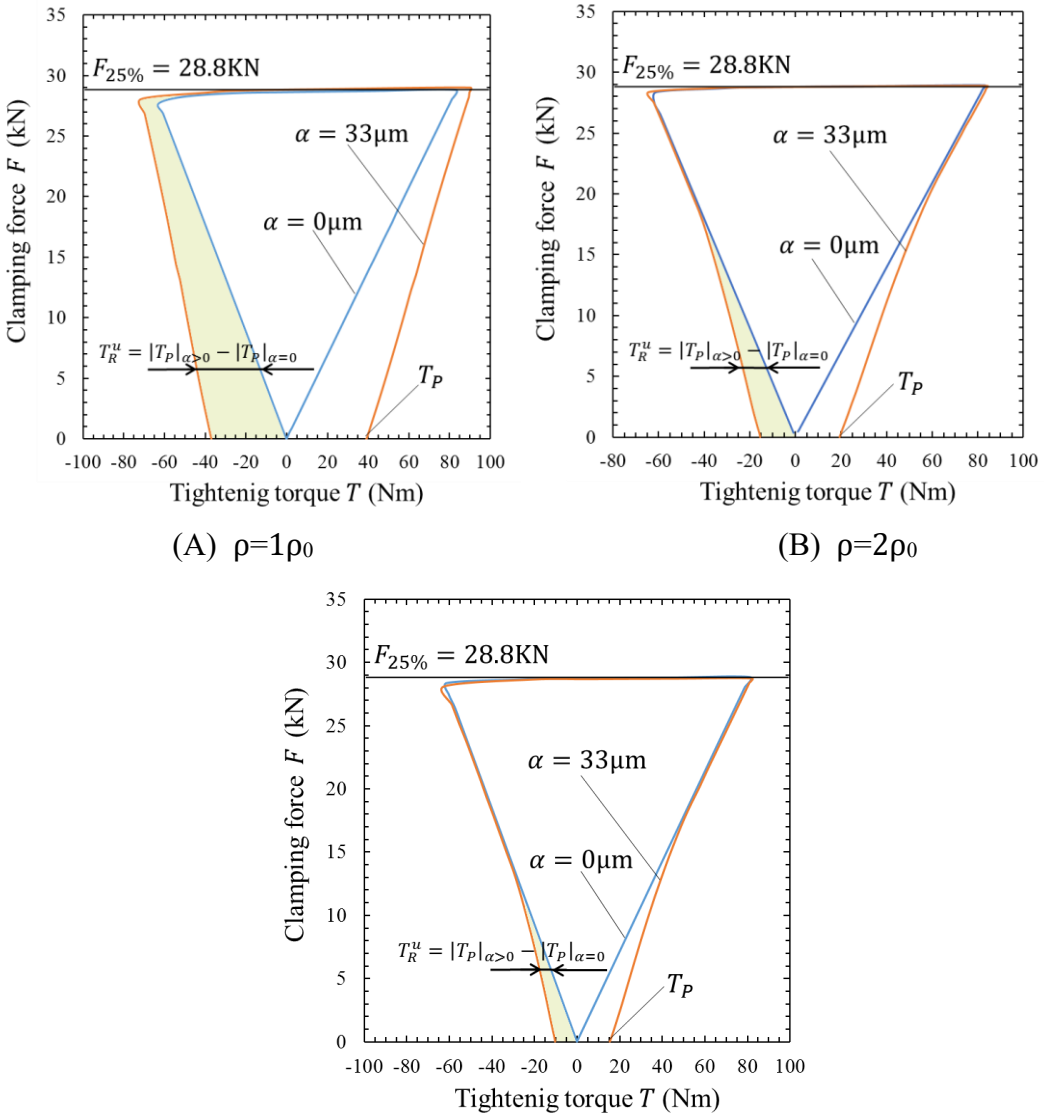

Fig. 3.17 Relation between tightening torque T and clamping force F.

Table 3.4 Prevailing torque T_P, residual prevailing torque T_P^u, median loosening resistance torque $\tilde{T}_R^u$ under $F = F_{25\%}$ for M16 with different root radii and a pitch difference of $\alpha = 33\mu m$

	T_P (Nm)	T_P^u (Nm)	$\tilde{T}_R^u$(Nm)
$\rho = \rho_0$	39.0	37.0	20.0
$\rho = 2\rho_0$	19.3	15.5	7.7
$\rho = 3\rho_0$	15.4	10.3	5.1

It should be noted that common bolted joints $\alpha = 0$ are loosening resistant only when sufficient tightening force F is provided; therefore, for example, no loosening resistance at F=0 in Fig. 3.17. Instead, $\alpha = 33\mu m$ has larger loosening resistance as and even at F=0, the residual previaling torque for $\rho = 2\rho_0$ and $\rho = 3\rho_0$ are 19.3Nm and 15.4Nm, and are in the range of residual prevaing torque of M16 SLN [60].

3.5 Conclusions

Since the authors' previous research showed that a slight pitch difference might improve the fatigue life, in this paper, the effect of root radius on the fatigue limit was investigated by varying the pitch difference in JIS M16 bolt-nut connections. Although increasing the root radius of the bolt thread necessitates truncating the internal thread, which may reduce the shear strength of the bolt thread, no thread stripping can be seen for the enlarged root radius of the bolt within this experiment. Conclusions can be summarized as follows.

(1) Fatigue tests were performed when the root radius is twice or three times larger than the standard bolt-nut root radius. This experiment verified that the fatigue limit could be improved by more than 30% by enlarging the bolt root radius. The FEM analysis showed that when the bolt root radius is enlarged, both stress amplitude and mean stress at each thread root can be reduced significantly.

(2) When the root radius is larger than the standard one, the fatigue limit can be improved further by more than 25% by introducing a suitable pitch difference. When there is no pitch difference, the crack initiation always occurs at $No.1$ or $No.2$ threads close to the bolt head causing the final failure at the same thread. When there is a pitch difference, the crack initiation occurs at $No.6$ or $No.7$ threads far away from the bolt head. Then the crack initiation and propagation expand toward the bolt head until the final failure occurs at $No.1$ or $No.2$ threads.

(3) By varying the root radius ρ and the pitch differences α, $F-T$ relation, that is, the clamping force F vs. the tightening torque T relation, was clarified by applying 3D FEM. When $\rho = 2\rho_0$ and $\alpha = 33\mu m$, it was confirmed that the prevailing torque T_P= 19Nm and the residual prevailing torque $T_P^u = 10\text{Nm}$ even at F=0. Since those

values are not smaller compared to other special nuts, good anti-loosening performance can be expected for the enlarged root radius of bolt-nut connections under the suitable pitch difference.

Chapter 4. Nut height effect on fatigue strength and anti-loosening performance of pitch difference bolt nut connections

4.1 Introduction

As shown in Fig. 1.12, introducing a pitch difference between the bolt and the nut and improve anti-loosening performance and fatigue life of bolt nut connections, but fatigue life improvement reaches the maximum value at smaller pitch difference, and large pitch difference is needed for excellent anti-loosening performance.

In this chapter, M12 bolt nut connections with two different nut heights, i.e., $H = 10.5\text{mm}$ and $H = 14.0\text{mm}$, and with a series of pitch differences are used to investigate the nut height effect of bolt nut connections with pitch difference on anti-loosening performances and fatigue properties. The relations between tightening torque and clamping forces are obtained by experiments and FE analysis. Moreover, the Junkers' loosening experiments of the specimens are also simulated by using FEM. Besides, the fatigue limit diagrams of the bolt nut connections are obtained by the axisymmetric model. It is found that by increasing the nut height for pitch difference bolt nut connections, the most suitable pitch difference of anti-loosening performance will decrease and the most suitable pitch difference for fatigue life improvement almost remains the same, the schematic illustration is shown in Fig. 4.1. Thus, a better combination of fatigue life improvement and anti-loosening performance of pitch difference bolt nut connections.

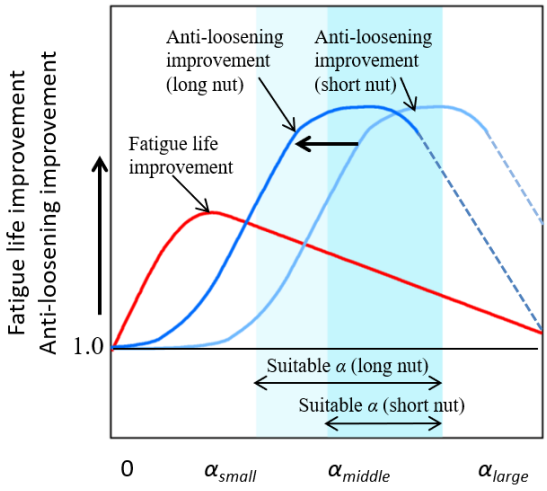

Fig. 4.1 Schematic illustration of the anti-loosening and fatigue life improvement

4.2 tightening and loosening process of Specimen

4.2.1 Size of specimens

Fig. 4.2 illustrates the size M12 bolt nut connections with a standard nut height of H =10.5mm and a longer nut with a height of H =14.0mm in this paper. Both the Japanese Industry Standard (JIS) bolt and nut are the same, and the pitch is p=1750μm. However, in this study, although the bolt pitch is p =1750μm, the nut pitch is α μm than that of the bolt. Fig. 4.2(b) illustrates the thread clearance in the axial-direction C_z=59μm and the one in the transverse-direction C_x=102μm. Both the bolt and the nut are made by rolling with less than 3μm manufacturing error. For all the specimens used in this study, both sides of the nut thread are chamfered. The chamfer plane angle is 45 degrees, and the chamfer distances from the edges are 1.5 mm. Fig. 4.2(c) illustrates nut thread geometry for the normal nut height $H = 10.5$mm with $m = 4$ and $H = 14.0$mm with $m = 6$. Here, n is number of complete threads excluding chamfered threads at both ends in Fig. 4.2(c). Table 2.1 shows the properties of the bolt material, JIS Chromium-molybdenum steel SCM 435 and the nut material medium carbon steel, JIS S45C.

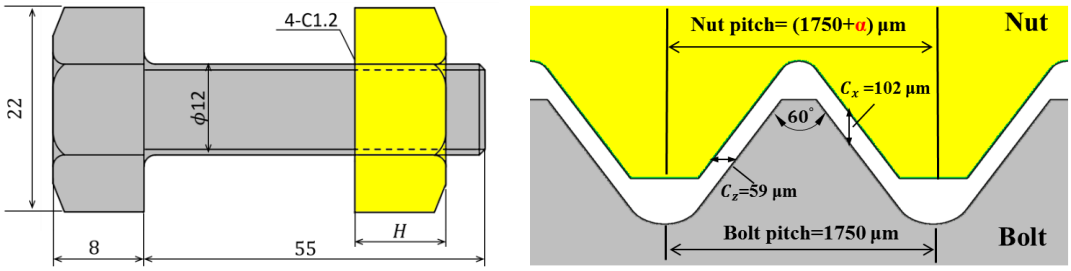

(a) Nut height H =10.5mm, H =14.0mm (b) Pitch difference and clearance

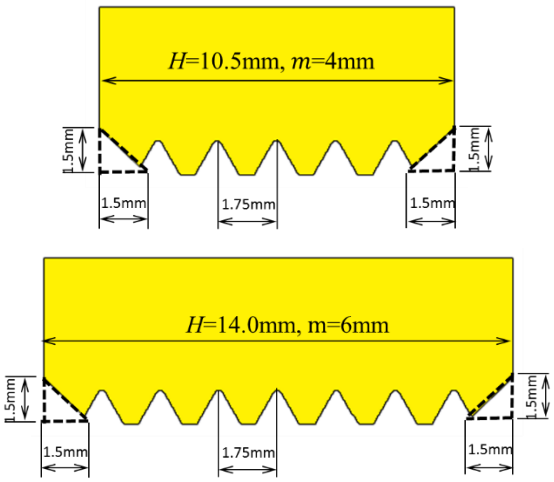

(c) Nut thread geometry when H =10.5mm m =4 and H =14.0mm m =6 where m is the complete thread number excluding chamfered threads at both nut ends

Fig. 4.2 M12 bolt nut connections used in the experiments

4.2.2 experimental and FEM conditions

Fig. 4.3 shows the picture of the experiment device based on NST series (JIS B 1084) and a sketch of the state of the bolt nut connections on the machine. Molybdenum disulfide lubricant spray is used as the lubricating oil between the thread surface between the bolt and the nut. In the screwing in process, as shown in Fig. 2.3(a), the nut is screwed in by using a torque wrench (DB 50N) until the nut contacts the clamped body. The tightening torque and the axial force during the tightening process can be obtained by the torque sensor and the stress sensor, respectively. Besides, the under-head friction coefficient μ_w and the thread friction coefficient μ_s during the whole process can be obtained by the machine.

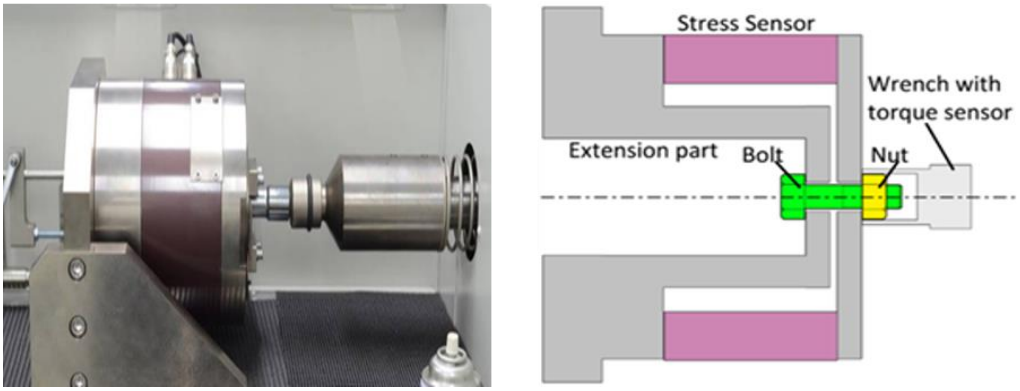

(a) experiment device (b) sketch of the device

Fig. 4.3 Nut tightening experiment device based on NST series (JIS B 1084)

Fig. 4.4(a) shows the experimental results of the relationship between the tightening torque and clamping force for M12 under different nut height. The yield stress of the material of the bolt is 800MPa, and the cross-sectional area of the bolt is about 84.3mm^2. Thus, the clamping force when the tensile stress in the bolt reaches the yield stress is $F_{100\%} = 68\text{kN}$. From Fig. 4.4(a), it can be seen that, when the clamping force is $F_{50\%} = 33.7\text{kN}$ and $F_{25\%} = 16.8\text{kN}$ of the yield stress, the corresponding tightening torque is 86Nm and 48Nm, respectively.

Motosh [22,102] proposed the following equation, which can express the relation between the tightening torque and the clamping force for standard bolt nut connections (see Appendix C)

Table 4.1 Variables used for Eq. C.1.

Pitch diameter d_2(mm)	Half angle of the thread β(°)	Friction coefficient		Thread pitch p(mm)	Bolt bearing surface outer diameter d_0(mm)	Bolt hole diameter d_h(mm)
		Thread surface μ_s	Bearing surface μ_w			
10.863	30	0.14	0.17	1.75	19	13.5

In practice, the thread friction coefficient μ_s and the under-head friction coefficient μ_w are sometimes assumed to be the same [103]. The two friction coefficients can be affected by many factors, such as, fastening speed, surface treatment, and lubrication [104,105]. In Liu's research [106], it is found that the μ_m can be denoted from 0.132 to 0.029 when using MoS_2 as the lubrication, and in the authors' another paper, the μ_m is assumed as 0.15 [71]. In Udagawa's research, the thread friction coefficient μ_s is between 0.09 and 0.12 when using MoS_2 as the lubrication [101].

In this study, during the tightening process, the under-head friction coefficient μ_w fluctuant between 0.16 and 0.18, and the thread friction coefficient μ_s is in the range between 0.11 and 0.15. Therefore, the under-head friction coefficient is chosen as 0.17. If the thread friction coefficient is chosen as 0.14, the tightening force is 33.8kN when the tightening force is 86Nm. The theoretical relation between the tightening torque and clamping force when $\mu_s = 0.14,\ \mu_w = 0.17$ is shown in Fig. 4.4(b).

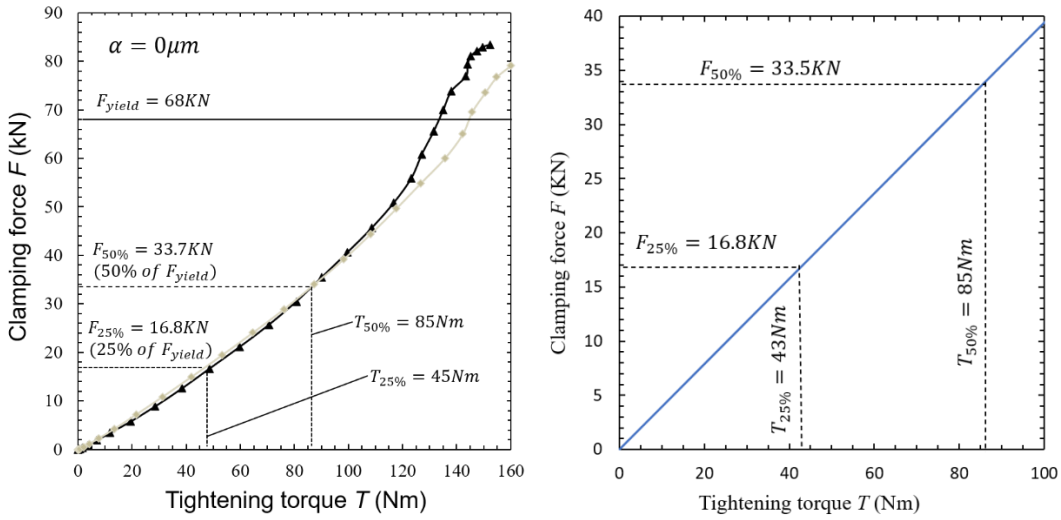

(a) experimental results (b) theoretical results

Fig. 4.4 Relation between tightening torque and clamping force

By comparing Fig. 4.4(a) and 4.4(b), it can be seen that the theoretical tightening torque at $F_{25\%} = 16.8$kN for $\mu_s = 0.14,\ \mu_w = 0.17$ is smaller than that of the experimental result. Table 4.2 shows the experimental, theoretical and FEM results of tightening torque under different tightening forces. From Table 4.2, it can be seen that the tightening torques at $F_{50\%} = 33.7$kN obtained by experiments, equation (4.1) and FEM are the same, the tightening torque at $F_{25\%} = 16.8$kN fluctuant within a small range. Therefore, in the following part of the tightening and untightening process of this study, the under-head friction coefficient μ_w and the thread friction coefficient μ_s are chosen as 0.17 and 0.14, respectively.

Table 4.2 The relation between tightening torque and clamping force at 25% and 50% of the material's yield stress of the bolts.

	Tightening torque T(Nm)		
	Experimental results	theoretical results $\mu_s = 0.14, \mu_w = 0.17$	FEM results $\mu_s = 0.14, \mu_w = 0.17$
$F_{25\%} = 16.8\text{kN}$	45	43	45
$F_{50\%} = 33.7\text{kN}$	85	85	85

4.3. comparison of the relation of tightening torque and clamping force under different nut height

4.3.1 FEM model and boundary conditions

The $F-T$ relation, that is, the clamping force F versus the tightening torque T relation is investigated by applying FEM during the tightening and untightening process (see Appendix A, B, C). Fig. 4.5 shows the FEM model for the $F-T$ relation where the cylindrical bolt head is fixed is fixed at the right side and the cylindrical clamped body is fixed at the left side with rotating the cylindrical nut. The clamped body height is set as 20mm. In Fig. 4.5, to save the calculation time, the initial nut position is just 0.05mm away from the clamped body. Table 1 shows the materials of the bolt, the nut, and the clamped body.

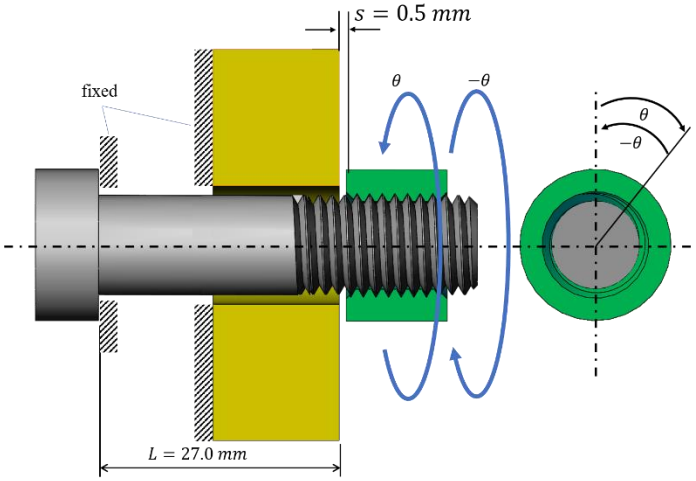

Fig. 4.5 boundary conditions

In this three-dimensional FEM simulation, the minimum element at the contact thread surfaces has a dimension 1.0mm; then, total number of elements is 55613, and the total number of nodes is 115852 when $H = 10.5\text{mm}$ and $p = 1750\mu\text{m}$. As described in Appendix C, to fit the FEM simulation results with the experimental results,

the friction coefficient at the thread surface is chosen as $\mu_s = 0.14$ and the friction coefficient at the bearing surface are chosen as $\mu_w = 0.17$. FEM software ANSYS workbench 16.2 is used for 3D FEM analysis. Bilinear elastoplastic stress-strain relations are applied to save the calculation time. Newton-Raphson's approach is used to solve the problem.

4.3.2 F-T relations obtained by experiment and FEM analysis

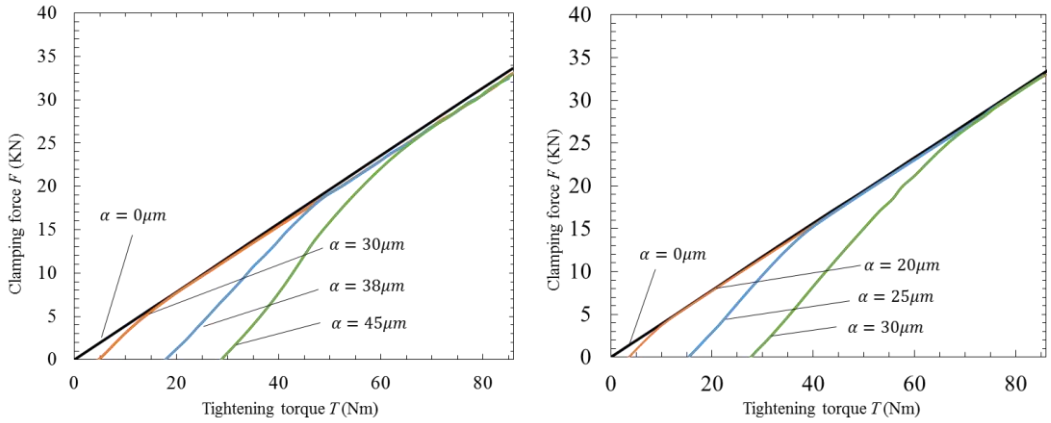

(a) $H = 10.5\text{mm}$ with number of threads m=4 (b) $H = 14.0\text{mm}$ with number of threads m=6

Fig. 4.6 $F-T$ relations are identical during tightening when (a) $H = 10.5\text{mm}, \alpha = 0\sim45\mu\text{m}$ and (b) $H = 14.0\text{mm}, \alpha = 0\sim30\mu\text{m}$

Fig. 4.6 shows the $F-T$ relation during tightening obtained by FEM analysis when (a) $H = 10.5\text{mm}$ and (b) $H = 14.0\text{mm}$. As shown in Fig. 4.6, the $F-T$ relation of $H = 10.5\text{mm}$, $\alpha = 30\mu m$ is almost the same as the $F-T$ relation of $H = 14.0\text{mm}$, $\alpha = 20\mu m$. Also, the $F-T$ relation of $H = 10.5\text{mm}$, $\alpha = 38\mu m$ is almost the same as the $F-T$ relation of $H = 14.0\text{mm}$, $\alpha = 25\mu m$. Similarly, the $F-T$ relation of $H = 10.5\text{mm}$, $\alpha = 45\mu m$ is almost the same as the $F-T$ relation of $H = 14.0\text{mm}$, $\alpha = 30\mu m$.

As shown in Fig. 4.2(c), the normal nut height$H = 10.5\text{mm}$ includes 4 threads, $m = 4$ excluding chamfered threads at both ends. The longer nut height $H = 14.0\text{mm}$ includes 6 threads, $m = 6$. These difference m=4 and m=6 affects anti-loosening coupled with pitch difference α. Focusing on the total pitch difference $m\alpha$, Table 4.3 illustrates several combinations m, α when $m\alpha$ is almost the same.

Fig. 4.7(a) shows the prevailing torque T_p versus α relation obtained by FEM analysis. It is seen that T_p increases with increasing α. As shown in Fig. 4.7(b), the same T_p can be provided when $m\alpha$ is the same. In Appendix B, some other anti-loosening parameters are discussed. More directly, under the same $m\alpha$, nut loosening simulation will be performed in the next section. Table 4.3 shows several combinations

m and α where the total pitch difference $m\alpha$ is almost the same.

Table 4.3 Combinations m, α where the total pitch difference $m\alpha$ is almost the same when $H = 10.5$mm, $m = 4$, and $H = 14.0$mm, $m = 6$ (m= number of complete threads excluding chamfered thread)

$H = 10.5$mm $(m = 4)$		$H = 14.0$mm $(m = 6)$	
Pitch difference α (μm)	$n\alpha$	Pitch difference α (μm)	$n\alpha$
25	100	17	102
30	120	20	120
38	152	25	150
45	180	30	180

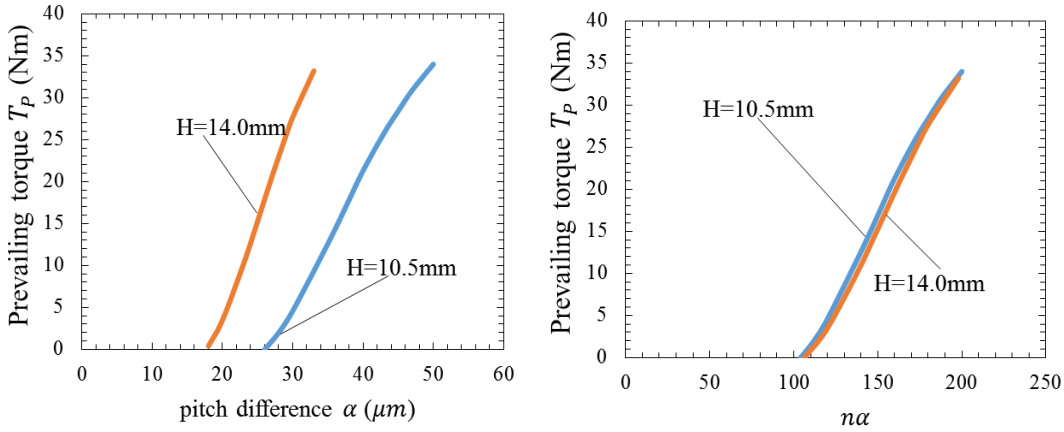

(a) T_p versus α (b) T_p versus $m\alpha$

Fig. 4.7 Prevailing torque T_p controlled by the total pitch difference $m\alpha$

Including untightening process, Fig. 4.8 shows the whole $F-T$ relation for (a) $H = 10.5$mm, $\alpha = 45$μm and (b) $H = 14.0$mm, $\alpha = 30$μm. The results for the common nut $\alpha = 0$ are also indicated by the solid grey lines. For $\alpha = 0$, $T_{25\%} = 45$Nm provides $F = F_{25\%} = 16.8$kN. When the nut is tightened by $T \leq T_{25\%} = 45$Nm, Fig. 4.8 shows the clamping force F is almost the same, which is about 72% of $F = F_{25\%} = 16.8$kN for $\alpha = 0$. Fig. 4.8 confirms that the $F-T$ relations are almost identical for (a) H =10.5mm, $\alpha = 45$μm and (b) H =10.5mm. In Fig. 4.8, the FEM results denoted by the solid line coincide well with the experimental results denoted by the doted points.

Fig. 4.9 shows the $F-T$ relation when the nut is tightened by $T \leq T_{50\%} = 85$Nm. For $\alpha = 0$, $T_{50\%} = 85$Nm provides $F = F_{50\%} = 33.8$kN. During the tightening $T \leq T_{50\%} = 85$Nm, the $F-T$ relation when $\alpha = 0$ coincides with the $F-T$ relation of $\alpha = 30\mu m$ and $\alpha = 45\mu m$ when T is large enough. As shown in Fig. 4.9, the $F-T$ relations are also identical for (a) H =10.5mm, $\alpha = 45$μm and (b) H =14.0mm, $\alpha = 30$μm.

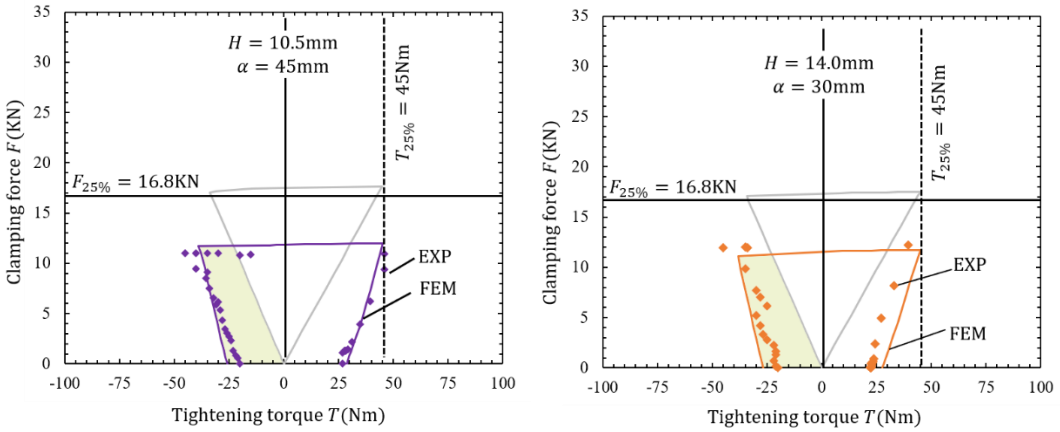

(a) $H = 10.5\text{mm}, \alpha = 45\mu\text{m}$ (b) $H = 14.0\text{mm}, \alpha = 30\mu\text{m}$

Fig. 4.8 F-T relations are identical when the total pitch difference $m\alpha = 180$ for (a) $H = 10.5\text{mm}, \alpha = 45\mu\text{m}$ and (b) $H = 14.0\text{mm}, \alpha = 30\mu\text{m}$ under $T \leq T_{25\%} = 45\text{Nm}$

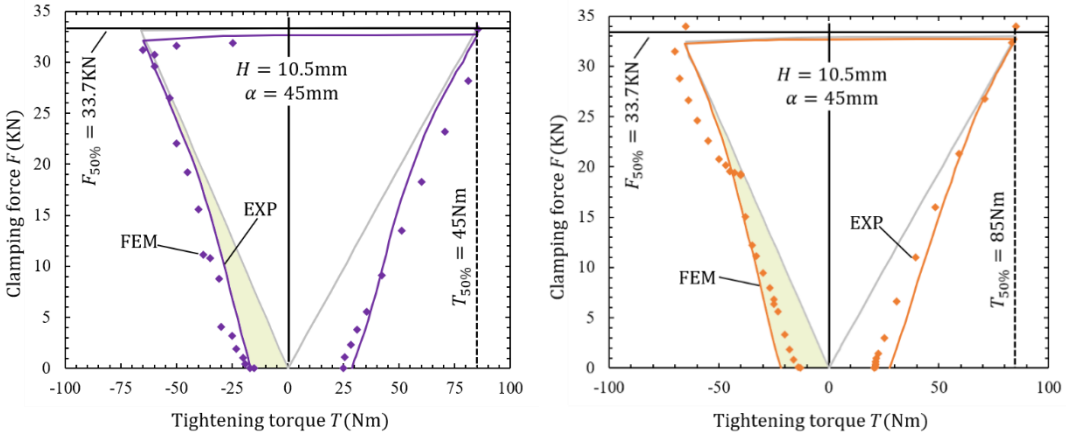

(a) $H = 10.5\text{mm}, \alpha = 45\mu\text{m}$ (b) $H = 14.0\text{mm}, \alpha = 30\mu\text{m}$

Fig. 4.9 F-T relations are identical when the total pitch difference $m\alpha = 180$ for (a) $H = 10.5\text{mm}, \alpha = 45\mu\text{m}$ and (b) $H = 14.0\text{mm}, \alpha = 30\mu\text{m}$ under $T \leq T_{50\%} = 85\text{Nm}$

In Fig. 4.8 and Fig. 4.9, $T \geq 0$ represents tightening, and $T < 0$ represents untightening. During $T \geq 0$, the nut can be tightened by the experimental device in Fig. 4.3, recording T and F on the device. However, during $T < 0$, the nut is untightened by a torque wrench by hand, including relatively larger errors in T and F. In addition, some other aspects may cause errors. First, there is a manufacturing error in the pitch, which has been discussed in the authors' previous paper [81]. Second, since the material is softer than that of the bolt, thread wear may happen during the tightening process, especially when the pitch difference is larger. Thus, there might be a slight shape change of the thread of the nut, and the friction coefficient may change accordingly. Furthermore, the friction coefficients are not the same in the tightening and untightening process, even though fluctuating in a small range. In the FE analysis, the

friction coefficients have to be a constant value. Overall, the $F-T$ relations are in good agreement in the experiment and FEM simulation. In the next section 4.3.3, the same anti-loosening will be confirmed directly by performing the loosening simulation for $H=10.5\text{mm}$ with $m=4$ and $H=14.0\text{mm}$ with $m=6$ in Table 4.3.

4.3.3 FEM simulation for nut loosening

In this study, FEM simulation is performed to confirm the anti-loosening ability more directly than the prevailing torque T_P and the $F-T$ relations. Two loosening tests are popularly used to measure the anti-loosening performance of bolt nut connections. One is the transverse impact vibration test based on NAS 3350 (National Aerospace Standard), and the other is the Junker test, whose loosening process is adopted in international fastener standards such as DIN 65151. Since the vibration in the NAS3350 test is time-depending and complex, this study focuses on the Junker test, where transverse cyclic vibration is applied based on DIN 65151.

Fig. 4.10(a) shows a schematic illustration of a Junker test. Under constant alternative transverse displacement is applied to the movable plate, the loosening of s. Fig. 4.10(b) shows the simplified model for FEM loosening simulation in this study. As a boundary condition, the bolt head is fixed, and the bolt head side of the clamped body is fixed in the bolt axial direction. Then, the cyclic transverse displacement is applied to the movable plate as $u_x=\pm u_{x0}=\pm 0.7\text{mm}$. In the simulation, the initial nut tightening force is set as $F_{25\%}=16.8\text{kN}$. Then, the clamped movable body vibrates for 20 cycles so that the change of clamping force can be obtained. FEM software ANSYS workbench 16.2 is used for 3D FEM simulation. Bilinear elastoplastic stress-strain relations are applied to save the calculation time. Newton-Raphson's approach is used to solve the problem.

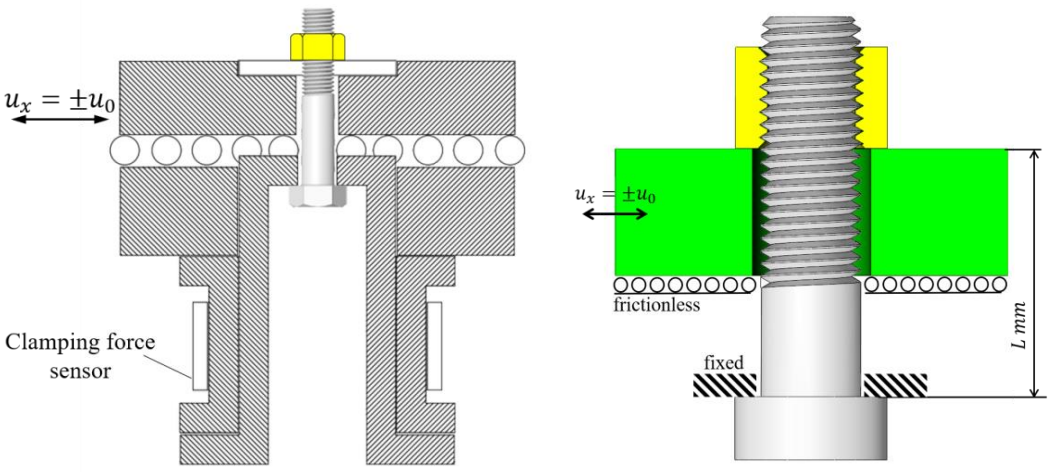

(a) Schematic illustration of a Junker test (b) Simplified FEM model

Fig. 4.10 Schematic illustration of a Junker test and FEM simulation model

Fig. 4.11 shows the variation of clamping forces F under alternative transverse

loading in Fig. 10 when the total pitch difference $m\alpha = 0, 100, 120, 150\mu m$. It is seen that with increasing $m\alpha$ the reduction rate of F decreases. For example, Fig. 4.11(b) shows some differences between the two lines, but they are close and different from Fig. 4.11(a) and Fig. 4.11(c). From Fig. 4.11(a)-(d), it may be concluded that the anti-loosening performance is almost the same under the same $m\alpha$. In other words, the same anti-loosening performance can be expected under the same $m\alpha$. Therefore, the same anti-loosening can be obtained by smaller α with increasing H. This is useful for improving anti-loosening because under standard H the suitable $\alpha 1$ for the fatigue strength is relatively smaller than the suitable $\alpha 2$ for the anti-loosening as $\alpha 1 < \alpha 2$ (see Fig. 4.1).

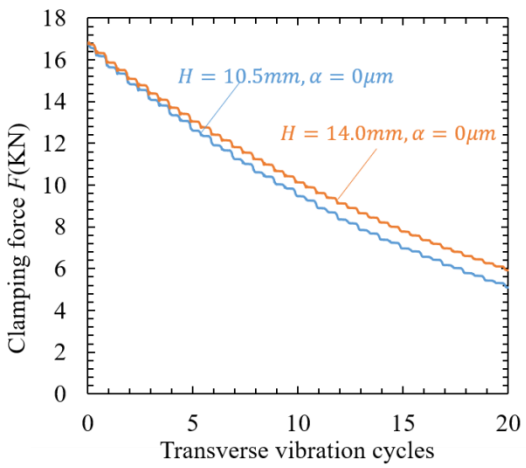

(a) $m\alpha = 0$, H=10.5mm, $\alpha = 0\mu m$ vs $m\alpha = 0$, H=14.0mm, $\alpha = 0\mu m$

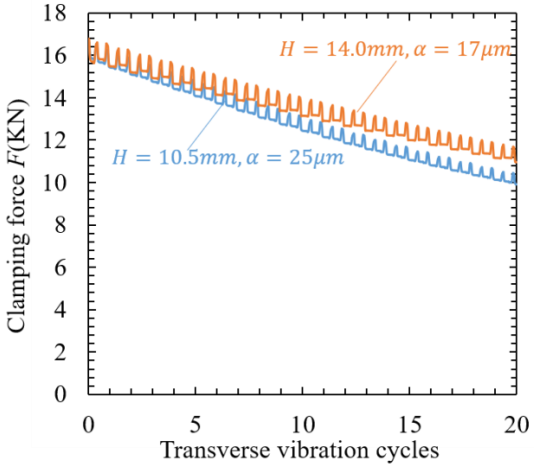

(b) $m\alpha = 100$, H=10.5mm, $\alpha = 25\mu m$ vs $m\alpha = 102$, H=14.0mm, $\alpha = 17\mu m$

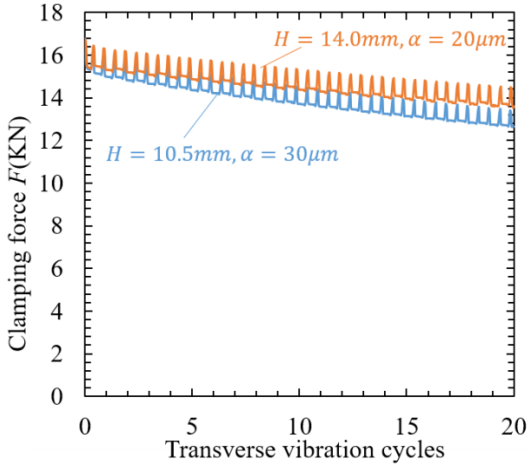

(c) $m\alpha = 120$, H =10.5mm, $\alpha = 30\mu m$ vs $m\alpha = 120$, H=14.0mm, $\alpha = 20\mu m$

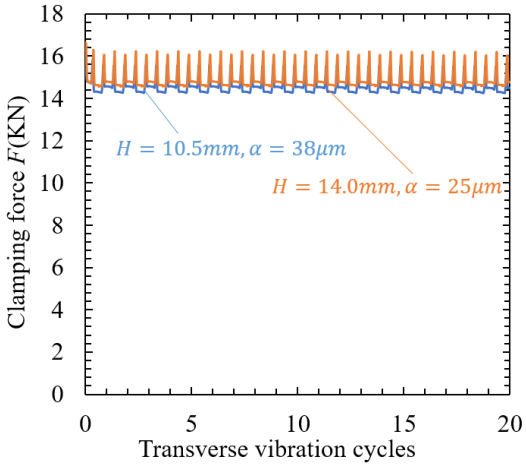

(d) $m\alpha = 152$, H=10.5mm, $\alpha = 38\mu m$ vs $m\alpha = 150$, H=14.0mm, $\alpha = 25\mu m$

Fig. 4.11 Variation of clamping forces F due to alternative transverse vibration in Fig. 4.10

4.4 Fatigue strength by varying nut height and pitch difference

4.4.1 FEM simulation for fatigue strength

In this section, the effect of H on fatigue strength is discussed. The authors' previous studies [76,77] indicated that $\alpha = 15\mu m$ in JIS M16 bolt–nut improves the fatigue life by about 1.5 times compared to $\alpha = 0$ although the fatigue limit does not increase. The recent study [107] showed that both the fatigue limit and the fatigue life can be significantly improved by enlarging the thread root radius and introducing an appropriate pitch difference at the same time.

Fig. 4.12(a) and 4.12(b) illustrate the axisymmetric FEM model for the nut heights $H = 10.5\text{mm}$ and $H = 14.0\text{mm}$ considering the real nut thread in Fig. 4.2(c). To clarify the stress concentration, the bolt thread roots are numbered as -3, -2, -1, 1, 2, 3, …as shown in Fig. 4.12(a) and 4.12(b). In this modeling, the bolt head side of the clamped body is fixed as shown in Fig. 4.12(c); then, after tightening of the nut, a sinusoidal periodic load is applied on the bolt head. The average stress $\sigma_m = 213\text{MPa}$ and the stress amplitude $\sigma_a = 100\text{MPa}$ are applied, which are used in the authors' previous research [76]. Then, the corresponding cyclic load F_c is $F_c = 16.2 \pm 7.6KN$.

The bolt material and the clamped plate material are SCM435 and the nut material is S45C to match the experiment. Multi-linear isotropic hardening shown in Fig. 3.10 is applied to express the plasticity following Von Mises yield criterion. The smallest element dimensions around the thread roots are about $0.01mm \times 0.005mm$. FEM software MSC.Marc/Mentat 2012 is used for the axisymmetric analysis. The total number of elements is 10680 for the nut $H = 10.5\text{mm}$, and about 40000 for the bolt and the clamped body.

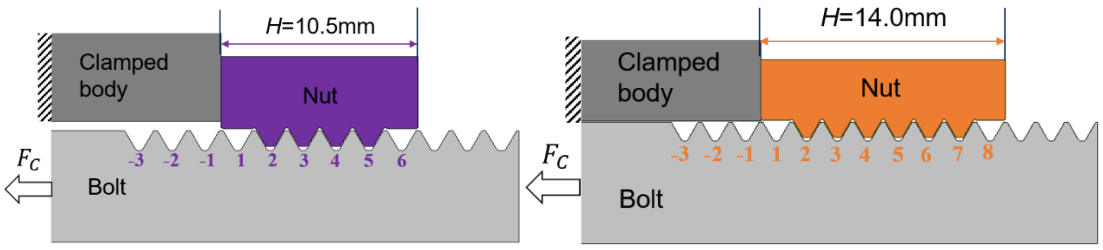

(a) Axisymmetric model for H =10.5mm (b) Axisymmetric model for H =14.0mm

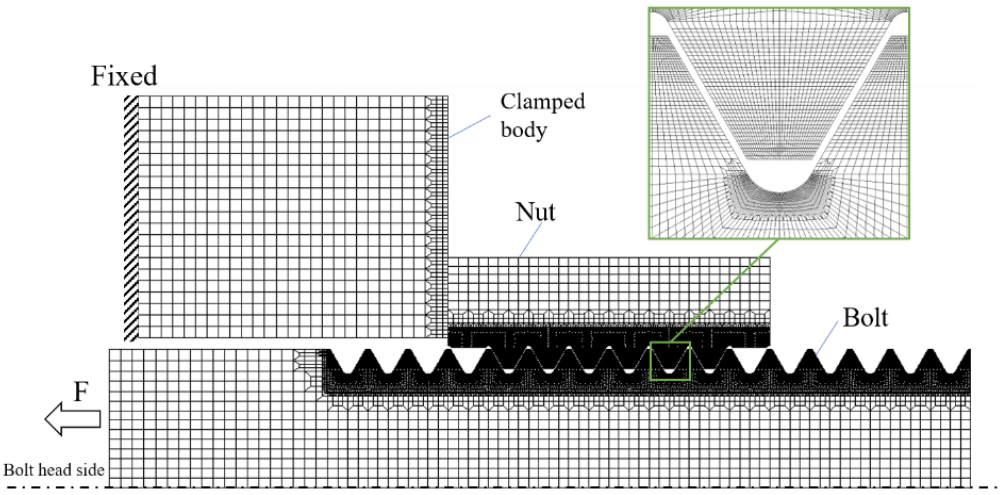

(c) FEM mesh for H =14.0mm, $\alpha = 0\mu m$

Fig. 4.12 Axisymmetric FEM model with the bolt thread number and FEM mesh for fatigue strength analysis where the bolt root radius $\rho = \rho_0 = 0.25mm$ is the standard of M12 bolt

4.4.2 Endurance limit diagram with stress at each thread

Fig. 4.13(a) shows the endurance limit diagram at each thread under the average stress $\sigma_m = 213\text{MPa}$ and the stress amplitude $\sigma_a = 100\text{MPa}$. In this paper, among the several studies [97–100] the Soderberg line of a plain specimen is used to discuss the relative hazard at the bolt roots. Here, σ_w represents the fatigue strength under reversal stress σ_m =0 and σ_y is the yield strength. The maximum tangential stress at each thread obtained by the FEM is plotted in terms of the stress amplitude σ_a = $(\sigma_{max} - \sigma_{min})$ / 2 and the mean stress σ_m = $(\sigma_{max} + \sigma_{min})$ / 2. Due to no stress gradient in plain specimens, the fracture stress in notched specimens is always larger than that in the plain specimens. Therefore, it should be noted that the stress data plotted beyond the line ((σ_m/σ_y)+(σ_a/σ_w) >1) does not represent the real fracture at the bolt thread.

When $\alpha = 0$, independent of H, Fig. 4.13(a) illustrates the most dangerous position locates at $No.2$ thread, which is the first engaged thread from the bolt head side. Fig. 4.13(b) and 4.13(c) show the maximum and minimum tangential stress along the arc of the thread roots. The stress amplitude at $No.2$ thread for $H = 10.5\text{mm}$ is almost the same as that of $H = 14.0\text{mm}$. When $\alpha = 0$, independent of H, the crack initiates at $No.2$ threads, causing a final fracture at the same thread [ref].

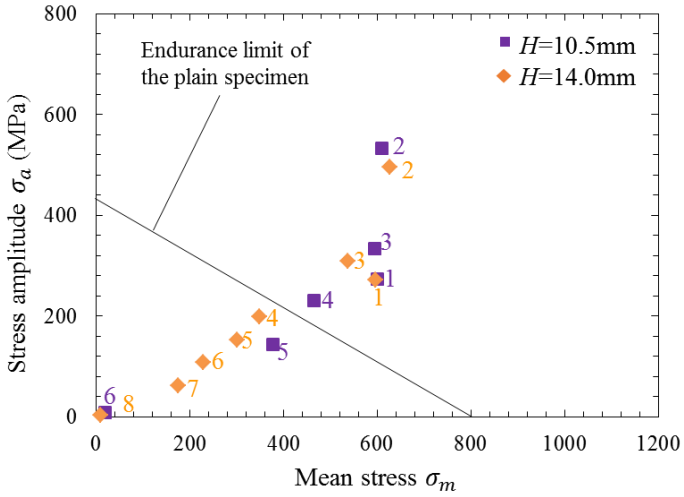

(a) Endurance limit for $H = 10.5\text{mm}$, $\alpha = 0$ and $H = 14.0\text{mm}$, $\alpha = 0$ where the bolt thread number in Fig. 4.12(a),(b) is indicated

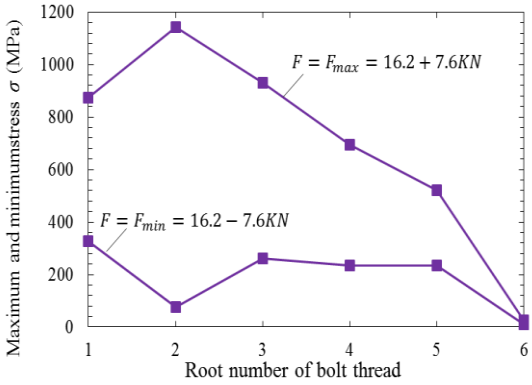

(b) Maximum and minimum stresses at each thread root for $H = 10.5\text{mm}$, $\alpha = 0$

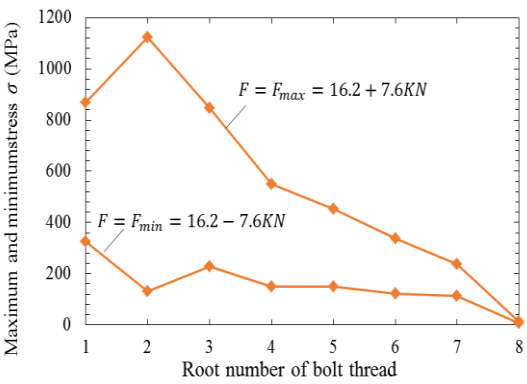

(c) Maximum and minimum stresses at each thread root for $H = 14.0\text{mm}$, $\alpha = 0$

Fig. 4.13 Stress at each thread under the average stress $\sigma_m = 213\text{MPa}$ and the stress amplitude $\sigma_a = 100\text{MPa}$ for $H = 10.5\text{mm}$, $\alpha = 0$ and $H = 14.0\text{mm}$, $\alpha = 0$ where the bolt thread number in Fig. 4.12 (a),(b) is indicated

For $\alpha = 15\mu\text{m}$ in M12 bolt-nut, Fig. 4.14(a) shows the endurance limit diagram under the average stress $\sigma_m = 213\text{MPa}$ and the stress amplitude $\sigma_a = 100\text{MPa}$. It is seen that the most dangerous thread is $No.5$ or $No.6$ when $H = 10.5\text{mm}$ and $No.6$ or $No.7$ when $H = 14.0\text{mm}$. The previous studies also showed that for $\alpha = 15\mu\text{m}$ in JIS M16 bolt-nut, the most dangerous thread is $No.6$ or $No.7$ [ref]. Fig. 4.14(b) and 4.14(c) show the maximum and minimum tangential stress along the arc of the thread roots with $\alpha = 15\mu\text{m}$. For $H = 10.5\text{mm}$, the maximum stress amplitude and the maximum mean stress loactes at $No.4$ and $No.5$ thread, and for $H = 14.0\text{mm}$, the maximum stress amplitude and the maximum mean stress locates at $No.6$ and $No.7$ thread. As shown in Fig. 4.14(a), (b), (c), the maximum stress amplitude and the maximum mean stress are almost the same for $H = 10.5\text{mm}$ to $H = 14.0\text{mm}$. In other words, the fatigue life of the nut with a pitch difference $\alpha = 15\mu\text{m}$ is almost the

same independent of the nut height form H. Different from $\alpha = 0$, when $\alpha \geq 15\mu m$ the initial crack occurs from the right bolt end side and then propagate to the left bolt head side. Since the crack initiates at $No.2$ threads causing final fracture, the fatigue life can be extended [76].

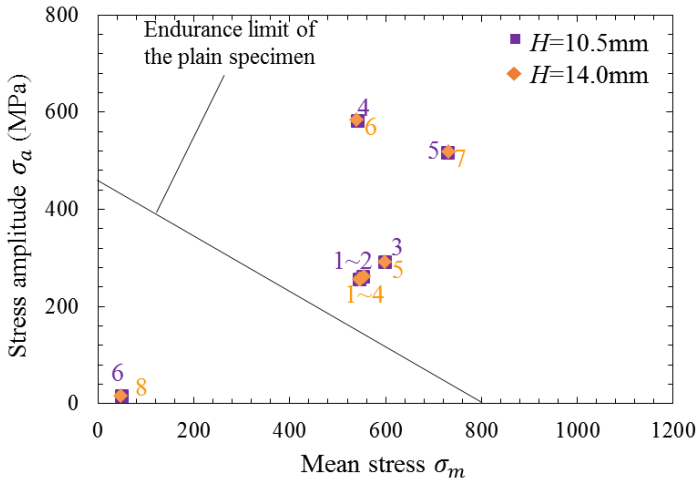

(a) Endurance limit for $H = 10.5\text{mm}$, $\alpha = 15\mu m$ and $H = 14.0\text{mm}$, $\alpha = 15\mu m$ where the bolt thread number in Fig. 4.12(a),(b) is indicated

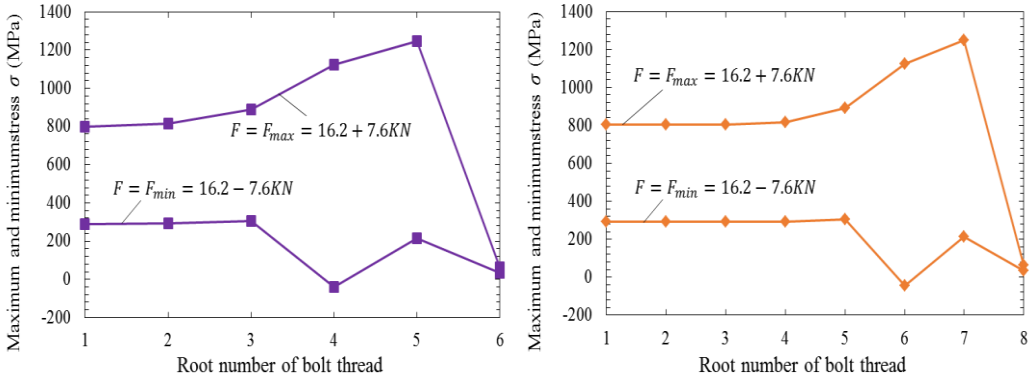

(b) Maximum and minimum stresses at each thread root for $H = 10.5\text{mm}$, $\alpha = 15\mu m$

(c) Maximum and minimum stresses at each thread root for $H = 14.0\text{mm}$, $\alpha = 15\mu m$

Fig. 4.14 Stress at each thread under the average stress $\sigma_m = 213\text{MPa}$ and the stress amplitude $\sigma_a = 100\text{MPa}$ for $H = 10.5\text{mm}$, $\alpha = 15\mu m$ and $H = 14.0\text{mm}$, $\alpha = 15\mu m$ where the bolt thread number in Fig. 4.12 (a),(b) is indicated

For $\alpha = 25\mu m$ in M12 bolt-nut, Fig. 4.15 shows the endurance limit diagram when $H = 10.5\text{mm}$ and $H = 14.0\text{mm}$. It is seen that the most dangerous thread is $No.5$ when $H = 10.5\text{mm}$ and $No.7$ when $H = 14.0\text{mm}$, and the second most dangerous thread is $No.4$ when $H = 10.5\text{mm}$ and $No.6$ when $H = 14.0\text{mm}$. The stress amplitude for $H = 10.5\text{mm}$ at $No.5$ thread is 10.0% larger than the stress amplitude for $H = 14.0\text{mm}$ at $No.7$ thread, but the mean stress for $H = 14.0\text{mm}$ at $No.7$

thread is 4.7% larger than the mean stress for $H = 10.5\text{mm}$ at $No.5$ thread. Overall, it may be concluded that the fatigue strength is almost the same independent of H under $\alpha = 25\mu\text{m}$.

In this section 4.4, the FEM simulation was performed to investigate the effect of H on fatigue strength. From Fig. 4.13, Fig. 4.14, Fig. 4.15, it may be concluded that the fatigue strength of pitch difference nut connections is controlled by α alone independent of H. In section 4.3, it was found that the same anti-loosening can be obtained by smaller α with increasing H. Therefore, both fatigue strength and anti-loosening can be improved by the larger nut height H and relatively smaller α.

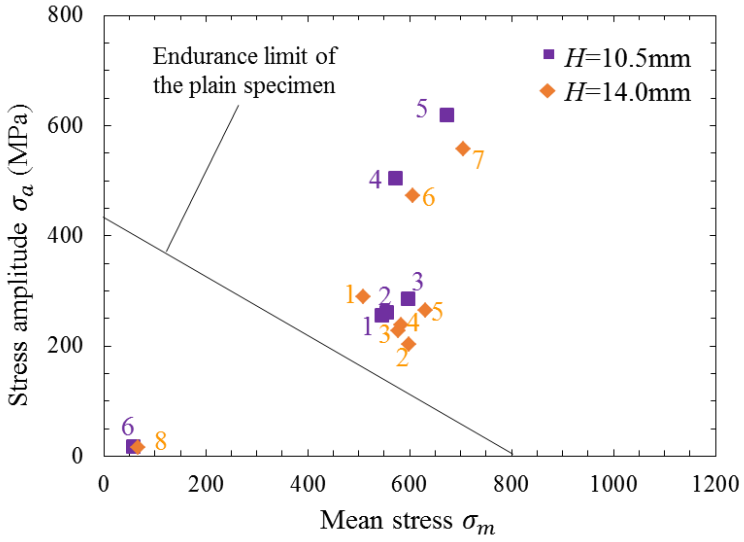

Fig. 4.15 Endurance limit under the average stress $\sigma_m = 213\text{MPa}$ and the stress amplitude $\sigma_a = 100\text{MPa}$ for $H = 10.5\text{mm}$, $\alpha = 25\mu\text{m}$ and $H = 14.0\text{mm}$, $\alpha = 25\mu\text{m}$ where the bolt thread number in Fig. 4.12(a),(b) is indicated

4.5. Conclusions

In this paper, how to improve both anti-loosening and fatigue strength with low cost was newly proposed for bolt-nut connection. The authors' previous study clarified that the most suitable pitch difference $\alpha = \alpha 1$ for the fatigue strength is smaller than the most suitable pitch difference $\alpha = \alpha 2$ for the anti-loosening (see Fig. 4.1). Toward improving both fatigue strength and anti-loosening, this study newly considers larger nut height coupled with pitch difference. The conclusions are summarized as follows.

(1) The anti-loosening performance of pitch difference nut is controlled by the total pitch difference $m\alpha$, that is, the product of the number of nut thread m and pitch difference α. The same anti-loosening performance was confirmed under the same $m\alpha$.

(2) When the pitch difference is within 25μm, the fatigue strength of pitch difference nut connections is controlled by α alone independent of m. The same fatigue strength

was confirmed under the same α independent of m.

(3) A larger nut height having relatively smaller pitch difference $\alpha = \alpha 3 \approx \alpha 1 < \alpha 2$ is suitable for improving both fatigue strength and anti-loosening.

Chapter 5. Conclusions and suggestions for future works

5.1 main conclusions

The anti-loosening performance of bolt nut connections with difference pitches is studied by Junker's type loosening test. Besides, the anti-loosening mechanism of bolt nut connections with pitch differences are investigated by using finite simulation. Moreover, aiming at obtaining better combination of fatigue life and anti-loosening performance of low-cost pitch bolt nut connections, pitch difference effect and nut height effect on fatigue and anti-loosening of pitch difference bolt nut connections are studied. The conclusions and suggestions are summarized as following.

(1) The anti-loosening performance of M12 bolt nut connections with a height of H=10.0mm and a pitch difference of $\alpha = 0, 35, 40, 50\mu m$ are obtained by experiments and FE analysis. It is found when the clamping force F is 15kN, the anti-loosening performance of $\alpha = 40, 50\mu m$ meets the DIN standard, for which the residual clamping force should be no less than 80% of the initial clamping force after a certain transverse vibration cycle. When the pitch difference is $\alpha = 35\mu m$, although the residual clamping force is less than 80% of the initial clamping force, the residual clamping force is about 4.5kN after 500 cycles of vibration and is about 4kN after 1500 cycles of vibration and almost remains steady. That is to say, a loosening resistance of the bolt nut connection is remaining.

(2) The loosening process of the nuts is simulated by using a simplified 3D Junker's type loosening test model, and the findings are as following. For common bolt nut connections, the loosening and the un-loosening process occurs alternately until the residual clamping force decreases to 0. When the pitch difference is $\alpha = 35\mu m$, the loosening and the un-loosening process occurs alternately as common bolt nut connections at the early stage of loosening until two ends of the nut contacts the bolt, and the loosening, un-loosening, and tightening process occurs alternately. Besides, with the decreasing of clamping force, the tightening angle increases, and the tightening angle almost equals to the loosening angle in one cycle until the clamping force decreases to a certain value.

(3) In the FEM analysis, when the pitch difference is no less than 40 μm, the clamping force decreases at the beginning of vibration. This is mainly due to the elastic twist energy stored in the tightening process released. After this, loosening, un-loosening, and the tightening process occur alternately, and the tightening angle almost equals to the loosening angle in one vibration cycle, it means the nut does not loose. This coincides with the experimental results well.

(4) For high strength JIS M16 bolt nut connections, the fatigue life can be extended by introducing a suitable pitch difference between the nut and the bolt. The stress concentration factor at thread roots can be decreased by increasing the thread root radius.

Thus, the fatigue life of bolt nut connections can be further extended; besides, the fatigue strength of the bolt nut connections can also be extended. For example, the stress concentration factor at thread roots can be decreased from 4.53 to 2.90 by increasing the thread root radius from ρ to 2ρ, and the fatigue life and fatigue strength of bolt nut connections with a pitch difference of $\alpha = 15\mu m$ and $\rho = 2\rho_0$ is about 2.6 times and 1.67 times of that of common bolt nut connections ($\alpha = 0\mu m$ and $\rho = \rho_0$).

(5) From the observation of the specimens after the fatigue test, it is confirmed that for the bolt nut connections with enlarged root radius, both the initial cracks and final fracture occurs at the first engaged thread at the bearing surface side of the nut (No. 6 or No. 7 thread) when there is no pitch difference between the bolt and the nut. Initial cracks occur at the free end side of the engaged part and extend to the other side until the final fracture occurs at the bearing surface side (No. 1 or No. 2 thread).

(6) According to the F-T relation by 3D FEM, when $\rho = 2\rho_0$ and α=33μm, it was confirmed that the prevailing torque T_P= 19Nm and the residual prevailing torque $T_P^u = 10\text{Nm}$ even at F_t=0. Since those values are not smaller compared to other special nuts, good anti-loosening performance can be expected for the enlarged root radius of bolt-nut connections under the suitable pitch difference.

(7) The F-T relation for bolt nut connections are obtained by experiments and 3D simulation. It is found that the prevailing torque is close when the product of the pitch difference α and complete thread number m is the same. Besides, the anti-loosening performance of bolt nut connections with different pitch differences and nut height are simulated by Junker's type loosening test. It is confirmed that the anti-loosening performance of pitch difference nut is controlled by the total pitch difference $m\alpha$, that is, the product of the number of nut thread m and pitch difference α.

(8) For bolt nut connections with a pitch difference within $\alpha = 25\mu m$, the fatigue strength of pitch difference nut connections is controlled by α alone independent of n. The same fatigue strength was confirmed under the same pitch difference α independent of complete thread number m.

(9) A larger nut height having relatively smaller pitch difference $\alpha = \alpha 3 \approx \alpha 1 < \alpha 2$ is suitable for improving both fatigue strength and anti-loosening.

5.2 Suggestions for future works

For prevailing torque type nut, the geometry change of the nut creates interference between the nut and bolt threads, and thereby helps the fastener resist loosening. Bickford thinks the prevailing torque is not an addition to the thread friction component of torque but a function of the design of the nut, and of the material used, as well as geometry [36]. The relation between the torque and clamping force in the tightening process (Eq. 5.1) and the loosening process (Eq. 5.2) suggested as following[36-38]:

$$T = \frac{F}{2}\left(\frac{d_2}{cos\beta}\mu_s + \frac{P}{\pi} + d_w\mu_w\right) + T_P = FKD + T_P \quad (5.1)$$

$$T = \frac{F}{2}\left(-\frac{d_2}{cos\beta}\mu_s + \frac{P}{\pi} - d_w\mu_w\right) - T_P \tag{5.2}$$

Here, T_P represents the prevailing torque, and all other terms are the same as Eq. (4.1).

Fig. 4.8 and Fig. 4.9 show the relationship between tightening torque and clamping force with different nut height and pitch differences. In those sub-figures, the part where the tightening torque is positive represents the tightening process, and the part where the tightening torque is negative represents the untightening process. In the tightening process, the nut can be tightened by the machine, and in the meanwhile, the values of tightening torque and clamping force can be recorded. In the untightening process, the nuts are untightened by a torque wrench. Therefore, the error of the tightening torque and the clamping force in the untightening process may be larger than that of the tightening process. In addition, some other aspects may cause errors. First, there is a manufacturing error in the pitch. Second, since the material is softer than that of the bolt, thread wear may happen during the tightening process, especially when the pitch difference is too big. Thus, there might be slightly shape change of the thread of the nut, and friction coefficient may change accordingly. Furthermore, the friction coefficients are not the same in the tightening and untightening process, even though fluctuating in a small range. In the FE analysis, the friction coefficients are assumed to be a constant value. In a general view, the experimental results and FEM results of the relation between tightening torque and clamping force coincide with each other.

From Fig. 4.8 and Fig. 4.9, it can be seen that Eq. 5.1 and Eq. 5.2 are not proper for pitch difference bolt nut connections. For pitch difference bolt nut connections, the slope ratio of the relation between tightening torque and clamping force of pitch difference bolt nut connections is greater than that of common bolt nut connections in the early stage of the tightening process. When the clamping force reaches to a certain value, the relation between the pitch difference bolt nut connections and common bolt nut connections become the same. This is different from Eq. 5.1. This may be caused by the plastic deformation of the thread and even by wear. The present work does not provide an equation of F-T relation for pitch difference bolt nut connection, and this can be studied in a further step.

Appendix A

Fig. A.1 illustrates the $F-T$ relation (the clamping force F versus the tightening torque T) for $\alpha = 45\mu m$ and $H = 10.5mm$ obtained by FEM analysis [81,84,85]. The green line of $\alpha = 45\mu m$ is compared with the gray line of $\alpha = 0$. For example, Fig. A.1(b) shows the $F-T$ relation during the nut position changed as $E \rightarrow F \rightarrow G \rightarrow G_u \rightarrow F_u \rightarrow E_u$ in Fig. 3.13.

The clamping force *F* appears by applying $T > 0$ for $\alpha = 0$. Instead, the clamping force F of $\alpha = 45\mu m$ appears by applying $T \geq T_P$ when the torque exceeds the prevailing torque T_P. The prevailing torque T_P can be defined in Eq. (A.1) at E in Fig. 3.13.

$$T_P \equiv \sup T \ when \ F = 0, \ T > 0 \tag{A.1}$$

With increasing $T \geq T_P$, the clamping force F increases. When $T = T_{25\%}$ or $T = T_{50\%}$, F becomes largest as $F = F_{max}$ at F in Fig. 3(e) as shown in Eq. (A.2).

$$F_{max} \equiv Max|F| \ when \ T = T_{25\%} \ or \ T = T_{50\%} \tag{A.2}$$

Here, $T_{25\%} = 45Nm$ is the torque T producing $F = F_{25\%} = 16.8kN$ for $\alpha = 0$ and $T_{50\%} = 85Nm$ is the torque T producing $F = F_{50\%} = 33.8kN$ for $\alpha = 0$. It should be noted that $F = F_{max}$ varies depending on α.

After T reaches $T = T_{25\%}$ or $T = T_{50\%}$, untightening torque is applied as $T < 0$. Initially, F is almost constant as $F \approx F_{max}$ since the bolt-nut rotates together. After $|T|$ reaches the slip torque T_{slip} defined in Eq. (A.3), the nut rotates independently. Then, F starts decreasing with decreasing $|T|$ as $F < F_{max}$ from Point G_u in Fig. A1(b).

$$T_{slip} \equiv Max|T| \ when \ T < 0 \ after \ T = T_{25\%} \ or \ T = T_{50\%} \tag{A.3}$$

As shown in $G_u \rightarrow F_u$ in Fig. A1, during F decreasing under untightening $T < 0$, initially the $F-T$ relations are equal for $\alpha = 45\mu m$ and $\alpha = 0$. During $F_u \rightarrow E_u$ in Fig. A1, the light green zone illustrates the difference between $\alpha = 0$ and $\alpha = 45\mu m$. The difference can be considered as a loosening resistance torque T_R^u contributing to anti-loosening, which is defined in Eq. (A.4) [85].

$$T_R^u \equiv |T|_{\alpha>0} - |T|_{\alpha=0} \ when \ T < 0,$$

$$T_R^u > 0 \ when \ 0 \leq F < h, \ i.e. \ h \equiv \sup F \ when \ T_R^u > 0 \tag{A.4}$$

At E_u in Fig. A.1, even no tightening force $F = 0$, $T_R^u > 0$. Therefore, the loosening resistance torque T_R^u can be characterized at the value when $F = 0$. The value T_R^u at $F = 0$ can be named the residual prevailing torque and defined in Eq. (A.5).

$$T_P^u \equiv T_R^u \ when \ F = 0 \tag{A.5}$$

The residual prevailing torque T_P^u above may represent the anti-loosening performance [85]. However, T_R^u is changing during $F_u \rightarrow E_u$. Therefore, the median

loosening resistance torque can be considered and defined in Eq. (A.6).

$$\tilde{T}_R^u \equiv |T|_{\alpha>0} - |T|_{\alpha=0} \ when \ F = h/2 \ and \ T < 0 \tag{A.6}$$

The median loosening resistance torque may represent T_R^u variation during $F_u \rightarrow E_u$. Regarding the normal nut $\alpha = 0$, $T_P = T_R^u = T_P^u = \tilde{T}_R^u = 0$.

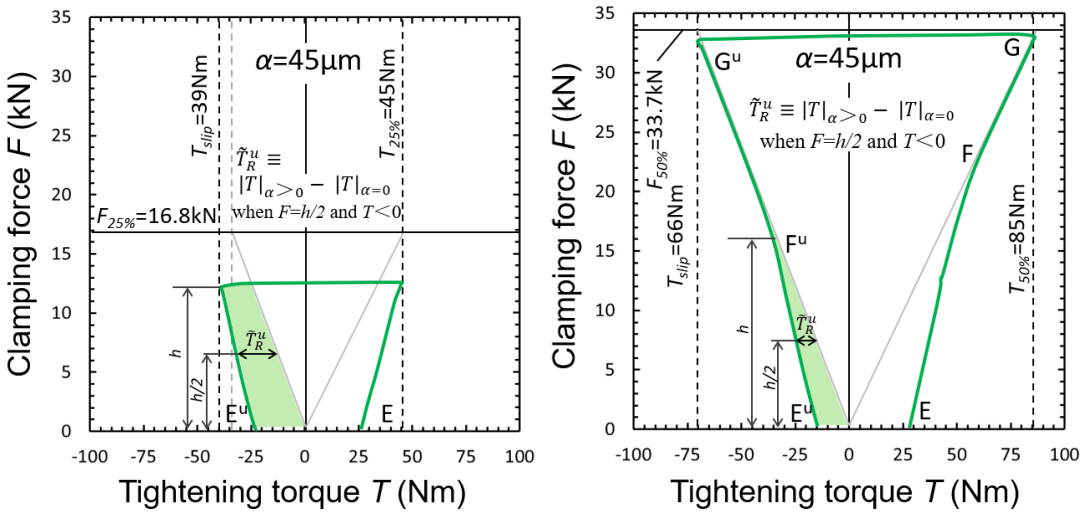

(a) $F-T$ relation when $\alpha = 45\mu m$ under $T \leq T_{25\%} = 45Nm$. (b) $F-T$ relation when $\alpha = 45\mu m$ under $T \leq T_{50\%} = 85Nm$.

Fig. A 1 $F-T$ relation (Clamping force F versus tightening torque T relation)

Appendix B

Table B.1 summarizes experimentally obtained prevailing torque T_P, residual prevailing torque T_P^u, median loosening resistance torque $\tilde{T}_R^u$, clamping force F, slipping torque T_{slip} defined in Appendix A by varying M12 pitch difference α when the nut height $H = 10.5\text{mm}$ and $H = 14.0\text{mm}$.

Table B. 1 Prevailing torque T_P, residual prevailing torque T_P^u, median loosening resistance torque $\tilde{T}_R^u$, tightening force F, slip torque T_{slip} for (a) $T \leq T_{25\%} = 45Nm$ and (b) $T \leq T_{25\%} = 85Nm$ obtained by FEM (Definitions of T_P, F, T_{slip}, T_P^u, $\tilde{T}_R^u$ are indicated in Appendix A)

(a) $T \leq T_{25\%} = 45Nm$

Nut Height(mm)	Pitch difference (μm)	T_P (Nm)	F (kN)	T_{slip} (Nm)	T_P^u (Nm)	$\tilde{T}_R^u$	$m\alpha$
10.5	28	2.0	17.3	34.8	1.7	0.8	112
	30	4.6	17.3	34.8	4.1	2.1	120
	35	12.6	17.3	34.8	12.0	6	140
	38	17.8	16.9	34.8	16.9	8.9	152
	40	21.5	15.6	35.5	20.1	12.2	160
	45	28.8	12.0	38.9	25.7	20	180
14.0	*18*	0.4	17.4	35.0	0.3	0.2	108
	20	3.5	17.4	34.5	3.3	1.7	120
	25	15.3	17.3	34.1	15.2	7.6	150
	30	27.7	11.7	38.2	26.8	21.5	180
	35	36.7	4.5	41.5	36.5	34.8	210

(a) $T \leq T_{50\%} = 85Nm$

Nut Height(mm)	Pitch difference (μm)	T_P (Nm)	F (kN)	T_{slip} (Nm)	T_P^u (Nm)	$\tilde{T}_R^u$	$m\alpha$
10.5	28	2.0	32.8	65.7	0.6	0.29	112
	30	4.6	32.8	65.3	1.1	0.55	120
	35	12.6	32.7	64.3	4.8	2.4	140
	38	17.8	32.5	64.6	8.0	4	152
	40	21.5	32.4	64.8	10.5	5.25	160
	45	28.8	32.4	64.9	16.6	8.3	180
14.0	*18*	0.4	32.6	65.0	0.1	0.05	108
	20	3.5	32.6	65.3	1.6	0.8	120
	25	15.3	32.6	65.0	10.8	5.4	150
	30	27.7	32.7	65.5	21.8	10.9	180
	35	36.7	31.9	67.1	32.0	16	210

From Table B.1, it is found that both prevailing torque T_P and residual prevailing torque T_P^u increase with α. When the tightening torque is $T_{25\%} = 45Nm$, with increasing α, the clamping force F remains steady at first and then decreases. When the tightening torque is $T_{50\%} = 85Nm$, the clamping force F remains steady with increasing α The residual prevailing torque T_P^u under a tightening torque of $T_{25\%} = 45Nm$ is larger than that of $T_{50\%} = 85Nm$.

Fig. B.1(a) shows median loosening resistance torque $\tilde{T}_R^u$ vs. α relation obtained by FEM analysis. The loosening resistance torque $\tilde{T}_R^u$ can be larger when the tightening force is not very large. Fig. B.1(b) shows the same $\tilde{T}_R^u$ can be provided when $m\alpha$ is the same.

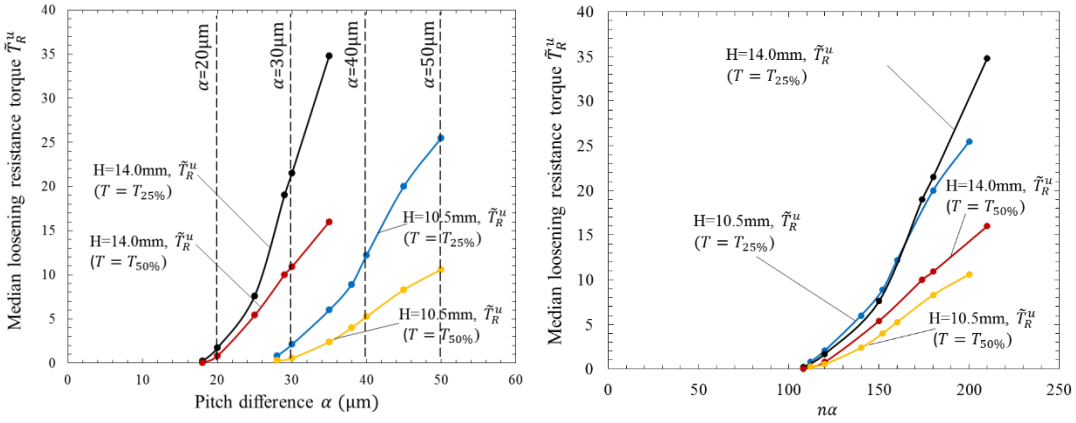

(a) $\tilde{T}_R^u$ versus α relation (b) $\tilde{T}_R^u$ versus mα relation

Fig. B 1 Median loosening resistance torque $\tilde{T}_R^u$ controlled by the total pitch difference $m\alpha$

Appendix C

In Fig. 4.6, Fig. 4.7, Fig. 4.8, Fig. A1, the $F-T$ relations are discussed for $\alpha \geq 20\mu m$ in comparison with the normal nut $\alpha = 0$. To obtain the $F-T$ relation of the normal nut $\alpha = 0$, the following equation proposed by Motosh [102] in Eq. (C.1) can be used conveniently.

$$T = \frac{F}{2}\left(\frac{d_2}{cos\beta}\mu_s + \frac{p}{\pi} + d_w\mu_w\right) \quad \text{(C.1)}$$

where T is the tightening torque, F is the tightening force, d_2 is the pitch diameter of the bolt, β is the half-angle of the thread, μ_s is the thread friction coefficient, p is the pitch of the bolt and nut, d_w is the effective diameter of the bearing surface, μ_w is the under-head friction coefficient, K is the nut factor, D is the nominal diameter.

During untightening $T < 0$ after $|T| = T_{slip}$, the $F-T$ relation of the normal nut $\alpha = 0$ can be expressed in Eq. (C.2) [22].

$$T = \frac{F}{2}\left(-\frac{d_2}{cos\beta}\mu_s + \frac{p}{\pi} - d_w\mu_w\right) \quad \text{(C2)}$$

Regarding the friction coefficients μ_s and μ_w, sometimes the same values are used in the previous studies [103]. The friction coefficients measured in the experiment are in the range μ_s=0.11-0.15 and μ_w=0.16-0.18 at the bearing surface. The ranges of those friction coefficients are close to the values obtained by Liu et al [71,106] and Udagawa[101]. To fit the FEM simulation results with the experimental results, the friction coefficient at the thread surface are chosen as μ_s=0.14 and the friction coefficient at the bearing surface are chosen as μ_w=0.17.

References

[1] F.E.Graves, Nuts and bolts, Sci. Am. (1984) 136–145. https://doi.org/10.1038/scientificamerican0684-136.

[2] P.A.Sidders, Guide to World Screw Threads, Illustrated, Industrial Press, New York, 2009.

[3] W.Sellers, on a system of screw threads and nuts, Seller's Present. to Franklin Inst. (1864) 1–5.

[4] H.Tore, Bolted Joints Study on bolt incidents, Pet. Saf. Authourity Report. No. 2018-5333 Rev. 3. (2019) 1–30.

[5] G.S.Campbell, R.Lahey, A survey of serious aircraft accidents involving fatigue fracture, Int. J. Fatigue. 6 (1984) 25–30. https://doi.org/10.1016/0142-1123(84)90005-7.

[6] N.Goto, S.Endoh, T.Ishikawa, S.Tamura, Y.Shuto, K.Tanak, Aircraft Serious Incident Investigation Report J-Air Corporation JA206J, Janpan Transp. Saf. Board. AI2015 (2015) 1–38. http://www.mlit.go.jp/jtsb/eng-air_report/JA206J.pdf.

[7] J.H.Harris, Summary of Facts and Statement of Opinion RC-135V, T/N 64-14848, United States Air Force Aircr. Accid. Investig. Board Rep. (2015) 1–22.

[8] G.H.Majzoobi, G.H.Farrahi, S.J.Hardy, M.K.Pipelzadeh, N.Habibi, Experimental results and finite-element predictions of the effect of nut geometry, washer and Teflon tape on the fatigue life of bolts, Fatigue Fract. Eng. Mater. Struct. 28 (2005) 557–564. https://doi.org/10.1111/j.1460-2695.2005.00899.x.

[9] F.D.A.Silva, E.S.Guidi, Influence Analysis of Washers Material in Fatigue Life of Bolted Joints, SAE Int. 36 (2015). https://doi.org/10.4271/2015-36-0112.

[10] L.Ji, C.L.Li, X.F.Lu, J.Q.Tang, Z.J.Lin, Y.Liu, Study on the impact on wind power blade root bolt fatigue property of ceramic gasket, FRP/CM. 9 (2017) 93–96.

[11] S.Griza, M.E.G.daSilva, S.V.dosSantos, E.Pizzio, T.R.Strohaecker, The effect of bolt length in the fatigue strength of M24×3 bolt studs, Eng. Fail. Anal. 34 (2013) 397–406. https://doi.org/10.1016/j.engfailanal.2013.09.010.

[12] R.B.Heywood, The Relationship Between Fatigue and Stress Concentration, Aircr. Eng. Aerosp. Technol. 19 (1947) 81–84. https://doi.org/10.1108/eb031482.

[13] C.W.Macgregor, N.Grossman, Effects of cyclic loading on mechanical behavior of 24S-T4 and 75S-T6 aluminum alloys and SAE 4130 steel, 1952.

[14] E.I.Batahgy, A.Monem, Influence of HAZ microstructure and stress concentration on fatigue strength of welded structural steel, Mater. Lett. 21 (1994) 415–423. https://doi.org/10.1016/0167-577X(94)90252-6.

[15] R.A.Walker, R.J.Finkelston, Effect of basic thread parameters on fatigue life, SAE Tech. Pap. (1970) 2529–2539. https://doi.org/10.4271/700851.

[16] E.Dragoni, Effect of thread pitch on the fatigue strength of steel bolts, 211 (1997) 591–600. https://doi.org/10.1243/0954406981521970.

[17] G.H.Majzoobi, G.H.Farrahi, N.Habibi, Experimental evaluation of the effect of thread pitch on fatigue life of bolts, Int. J. Fatigue. 27 (2005) 189–196. https://doi.org/10.1016/j.ijfatigue.2004.06.011.

[18] I.Yoshimoto, K.Maruyama, K.Hongo, T.Sasaki, Investigation on the screw threads profile to improve the fatigue strength, J. Japan Soc. Precis. Eng. 44 (1978) 96–101. https://doi.org/10.2493/JJSPE1933.44.1508.

[19] P.Honarmandi, J.W.Zu, K.Behdinan, Elasto-plastic fatigue life improvement of bolted joints and introducing FBI method, Mech. Based Des. Struct. Mach. 33 (2005) 311–330. https://doi.org/10.1080/15367730500374381.

[20] S.I.Nishida, C.Y.Urashima, H.T.Tamasaki, A new method for fatigue life improvement of screws, Eur. Struct. Integr. Soc. 22 (1997) 215–225. https://doi.org/10.1016/S1566-1369(97)80021-0.

[21] S.I.Nishida, Failure of Fastening Screws and Their Preventive Methods, Faster World. (2019) 290–295.

[22] J.H.Bickford, Introduction to the Design and Behavior of Bolted Joints: Non-Gasketed Joints, in: Fourth edition, CRC Press, 2007: pp. 467–494.

[23] Y.I.Babei, Z.G.Dutsyak, Effect of thread cutting techniques on the fatigue and corrosion-fatigue strength of steel, Sov. Mater. Sci. a Transl. Fiz. Mekhanika Mater. Sci. Ukr. SSR. 3 (1967) 383–391.

[24] M.J.Knight, F.P.Brennan, W.D.Dover, Fatigue life improvement of threaded connections by cold rolling, J. Strain Anal. Eng. Des. 40 (2005) 83–93. https://doi.org/10.1243/030932405X7818.

[25] F.L.Liu, M.L.Sui, MJ screw outer diameter amendment of titanium alloy fasteners , Aeronaut. Stand. &Quality. 3 (2005) 48–50.

[26] P.Zhang, Y.J.Lai, Y.Z.Wang, L.Tian, Y.L.Zhu, Fatigue fracture of TC4 fasteners, Chinese J. Nonferrous Met. 20 (2010) 849–851.

[27] S.Ifergane, N.Eliaz, N.Stern, E.Kogan, G.Shemesh, H.Sheinkopf, D.Eliezer, The effect of manufacturing processes on the fatique lifetime of aeronautical bolts, Eng. Fail. Anal. 8 (2001) 227–235. https://doi.org/10.1016/S1350-6307(00)00013-3.

[28] R.I.Stephens, N.J.Bradley, N.J.Horn, J.J.Gradman, J.M.Arkema, C.S.Borgwardt, Fatigue of high strength bolts rolled before or after heat treatment with five different preload levels, SAE Tech. Pap. (2005). https://doi.org/10.4271/2005-01-1321.

[29] SPS Technologies, Product Engineering Report Number 4718, Fasten. Semin. 1974, Jenkintown, PA 19046, Third Print. (1980).

[30] J.A.Collins, H.Busby, G.Staab, eds., Machine Joints and Fastening Methods, in: Mech. Des. Mach. Elem. Mach. a Fail. Prev. Perspect., Second, John Wiley & Sons, 2010: pp. 485–492.

[31] R.F.Li, D.Y.Zhang, M.L.Cheng, High strength steel large diameter internal thread strengthening by ultrasonic burnishing technology, China Surf. Eng. 27 (2014) 63–68.

[32] M.Cheng, D.Zhang, H.Chen, W.Qin, Development of ultrasonic thread root rolling technology for prolonging the fatigue performance of high strength thread, J.

Mater. Process. Technol. 214 (2014) 2395–2401. https://doi.org/10.1016/j.jmatprotec.2014.05.019.

[33] J.T.Wang, Y.K.Zhang, J.F.Chen, J.Y.Zhou, K.Y.Luo, W.S.Tan, L.Y.Sun, Y.L.Lu, Effect of laser shock peening on the high-temperature fatigue performance of 7075 aluminum alloy, Mater. Sci. Eng. A. 704 (2017) 459–468. https://doi.org/10.1016/j.msea.2017.08.050.

[34] S.Yang, W.Zeng, J.Yang, Characterization of shot peening properties and modelling on the fatigue performance of 304 austenitic stainless steel, Int. J. Fatigue. 137 (2020) 105621. https://doi.org/10.1016/j.ijfatigue.2020.105621.

[35] V.Singh, V.Pandey, S.Kumar, N.C.S.Srinivas, K.Chattopadhyay, Effect of Ultrasonic Shot Peening on Surface Microstructure and Fatigue Behavior of Structural Alloys, Trans. Indian Inst. Met. 69 (2016) 295–301. https://doi.org/10.1007/s12666-015-0771-x.

[36] C.B.O'Sullivan, A.L.Bertone, A.S.Litsky, J.T.Robertson, Effect of laser shock peening on fatigue life and surface characteristics of stainless steel cortical bone screws, Am. J. Vet. Res. 65 (2004) 972–976. https://doi.org/10.2460/ajvr.2004.65.972.

[37] X.Shen, L.Lu, D.Zeng, M.Zhang, Improving fatigue resistance of high strength bolt under cyclic transverse loading by fine particle peening, Eng. Struct. 210 (2020) 110359. https://doi.org/10.1016/j.engstruct.2020.110359.

[38] Y.T.Zhan, J.H.Wang, K.Jin, J.BinChen, H.J.Wang, J.Fang, W.L.Chen, L.Sui, Effect of shot peening on fatigue life performance of homemade nut, J. Chinese Soc. Corros. Prot. 41 (2021) 395–399.

[39] F.Sun, L.Wang, X.C.Li, W.Cheng, Z.Lin, D.C.Ba, G.Q.Song, C.S.Sun, Effect of surface modification on the long-term stability of dental implant abutment screws by plasma nitriding treatment, Surf. Coatings Technol. 399 (2020) 126089. https://doi.org/10.1016/j.surfcoat.2020.126089.

[40] G.H.Junker, New criteria for self-loosening of fasteners under vibration, SAE Tech. Pap. (1969) 314–335. https://doi.org/10.4271/690055.

[41] Deutsches Institut für Normung. Dynamic testing of the locking characteristics of fasteners under transverse loading conditions (vibration test), DIN 65151 2002-08. Berlin DIN; (2002).

[42] N.G.Pai, D.P.Hess, Experimental study of loosening of threaded fasteners due to dynamic shear loads, J. Sound Vib. 253 (2002) 585–602. https://doi.org/10.1006/jsvi.2001.4006.

[43] G.E.Ramey, R.C.Jenkins, Experimental Analysis of Thread Movement in Bolted Connections Due to Vibrations, 1995.

[44] J.Liu, H.Ouyang, Z.Feng, Z.Cai, X.Liu, M.Zhu, Study on self-loosening of bolted joints excited by dynamic axial load, Tribol. Int. 115 (2017) 432–451. https://doi.org/10.1016/j.triboint.2017.05.037.

[45] T.Sawa, M.Ishimura, H.Yamanaka, Y.Fukuba, Mechanism of rotational screw thread loosening in bolted joints under repeated temperature changes, in: PVP, San Antonio, Texas, 2007. https://doi.org/10.1115/PVP2007-26439.

[46] M.Ishimura, S.Sawa, Y.Omiya, T.Sawa, Mechanism of Screw Thread Loosening in Bolted Joints With Dissimilar Clamped Parts Under Repeated Temperature Changes, in: IMECE, 2014: pp. 1–7. https://doi.org/10.1115/IMECE2014-38077.

[47] M.Ishimura, T.Sawa, A.Karami, T.Nagao, Bolt nut loosening in bolted flange connections under repeated bending moments, in: K-PVP, Bellevue,USA, 2010: pp. 1–9. https://doi.org/10.1115/PVP2010-25326.

[48] K.Koga, Loosening by repeated impact of threaded fastenings, Bull. JSME. 13 (1970) 140–149. https://doi.org/10.1299/jsme1958.13.140.

[49] Q.Zheng, Y.Guo, Y.Wei, Y.Wang, X.Wang, Loosening of steel threaded connection subjected to axial compressive impact loading, Int. J. Impact Eng. 144 (2020) 103662. https://doi.org/10.1016/j.ijimpeng.2020.103662.

[50] M.Andersson, Locking system and fastening elements, U.S. Patent Application 12/438,825, 2010.

[51] T.Sawa, H.Yamanaka, M.Ishimura, Y.Shoji, Experimental evaluation of screw thread loosening in bolted joint with some parts for preventing the loosening under transverse repeated loadings, in: SAE Tech. Pap., 2006: pp. 1–10. https://doi.org/10.4271/2006-01-0988.

[52] Y.Shoji, T.Sawa, Self-loosening mechanism of nuts due to lateral motion of fastened plate, in: ASME Press. Vessel. Pip. Conf., ASME, San Antonio, Texas, 2007: pp. 223–230. http://www.asme.org/about-asme/terms-of-use.

[53] S.Dravid, K.Tripathi, M.Chouksey, Role of Washers in Controlling Loosening of Full Threaded Bolted Joints, Procedia Technol. 14 (2014) 543–552. https://doi.org/10.1016/j.protcy.2014.08.069.

[54] Nabeya Bi-tech Kaisha, anti-loosening product, (2021). www.nbk1560.com/products/specialscrew/nedzicom/stoplooseningparts/SWAS-EW/?SelectedLanguage=ja-JP (accessed May29, 2021).

[55] B.Panja, S.Das, Development of an anti-loosening fastener and comparing its performance with different other threaded fasteners, Sadhana - Acad. Proc. Eng. Sci. 42 (2017) 1793–1801. https://doi.org/10.1007/s12046-017-0719-4.

[56] R.T.Barrett, NASA reference publication 1228 Fastener Design Material, NASA, Off. Manag. Sci. Tech. Inf. Devision. (1990) 6–9. http://ntrs.nasa.gov/archive/nasa/casi.ntrs.nasa.gov/19900009424.pdf.

[57] product information: Antiloosening solution, IMJINST. (2021). http://imjinst.co.kr/en/product01/?ckattempt=1 (accessed May29, 2021).

[58] W.Eccles, I.Sherrington, R.D.Arnell, Towards an understanding of the loosening characteristics of prevailing torque nuts, Proc. Inst. Mech. Eng. Part C J. Mech. Eng. Sci. 224 (2010) 483–495. https://doi.org/10.1243/09544062JMES1493.

[59] W.Eccles, Tribological Aspects of the Self-Loosening of Threaded Fasteners, University of Central Lancashire, 2010.

[60] S.Izumi, T.Yokoyama, T.Teraoka, A.Iwasaki, S.Sakai, K.Saito, M.Nagawa, H.Noda, Verification of Anti-Loosening Performance of Super Slit Nut by Finite Element Method, Trans. Japan Soc. Mech. Eng. Ser. A. 71 (2005) 380–386. https://doi.org/10.1299/kikaia.71.380.

[61] S.Nishiyama, H.Migita, M.Kataoka, N.Nakasaki, K.MuranoURANO, Development of Anti-Loosening Performance of Hyper Lock Nut, J. Syst. Des. Dyn. 3 (2009) 147–161. https://doi.org/10.1299/jsdd.3.147.

[62] U-NUT Product information. Comprehensive manufacturer of anti-loosening nuts, Fuji Seimitsu Co., Ltd. (n.d.). https://www.fun.co.jp/products/detail.php?no=Ng== (accessed December28, 2020).

[63] N.-A.Noda, Y.Xiao, M.Kuhara, K.Saito, M.Nagawa, A.Yumoto, A.Ogasawara, Optimum Design of Thin Walled Tube on the Mechanical Performance of Super Lock Nut, J. Solid Mech. Mater. Eng. 2 (2008) 780–791. https://doi.org/10.1299/jmmp.2.780.

[64] N.A.Noda, M.Kuhara, Y.Xiao, S.Noma, K.Saito, M.Nagawa, A.Yumoto, A.Ogasawara, Stress Reduction Effect and Anti-Loosening Performance of Outer Cap Nut by Finite Element Method, J. Solid Mech. Mater. Eng. 2 (2008) 801–811. https://doi.org/10.1299/jmmp.2.801.

[65] K.Wakabayashi, Hard Lock Kogyo,Hard Lock Nut, Japanese Patent, 195236, 2002.

[66] N.Sase, K.Nishioka, S.Koga, H.Fujii, An anti-loosening screw-fastener innovation and its evaluation, J. Mater. Process. Technol. 300 (1998) 209–215. https://doi.org/10.1016/s0924-0136(97)00419-6.

[67] N.Sase, H.Fujii, Optimizing study of SLBs for higher anti-loosening performance, J. Mater. Process. Technol. 119 (2001) 174–179. https://doi.org/10.1016/S0924-0136(01)00935-9.

[68] T.Takemasu, H.Miyahara, Development of thread rolled anti-loosening bolts based on the double thread mechanism and a performane evaluation, JSME Int. Journal, Ser. A Solid Mech. Mater. Eng. 48 (2006) 305–310. https://doi.org/10.1299/jsmea.48.305.

[69] T.Shinbutsu, S.Amano, T.Takemasu, T.Kuwabara, J.Shimura, Thread rolling and performance evaluations of a new anti-loosening double thread bolt combining a single thread and multiple threads, Procedia Eng. 207 (2017) 603–608. https://doi.org/10.1016/j.proeng.2017.10.1028.

[70] T.Shinbutsu, S.Amano, T.Takemasu, T.Kuwabara, Thread Rolling and Performance Evaluation of New Double-Thread Bolt-Study on Development of Antiloosening Bolt Fasteners Based on Coarse-Single Coarse-Multiple Double-Thread Mechanism, 1st Report, J. Japan Soc. Technol. Plast. 58 (2017) 404–410.

[71] H.Gong, J.Liu, X.Ding, Study on local slippage accumulation between thread contact surfaces and novel anti-loosening thread designs under transversal vibration, Tribol. Int. 153 (2021) 106558. https://doi.org/10.1016/j.triboint.2020.106558.

[72] Z.C.Tang, Tang's Thread and the anti-loosening principle, J. Mech. Eng. 6 (2001) 21–23.

[73] F.Sun, Z.C.Tang, The anti-loosening principle and effect of Tang's thread, J. Mech. Eng. 5 (2002) 13–15.

[74] Y.Xiao, Q.Wan, N.A.Noda, Y.Akaishi, Y.Takase, S.Nishida, Stress reduction effect

of tapering thread bolts and nuts which have slightly different pitches, Trans. Soc. Automot. Eng. Japan. 42 (2011) 927–933. https://doi.org/10.11351/jsaeronbun.42.927.

[75] Y.Akaishi, X.Chen, Y.Yu, H.Tamasaki, N.A.Noda, Y.Sano, Y.Takase, Fatigue Strength Analysis for Bolts and Nuts Which Have Slightly Different Pitches Considering Clearance, Trans. Soc. Automot. Eng. Japan. 44 (2013) 1111–11117. https://doi.org/10.11351/jsaeronbun.44.1111.

[76] X.Chen, N.A.Noda, M.A.Wahab, Y.I.Akaishi, Y.Sano, Y.Takase, G.Fekete, Fatigue failure analysis for bolt-nut connections having slight pitch differences using experimental and finite element methods, Acta Polytech. Hungarica. 12 (2015) 61–79. https://doi.org/10.12700/APH.12.8.2015.8.4.

[77] X.Chen, N.A.Noda, M.A.Wahab, Y.Sano, H.Maruyama, H.Wang, R.Fujisawa, Y.Takase, Fatigue Life Improvement by Slight Pitch Difference in Bolt-Nut Connections, J. Chinese Soc. Mech. Eng. Trans. Chinese Inst. Eng. Ser. C. 37 (2016) 11–19.

[78] N.-A.Noda, Y.Sano, X.Chen, H.Maruyama, H.Wang, R.Fujisawa, Y.Takase, Fatigue strength for bolts and nuts having slight pitch difference considering incomplete threads of nut, Trans. JSME (in Japanese). 81 (2015). https://doi.org/10.1299/transjsme.15-00240.

[79] N.A.Noda, Y.Sano, Y.Takase, X.Chen, H.Maruyama, H.Wang, R.Fujisawa, Anti-Loosing Performance of Special Bolts and Nuts Having Enhanced Fatigue Life by Introducing Pitch Difference, Trans. Soc. Automot. Eng. Japan. 46 (2015) 121–126. https://doi.org/10.11351/jsaeronbun.46.121.

[80] N.A.Noda, X.Chen, Y.Sano, M.A.Wahab, H.Maruyama, R.Fujisawa, Y.Takase, Effect of pitch difference between the bolt-nut connections upon the anti-loosening performance and fatigue life, Mater. Des. 96 (2016) 476–489. https://doi.org/10.1016/j.matdes.2016.01.128.

[81] N.A.Noda, X.Liu, Y.Sano, K.Tateishi, B.Wang, Y.Takase, Three dimensional finite element analysis for prevailing torque of bolt nut connections having slight pitch difference, J. Mech. Sci. Technol. 34 (2020) 2469–2476. https://doi.org/10.1007/s12206-020-0522-8.

[82] N.A.Noda, X.Liu, Y.Sano, S.Kubo, Y.Huang, K.Tateishi, Y.Takase, Three-dimensional finite element analysis for prevailing torque in the screwing process of bolt and nut connections with pitch difference, Trans. JSME (in Japanese). 85 (2019). https://doi.org/10.1299/transjsme.19-00149.

[83] N.A.Noda, X.Liu, Y.Sano, K.Tateishi, B.Wang, Y.Inui, Y.Takase, Three-dimensional finite element analysis of tightening and untightening process of bolt and nut connections with slight pitch difference, Trans. JSME (in Japanese). 86 (2020). https://doi.org/10.1299/transjsme.19-00413.

[84] N.A.Noda, X.Liu, Y.Sano, K.Tateishi, B.Wang, Y.Inui, Y.Takase, Prevailing torque and residual prevailing torque of Bolt-Nut connections having slight pitch difference, Mech. Based Des. Struct. Mach. 0 (2020) 1–14. https://doi.org/10.1080/15397734.2020.1768114.

[85] X.Liu, B.Wang, N.A.Noda, Y.Sano, Y.Inui, K.Tateishi, Y.Takase, Bolt Clamping Force versus Torque Relation (F-T Relation) during Tightening and Untightening the Nut Having Slight Pitch Difference, Mech. Based Des. Struct. Mach. Int. J. (2021). https://doi.org/10.1080/15397734.2021.1931308.

[86] Junker tests - meeting vibbration tests standards, Hardlock Ind. Co. Ltd. (n.d.). https://heico-lock.us/technical-info/junker-tests/ (accessed May30, 2021).

[87] S.I.Nishida, Strength Design of Machine/Structure and Practical Examples, J. Soc. Mater. Sci. Japan. 59 (2010). https://doi.org/10.2472/jsms.59.476.

[88] M.Sivapathasundaram, M.Mahendran, Pull-out capacity of multiple screw fastener connections in cold-formed steel roof battens, J. Constr. Steel Res. 144 (2018) 40–52. https://doi.org/10.1016/j.jcsr.2018.01.013.

[89] L.H.Teh, M.E.Uz, Ultimate Tilt-Bearing Capacity of Bolted Connections in Cold-Reduced Steel Sheets, J. Struct. Eng. 143 (2017) 04016206-1-04016206–12. http://ro.uow.edu.au/eispapers1/118.

[90] K.Roy, J.B.P.Lim, A.M.Yousefi, G.C.Clifton, M.Mahendran, Low Fatigue Response of Crest-Fixed Cold-Formed Steel Drape Low Fatigue Response of Crest-Fixed Cold-Formed Steel Drape Curved Roof Claddings, in: Int. Spec. Conf. Cold-Form Steel Struct. 4, 2018. https://scholarsmine.mst.edu/isccss/24iccfss/session10/4.

[91] K.Roy, H.H.Lau, T.C.Huon Ting, R.Masood, A.Kumar, J.B.P.Lim, Experiments and finite element modelling of screw pattern of self-drilling screw connections for high strength cold-formed steel, Thin-Walled Struct. 145 (2019) 106393-undefined. https://doi.org/10.1016/j.tws.2019.106393.

[92] M.D.Elliott, L.H.Teh, A.Ahmed, Behaviour and strength of bolted connections failing in shear, J. Constr. Steel Res. 153 (2019) 320–329. https://doi.org/10.1016/j.jcsr.2018.10.029.

[93] E.A.Patterson, A comparative study of methods for estimating bolt fatigue limits, Fatigue Fracr. Engng Muter. Strucr. 13 (1990) 59–81.

[94] N.A.Noda, Y.Takase, Stress concentration formulae useful for any shape of notch in a round test specimen under tension and under bending, Fatigue Fract Engng Mater Struct. 22 (1999) 1071–1082.

[95] N.A.Noda, Y.Takase, Stress concentration formula useful for all notch shape in a round bar (comparison between torsion, tension and bending), Int. J. Fatigue. 28 (2006) 151–163. https://doi.org/10.1016/j.ijfatigue.2005.04.015.

[96] F.Esmaeili, M.Zehsaz, T.N.Chakherlou, Experimental investigations on the effects of torque tightening on the fatigue strength of double-lap simple bolted and hybrid (Bolted/Bonded) joints, Strain. 50 (2014) 347–354. https://doi.org/10.1111/str.12097.

[97] K.Gunn, Effect of Yielding on the Fatigue Properties of Test Pieces Containing Stress Concentrations, Aeronaut. Q. 6 (1955) 277–294. https://doi.org/10.1017/s0001925900010052.

[98] R.L.Burguete, E.A.Patterson, The effect of mean stress on the fatigue limit of high tensile bolts, in: Proc. Inst. Mech. Eng. Part C J. Mech. Eng. Sci., 1995. https://doi.org/10.1243/PIME_PROC_1995_209_152_02.

[99] B.S.Munn, K.Li, Investigation Into the Effect of Thread Root Condition on the High, in: PVP2010, 2010: pp. 1–15. https://doi.org/10.1115/PVP2010-25227.

[100] S.Hashimura, K.Kamibeppu, T.Nutahara, K.Fukuda, Y.Miyashita, Effects of Clamp Force on Fatigue Strength of Aluminum Alloy Bolts, Procedia Struct. Integr. 19 (2019) 204–213. https://doi.org/10.1016/j.prostr.2019.12.022.

[101] K.S.Udagawa, Survey report for standardization on fastening performance of high strength bolts, J. Japan Res. Inst. Screw Threads Fasten. 13 (1982) 165–172. https://iss.ndl.go.jp/books/R100000002-I000000018792-00.

[102] N.Motosh, Development of design charts for bolts preloaded up to the plastic range, J. Manuf. Sci. Eng. Trans. ASME. 98 (1976) 849–851. https://doi.org/10.1115/1.3439041.

[103] D.X.Cheng, Handbook of mechanical design, 6th ed., Chemical Industry Press, Beijing, 2016.

[104] T.Sakai, The friction coefficient of fasteners, Bull. JSME. 21 (1978) 333–340. https://doi.org/10.1299/jsme1958.21.333.

[105] Q.Zou, T.S.Sun, S.A.Nassar, G.C.Barber, A.K.Gumul, Effect of lubrication on friction and torque-tension relationship in threaded fasteners, Tribol. Trans. 50 (2007) 127–136. https://doi.org/10.1080/10402000601105490.

[106] J.Liu, H.Ouyang, J.Peng, C.Zhang, P.Zhou, L.Ma, M.Zhu, Experimental and numerical studies of bolted joints subjected to axial excitation, Wear. 346–347 (2016) 66–77. https://doi.org/10.1016/j.wear.2015.10.012.

[107] N.A.Noda, B.Wang, K.Oda, Y.Sano, X.Liu, Y.Inui, T.Yakushiji, Effects of root radius and pitch difference on fatigue strength and anti-loosening performance for high strength bolt–nut connections, Adv. Struct. Eng. (2021). https://doi.org/10.1177/1369433220988619.